Electronic Supplementary Information

Computationally Designed Tandem Direct Selective Oxidation using Molecular Oxygen as Oxidant without Coreductant

Bo Yang and Thomas A. Manz*

Department of Chemical & Materials Engineering, New Mexico State University, Las Cruces, NM 88003-8001.

*corresponding author email tmanz@nmsu.edu

CONTENTS:

All data presented in the figures and tables are based on DFT calculations using the B3LYP functional and LANL2DZ basis sets unless specified otherwise. All energies in the table beneath each optimized conformation are in Hartrees. $\mathbf{E_{SCF}}$ is the electronic energy without zero point vibrations or thermal contributions. $\mathbf{E_{ZP}}$ includes zero-point vibrations but no thermal contributions (i.e., the energy at 0 Kelvin). **H** and **G** are the computed enthalpy and Gibbs free energy at 298.15 Kelvin and 1 atmosphere pressure. For transition states, the imaginary frequency $\boldsymbol{f}$ (cm^{-1}) along the reaction coordinate is listed.

Note that $M(O_2)_2^S$, $M{\cdot}(O_2)_2^T$, $M'(O_2)_2^S$, and $M'{\cdot}(O_2)_2^T$ without any conformation label are the spiro conformations.

1. Additional Figures and Tables

1.1 Crossing Point Calculations

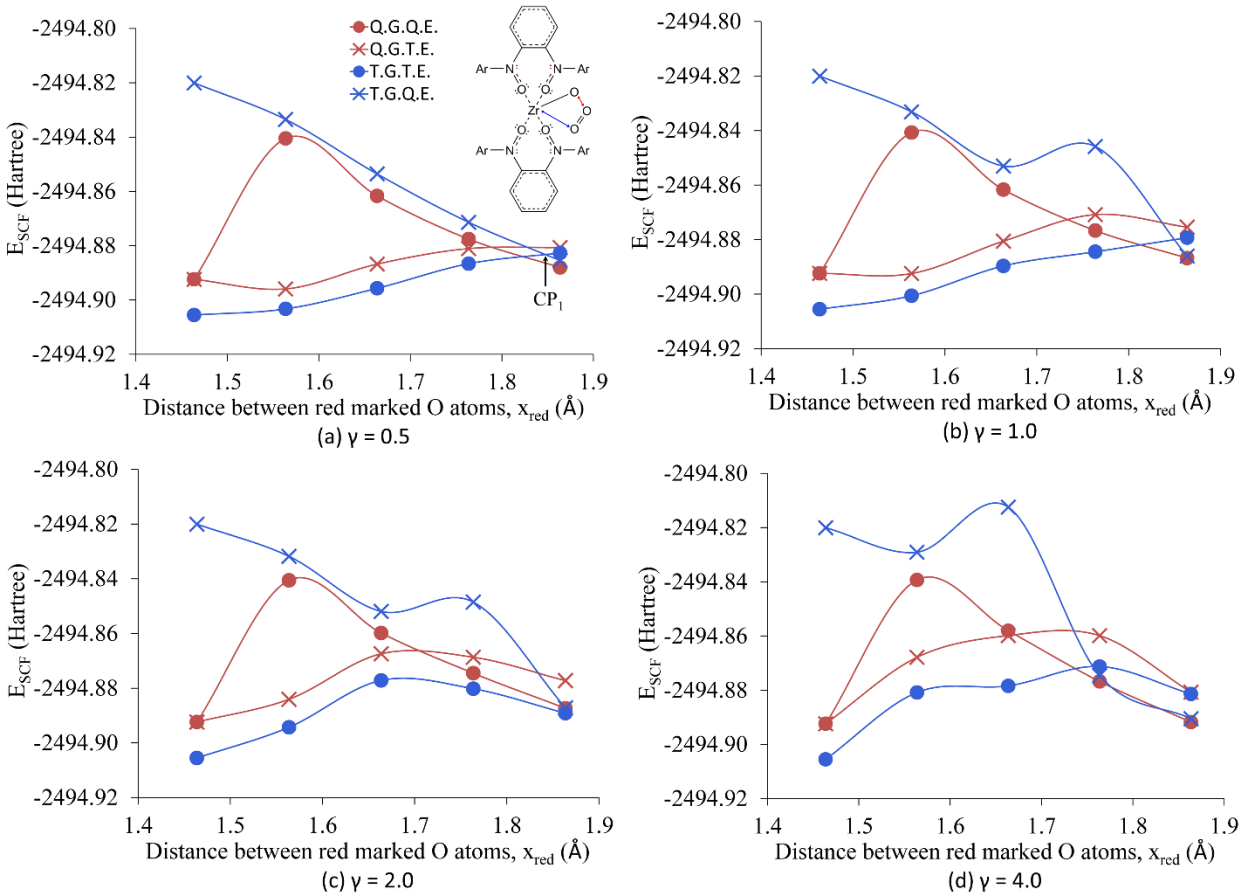

Fig. S1: Triplet-quintet crossing point for reaction in which molecular O_2 reacts with the triplet oxo complex to form the triplet η^2-ozone complex. The activation barrier for this reaction was estimated according to the triplet-quintet energy crossing point (CP_1) as marked in plot (a). Legend T.G. = triplet geometry, T.E. = triplet energy, Q.G. = quintet geometry, Q.E. = quintet energy. Each red dot in the two-dimensional chemical drawing represents one-half of an electron. (The two unpaired electrons in the triplet geometry are nominally shared between the four N atoms.) The constrained distances between two red (blue) marked atoms are defined as x_{red} (x_{blue}), with $x^0_{red} = 1.514$ Å ($x^0_{blue} = 2.092$ Å) as in the triplet η^2-ozone ground state. The ratio of elongation (γ) between two constrained distances is defined as: $\gamma = \Delta x_{blue}/\Delta x_{red}$ with $\Delta x_{blue} = x_{blue} - x^0_{blue}$, and $\Delta x_{red} = x_{red} - x^0_{red}$. For plot (a) γ = 0.5, (b) γ = 1.0, (c) γ = 2.0, and (d) γ = 4.0.

For reaction in which molecular O_2 reacts with the MO^T complex, a triplet-quintet crossing point calculation was constructed to determine the associated activation barrier. In this case, the activation barrier was defined by the triplet-quintet crossing point (CP_1) where a vertical transition (i.e., at constant geometry) occurred. As shown in Fig. S1, this crossing point was estimated by a series of constrained geometry optimizations over the potential energy surface. Starting with the fully optimized $M(\eta^2\text{-}O_3)^T$ structure, two distances were constrained simultaneously:

1) marked in red in Fig. S1: the distance between the outer O atom (the one that remains adsorbed to form the oxo group) and the middle O atom

2) marked in blue in Fig. S1: the distance between the Zr atom and the other outer O atom (the one that desorbs to form an O_2 molecule)

All other geometric parameters were relaxed for both triplet and quintet constrained geometry optimizations. Computed SCF energy (E_{SCF}) for each constrained geometry was plotted against independently constrained values of the two variables to create a two-dimensional potential energy surface. The triplet energies for constrained optimized triplet and quintet geometries, and quintet energies for constrained optimized triplet and quintet geometries were computed. As shown in Fig. S1, the crossing point (CP_1) was estimated as the lowest energy for which triplet and quintet energies were the same for the same geometry along this potential energy surface.

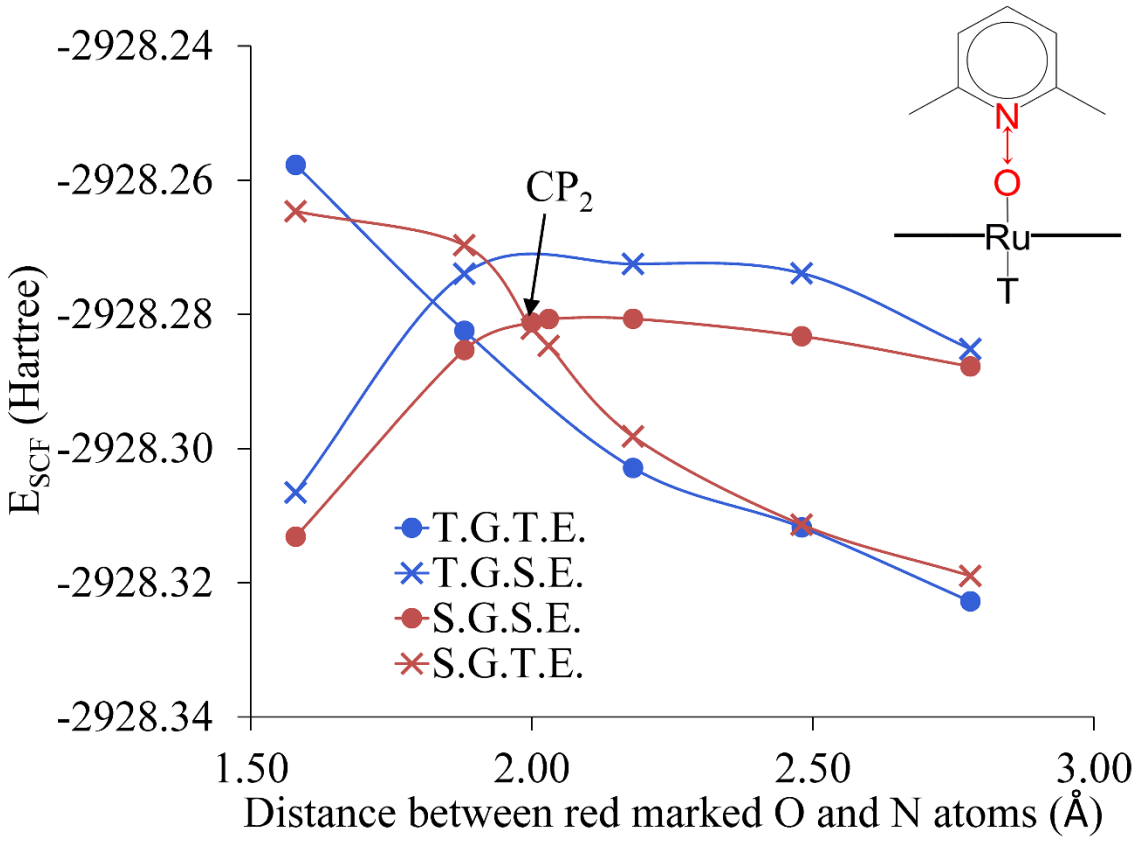

Fig. S2: Singlet-triplet crossing point for reaction in which Me_2PyO denotes an O atom to the bare RuTDCPP complex to form Me_2Py plus the RuTDCPP oxo complex. The activation barrier for this reaction was estimated according to the singlet-triplet energy crossing point (CP_2) as marked in the diagram. Legend: S.G. = singlet geometry, S.E. = singlet energy, T.G. = triplet geometry, T.E. = triplet energy. The distance between the two red marked atoms is constrained in each geometry optimization.

For reaction in which Me_2PyO denotes an O atom to the bare RuTDCPP complex to form Me_2Py plus the RuTDCPP oxo complex, a singlet-triplet crossing point calculation was constructed to determine the associated activation barrier. The activation barrier was defined by the singlet-triplet crossing point (CP_2) where a vertical transition occurred. As shown in Fig. S2, this crossing point was estimated by a series of constrained geometry optimizations over the potential energy surface. Starting with the fully optimized RuTDCPP(Me_2PyO)^T structure, the distance between the O atom and the N atom (marked in red in Fig. S2) was constrained. All other geometric parameters were relaxed for both singlet and triplet constrained geometry optimizations. Computed SCF energy (E_{SCF}) for the constrained geometry was plotted against the constrained distance. The singlet energies for constrained optimized singlet and triplet geometries, and triplet energies for constrained optimized singlet and triplet geometries were computed. As shown in Fig. S2, the crossing point was estimated as the lowest energy for which singlet and triplet energies were the same for the same geometry along this potential energy surface.

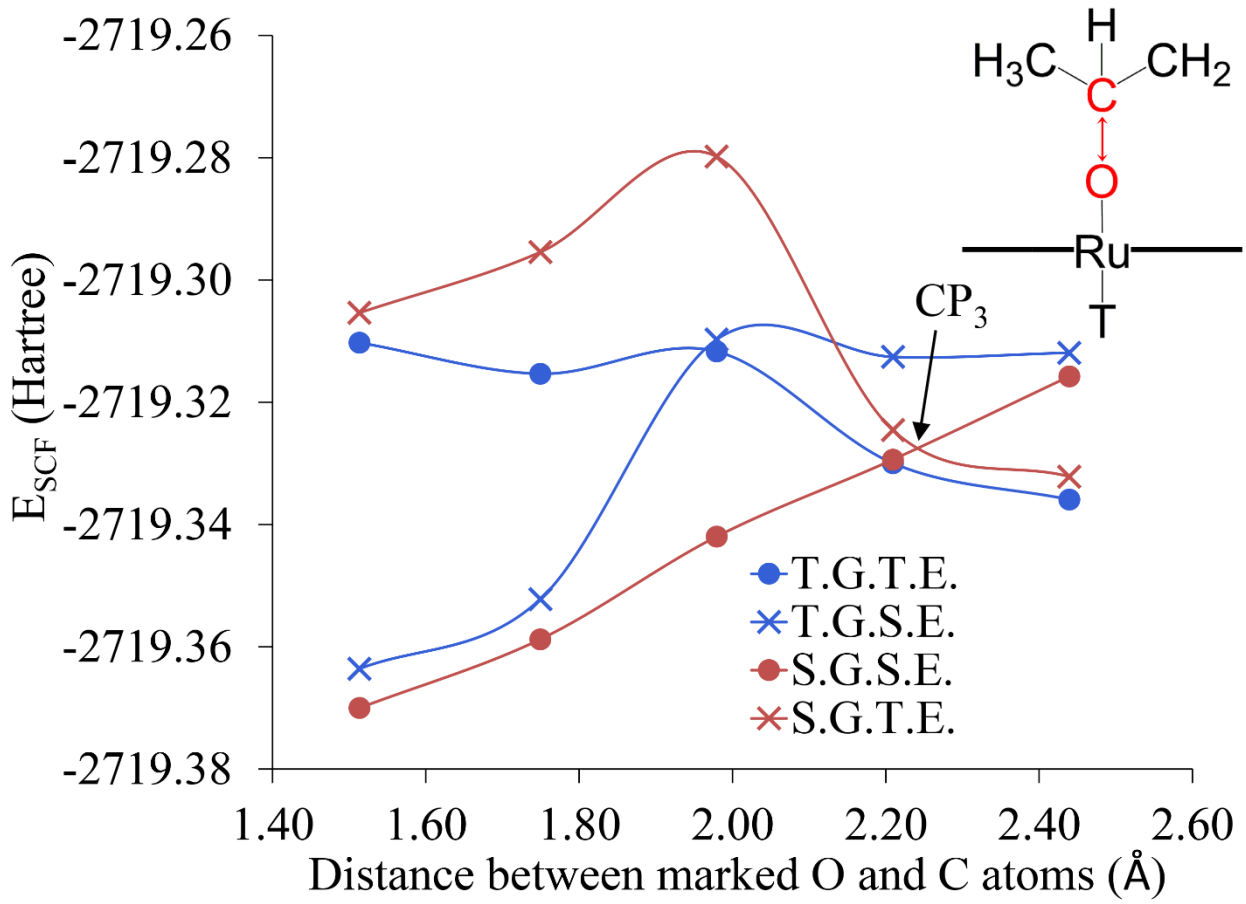

Fig. S3: Singlet-triplet crossing point for the reaction forming RuTDCPP(PO)^{S} from RuTDCPP(PO*)^{T}. The activation barrier for this reaction was estimated according to the singlet-triplet energy crossing point (CP_3) as marked in the diagram. Legend: S.G. = singlet geometry, S.E. = singlet energy, T.G. = triplet geometry, T.E. = triplet energy. The distance between the two red marked atoms is constrained in each geometry optimization.

For the reaction forming RuTDCPP(PO)^{S} from RuTDCPP(PO*)^{T}, a singlet-triplet crossing point calculation was constructed to determine the associated activation barrier. The activation barrier was defined by the singlet-triplet crossing point (CP_3) where a vertical transition occurred. As shown in Fig. S3, this crossing point was estimated by a series of constrained geometry optimizations over the potential energy surface. Starting with the fully optimized RuTDCPP(PO*)^{T} structure, the distance between the O atom and the middle C atom (marked in red in Fig. S3) was constrained. All other geometric parameters were relaxed for both singlet and triplet constrained geometry optimizations. Computed SCF energy (E_{SCF}) for the constrained geometry was plotted against the constrained distance. The singlet energies for constrained optimized singlet and triplet geometries, and triplet energies for constrained optimized singlet and triplet geometries were computed. As shown in Fig. S3, the crossing point was estimated as the lowest energy for which singlet and triplet energies were the same for the same geometry along this potential energy surface.

1.2. Relative Energies with Respect to Different Oxygen Chemical Potentials

Table S1: Summary of the computed relative energies for the DMZB catalyst with various oxygenated functional groups. The triplet spiro bisperoxo form of the DMZB catalyst ($M\cdot(O_2)_2^T$) is the reference state. The columns labeled Me_2PyO refer to the 2,6-dimethylpyridine *N*-oxide side and the columns labeled O_2 refer to the O_2 side.

DMZB	Relative Energy (kcal/mol)							
	E_{scf}		E_{zp}		H		G	
	Me_2PyO	**O_2**	**Me_2PyO**	**O_2**	**Me_2PyO**	**O_2**	**Me_2PyO**	**O_2**
M^S	-11.3	18.3	-4.8	17.0	-8.4	16.7	6.2	0.3
M^T	42.7	72.4	46.9	68.6	44.3	69.4	52.8	46.9
MO^S	-5.0	17.3	-1.2	15.2	-3.5	15.3	5.0	0.6
MO^T	-16.9	5.3	-13.4	3.0	-15.6	3.3	-8.2	-12.6
$M(O)_2^S$	16.2	31.1	19.8	30.7	18.5	31.1	23.2	20.2
$M(O)_2^T$	18.9	33.8	21.1	31.9	20.2	32.7	23.0	20.1
$M(O_2)^S$	2.3	17.2	5.2	16.1	3.8	16.4	9.5	6.6
$M(O_2)^T$	-7.9	6.9	-5.4	5.5	-7.2	5.3	-1.0	-3.9
$MO(O_2)^S$	16.1	23.5	18.0	23.4	17.4	23.6	20.5	19.1
$MO\cdot(O_2)^T$	-2.3	5.1	-1.4	4.1	-1.6	4.7	-1.3	-2.7
$M(\eta^2\text{-}O_3)^S$	15.5	23.0	17.5	22.9	16.5	22.8	20.4	18.9
$M(\eta^2\text{-}O_3)^T$	5.9	13.4	7.7	13.1	6.8	13.1	9.7	8.2
$M(\eta^3\text{-}O_3)^S$	19.9	27.3	21.5	27.0	20.7	27.0	24.1	22.6
$M(\eta^3\text{-}O_3)^T$	9.7	17.1	10.8	16.3	10.2	16.5	12.0	10.5
$M(O_2)_2^S$	25.3	25.3	26.0	26.0	25.6	25.6	27.2	27.2
$M\cdot(O_2)_2^T$	0.0	0.0	0.0	0.0	0.0	0.0	0.0	0.0
$MO(\eta^2\text{-}O_3)^S$	23.2	23.2	24.0	24.0	24.0	24.0	24.3	24.3
$MO\cdot(\eta^2\text{-}O_3)^T$	12.6	12.6	13.1	13.1	13.3	13.3	12.9	12.9
$MO\cdot(\eta^3\text{-}O_3)^T$	33.4	33.4	33.2	33.2	33.2	33.2	33.3	33.3
$M(O_2)(\eta^2\text{-}O_3)^S$	28.5	21.1	28.6	23.2	28.8	22.5	28.6	30.1
$M(\eta^2\text{-}O_3)\cdot(O_2)^T$	20.6	13.2	19.5	14.1	20.1	13.9	18.0	19.5
$M(O_2)(\eta^3\text{-}O_3)^S$	33.9	26.5	34.3	28.9	34.3	28.0	35.1	36.6
$M(\eta^3\text{-}O_3)\cdot(O_2)^T$	23.5	16.1	22.6	17.1	23.0	16.7	21.7	23.2
$M(\eta^2\text{-}O_3)_2^S$	44.1	29.3	43.3	32.5	44.0	31.5	41.5	44.5
$M\cdot(\eta^2\text{-}O_3)_2^T$	42.1	27.2	40.1	29.2	41.0	28.4	37.6	40.5
$M(\eta^2\text{-}O_3)(\eta^3\text{-}O_3)^S$	47.3	32.5	46.5	35.6	47.1	34.5	45.9	48.8
$M(\eta^3\text{-}O_3)\cdot(\eta^2\text{-}O_3)^T$	42.7	27.9	41.2	30.3	42.0	29.5	39.4	42.3
$M(O_2)^S_{2,butterfly}$	30.7	30.7	30.9	30.9	31.0	31.0	30.9	30.9
$M(O_2)\cdot(O_2)^T_{butterfly}$	11.0	11.0	10.6	10.6	10.7	10.7	10.0	10.0
$M(O_2)^S_{2,planar}$	19.5	19.5	20.3	20.3	20.0	20.0	21.8	21.8

Table S2: Summary of the computed relative energies for the DMZB catalyst with various oxygenated functional groups and adsorbed molecules. The triplet spiro bisperoxo form of the DMZB catalyst ($M\cdot(O_2)_2^T$ in Table S1) is the reference state. The columns labeled Me_2PyO refer to the 2,6-dimethylpyridine *N*-oxide side and the columns labeled O_2 refer to the O_2 side.

DMZB	**Relative Energy (kcal/mol)**							
	E_{scf}		**E_{zp}**		**H**		**G**	
	Me_2PyO	**O_2**	**Me_2PyO**	**O_2**	**Me_2PyO**	**O_2**	**Me_2PyO**	**O_2**
$MO\cdot Me_2Py^S$	-7.1	15.1	-1.5	14.9	-3.3	15.5	18.6	14.2
$M(O_2)\cdot Me_2Py^S$	8.0	22.9	13.0	23.9	11.3	23.9	33.4	30.5
$M(O_2)\cdot Me_2Py^T$	-3.9	10.9	0.7	11.6	-0.7	11.8	19.9	16.9
$M(\eta^2\text{-}O_3)\cdot Me_2Py^S$	22.7	30.1	26.2	31.7	24.8	31.1	45.2	43.8
$M(\eta^2\text{-}O_3)\cdot Me_2Py^T$	11.2	18.6	14.6	20.0	13.7	20.0	31.9	30.4
$M(\eta^3\text{-}O_3)\cdot Me_2Py^S$	31.5	39.0	34.7	40.2	33.8	40.1	53.1	51.6
$M(\eta^3\text{-}O_3)\cdot Me_2Py^T$	14.4	21.8	17.5	23.0	16.7	23.0	34.9	33.4
$MO\cdot Me_2PyO^S$	-13.4	8.8	-8.2	8.1	-9.9	9.0	10.8	6.4
$MO\cdot Me_2PyO^T$	-25.3	-3.1	-20.4	-4.1	-22.0	-3.1	-2.0	-6.4
$M(O_2)\cdot Me_2PyO^S$	-3.8	11.0	0.5	11.4	-0.9	11.7	19.0	16.0
$M(O_2)\cdot Me_2PyO^T$	-14.4	0.5	-10.4	0.5	-11.6	0.9	7.4	4.4
$M(\eta^2\text{-}O_3)\cdot Me_2PyO^S$	11.7	19.1	15.8	21.3	14.6	20.9	34.6	33.1
$M(\eta^2\text{-}O_3)\cdot Me_2PyO^T$	3.3	10.7	6.5	12.0	5.7	11.9	23.2	21.7
$M(\eta^3\text{-}O_3)\cdot Me_2PyO^S$	19.1	26.5	22.2	27.6	20.8	27.1	40.9	39.4
$M(\eta^3\text{-}O_3)\cdot Me_2PyO^T$	5.8	13.3	8.7	14.2	7.8	14.1	25.9	24.4
$MO\cdot EO^S$	-5.0	17.2	1.5	17.8	-0.7	18.1	20.2	15.8
$MO\cdot EO^T$	-28.3	-6.1	-22.9	-6.6	-24.7	-5.9	-5.9	-10.3
$M(O_2)\cdot EO^S$	-2.7	12.1	2.1	13.0	0.5	13.0	19.3	16.4
$M(O_2)\cdot EO^T$	-13.6	1.3	-9.1	1.8	-10.6	1.9	7.1	4.1
$M(\eta^2\text{-}O_3)\cdot EO^S$	11.0	18.4	15.1	20.5	13.8	20.1	31.4	29.9
$M(\eta^2\text{-}O_3)\cdot EO^T$	2.3	9.7	5.4	10.9	4.0	10.3	20.8	19.3
$M(\eta^3\text{-}O_3)\cdot EO^S$	17.6	25.0	21.3	26.7	20.0	26.3	37.8	36.3
$M(\eta^3\text{-}O_3)\cdot EO^T$	5.9	13.3	9.0	14.4	8.1	14.3	22.6	21.1

Table S3: Summary of the computed relative energies for the RuTDCPP catalyst with various oxygenated functional groups or adsorbed molecules. The triplet oxo form of the RuTDCPP catalyst (RuTDCPP(O)^{T}) is the reference state. The columns labeled Me_2PyO refer to the 2,6-dimethylpyridine *N*-oxide side and the columns labeled PO refer to the PO side.

RuTDCPP	**Relative Energy (kcal/mol)**							
	E_{scf}		**E_{zp}**		**H**		**G**	
	Me_2PyO	**PO**	**Me_2PyO**	**PO**	**Me_2PyO**	**PO**	**Me_2PyO**	**PO**
RuTDCPP^{S}	17.0	8.5	18.5	10.3	17.8	9.6	20.6	10.8
RuTDCPP^{T}	43.9	35.4	43.8	35.6	43.7	35.5	44.4	34.7
RuTDCPP^{Q}	71.0	62.5	69.2	60.9	69.3	61.1	68.6	58.8
RuTDCPP(O)^{S}	22.5	22.5	22.5	22.5	22.5	22.5	23.3	23.3
RuTDCPP(O)^{T}	0.0	0.0	0.0	0.0	0.0	0.0	0.0	0.0
RuTDCPP(O)^{Q}	39.4	39.4	36.3	36.3	36.8	36.8	35.3	35.3
RuTDCPP(Me_2Py)^{S}	15.5	7.0	18.7	10.5	17.9	9.7	36.2	26.5
RuTDCPP(Me_2Py)^{T}	41.9	33.4	43.9	35.7	43.2	35.0	61.6	51.8
RuTDCPP(Me_2Py)^{Q}	77.0	68.5	77.7	69.5	77.2	69.0	94.6	84.9
RuTDCPP(Me_2PyO)^{S}	1.3	-7.2	3.5	-4.7	3.3	-4.9	19.5	9.8
RuTDCPP(Me_2PyO)^{T}	24.0	15.5	25.4	17.2	25.2	17.0	41.3	31.6
RuTDCPP(Me_2PyO)^{Q}	51.5	43.0	50.5	42.2	51.2	43.0	62.6	52.9
RuTDCPP(P)^{S}	5.2	-3.4	8.3	0.1	7.4	-0.8	23.8	14.0
RuTDCPP(P)^{T}	34.7	26.2	36.6	28.4	35.9	27.7	51.2	41.4
RuTDCPP(P)^{Q}	70.8	62.3	71.2	63.0	70.7	62.5	85.2	75.4
RuTDCPP(PO)^{S}	-3.4	-12.0	-0.7	-9.0	-1.2	-9.4	14.2	4.5
RuTDCPP(PO)^{T}	34.2	25.7	35.2	26.9	35.1	26.9	48.3	38.6
RuTDCPP(PO)^{Q}	61.8	53.2	61.4	53.1	61.4	53.2	74.6	64.8
RuTDCPP(Py)^{T}	13.4	4.9	14.8	6.6	14.5	6.3	29.4	19.7
RuTDCPP(Py)^{S}	-14.5	-23.1	-11.5	-19.8	-12.1	-20.3	4.1	-5.7
RuTDCPP(PyO)^{T}	30.5	22.0	31.2	22.9	31.2	23.0	45.6	35.8
RuTDCPP(PyO)^{S}	-4.6	-13.2	-2.4	-10.7	-2.6	-10.8	11.5	1.7

1.3. Computed Activation Barriers and Net Reaction Energies

Table S4: The computed activation barriers and net reaction energies for various reaction steps in the 2,6-dimethylpyridine oxidation reaction using the DMZB catalyst. The computed overall energetic spans are listed at the bottom.

Reactant(s)	Product(s)	Activation Barrier (kcal/mol)				Net Rxn Energy (kcal/mol)			
		E_{SCF}	E_{ZP}	H	G	E_{SCF}	E_{ZP}	H	G
$MO{\cdot}(O_2)^T$	MO^T+O_2	8.0	7.5	7.2	8.0	0.3	-1.1	-1.4	-9.8
MO^T+O_2	$MO{\cdot}(O_2)^T$	7.7	8.6	8.6	17.9	-0.3	1.1	1.4	9.8
$MO{\cdot}Me_2PyO^T$	MO^T+Me_2PyO	8.4[a]	7.1[a]	6.4[a]	–[a]	8.4	7.1	6.4	-6.1
$MO{\cdot}(O_2)^T+O_2$	$M(\eta^2\text{-}O_3){\cdot}(O_2)^T$	15.8	18.1	16.7	31.1	8.1	10.0	9.1	22.2
$M(\eta^2\text{-}O_3){\cdot}(O_2)^T$	$M(\eta^3\text{-}O_3){\cdot}(O_2)^T$	4.4	4.1	3.7	4.6	2.9	3.0	2.9	3.7
$M(\eta^3\text{-}O_3){\cdot}(O_2)^T+Me_2Py$	$M{\cdot}(O_2)_2^T+Me_2PyO$	12.8	13.3	13.5	26.6	-23.5	-22.6	-23.0	-21.7
$M{\cdot}(O_2)_2^T+Me_2Py$	$M(O){\cdot}(O_2)^T+Me_2PyO$	25.4	26.0	26.1	39.1	-2.3	-1.4	-1.6	-1.3
$M(O_2)^T+Me_2Py$	MO^T+Me_2PyO	19.8	20.5	21.1	33.7	-9.0	-8.0	-8.3	-7.2
MO^T+O_2	$M(\eta^2\text{-}O_3)^T$	24.1	24.5	24.0	35.9	8.0	10.1	9.8	20.8
$M(\eta^2\text{-}O_3)^T$	$M(\eta^3\text{-}O_3)^T$	3.9	3.2	3.1	3.1	3.7	3.2	3.4	2.3
$M(\eta^3\text{-}O_3)^T+Me_2Py$	$M(O_2)^T+Me_2PyO$	13.8	15.0	14.5	31.1	-17.6	-16.2	-17.5	-13.0
$MO{\cdot}(O_2)^T+Me_2Py$	$M(O)_2^T+Me_2PyO$	36.7	37.1	36.9	51.6	21.3	22.4	21.8	24.3
$M(\eta^3\text{-}O_3){\cdot}(\eta^2\text{-}O_3)^T+Me_2Py$	$M(\eta^2\text{-}O_3){\cdot}(O_2)^T+Me_2PyO$	13.8	14.3	14.4	27.6	-22.2	-21.7	-21.9	-21.4
E_{span}		32.0[b]	34.5[b]	33.3[b]	54.2[c]				

[a] The transition state and product geometries are the same, because the reaction is completely uphill. [b] The TDI is $MO{\cdot}Me_2PyO^T$ and the TDTS is TS_3. [c] The TDI is MO^T and the TDTS is TS_8.

Table S5: The computed activation barriers and net reaction energies for various steps in the propene epoxidation reaction using the RuTDCPP catalyst. The computed overall energetic spans are listed at the bottom.

reactant	product	activation barrier (kcal/mol)				net rxn energy (kcal/mol)			
		E_{SCF}	E_{ZP}	H	G	E_{SCF}	E_{ZP}	H	G
RuTDCPP(Me_2PyO)^S	RuTDCPP^S+ Me_2PyO	15.7[a]	15.0[a]	14.5[a]	1.1[a]	15.7	15.0	14.5	1.1
RuTDCPP(Me_2PyO)^S	RuTDCPP(O)^T+Me_2Py	28.7	27.0	27.0	26.7	-1.3	-3.5	-3.3	-19.5
RuTDCPP(O)^T+P	RuTDCPP(PO*)^T	17.9	17.8	17.7	30.2	9.4	10.0	10.1	22.1
RuTDCPP(PO*)^T	RuTDCPP(PO)^S	7.1	7.0	5.9	9.4	-21.4	-19.0	-19.5	-17.6
RuTDCPP(PO)^S	RuTDCPP^S+PO	20.4[a]	19.2[a]	19.1[a]	6.4[a]	20.4	19.2	19.1	6.4
E_{span}		33.4[b]	31.3[b]	31.6[b]	32.0[b]				

[a] The transition state and product geometries are the same, because the reaction is completely uphill. [b] The TDI is RuTDCPP(PO)^S and the TDTS is CP_2.

Table S6: The computed activation barriers and net reaction energies for various reaction steps in direct ethylene epoxidation using the DMZB catalyst. The computed overall energetic spans are listed at the bottom.

Reactant(s)	Product(s)	Activation Barrier (kcal/mol)				Net Rxn Energy (kcal/mol)			
		E_{SCF}	E_{ZP}	H	G	E_{SCF}	E_{ZP}	H	G
MO·$(O_2)^T$	MO^T+O_2	8.0	7.5	7.2	8.0	0.3	-1.1	-1.4	-9.8
MO^T+O_2	MO·$(O_2)^T$	7.7	8.6	8.6	17.9	-0.3	1.1	1.4	9.8
MO·$(O_2)^T$+O_2	M(η^2-O_3)·$(O_2)^T$	15.8	18.1	16.7	31.1	8.1	10.0	9.1	22.2
M(η^2-O_3)·$(O_2)^T$	M(η^3-O_3)·$(O_2)^T$	4.4	4.1	3.7	4.6	2.9	3.0	2.9	3.7
MO^T+O_2	M(η^2-O_3)^T	24.1	24.5	24.0	35.9	8.0	10.1	9.8	20.8
M(η^2-O_3)^T	M(η^3-O_3)^T	3.9	3.2	3.1	3.1	3.7	3.2	3.4	2.3
M(η^3-O_3)·EO^T+E	M(O_2)·EO^T+EO	14.7	15.7	14.6	30.2	-25.8	-23.9	-24.6	-23.3
M(O_2)·EO^T+E	MO·EO^T+EO	21.7	22.3	22.0	34.3	-21.1	-19.6	-20.0	-20.7
MO·EO^T+O_2	M(η^2-O_3)·EO^T	25.7	27.2	26.1	38.7	15.8	17.5	16.2	29.6
M(η^2-O_3)·EO^T	M(η^3-O_3)·EO^T	4.9	4.6	4.7	4.1	3.6	3.5	4.1	1.8
MO·EO^T	MO^T+EO	11.4[a]	9.6[a]	9.2[a]	–[a]	11.4	9.6	9.2	-2.3
M(η^3-O_3)·$(O_2)^T$+E	M·$(O_2)_2^T$+EO	11.9	12.5	12.4	22.7	-29.9	-28.4	-28.9	-29.5
M·$(O_2)_2^T$+E	MO·$(O_2)^T$+EO	23.8	24.6	24.4	35.7	-8.7	-7.2	-7.5	-9.0
M(η^3-O_3)^T+E	M(O_2)^T+EO	13.1	14.1	13.1	27.4	-23.9	-22.0	-23.4	-20.7
MO·$(O_2)^T$+E	M$(O)_2^T$+EO	27.4	28.5	27.8	41.3	14.9	16.6	15.8	16.6
E_{span}		34.0[b]	36.2[b]	34.9[c]	58.4[d]				

[a] The transition state and product geometries are the same, because the reaction is completely uphill. [b] The TDI is MO·EO^T and the TDTS is TS_{15}. [c] The TDI is MO·EO^T and the TDTS is TS_{13}. [d] The TDI is MO^T and the TDTS is TS_{15}.

1.4. Computed ASMs

Table S7: Assigned spin magnetic moments (ASMs) for the DMZB triplet conformations that do not contain any adsorbed Me_2Py, Me_2PyO, or EO molecules.

Species	Zr	Non-ligand Oxygens		Nitrogens		Other Atoms
		Strongly Ads.	Weakly Ads.	Ligand 1	Ligand 2	
M^T	0.7069	—	—	0.5264	0.0396	0.7272
MO^T	0.0098	0.0194	—	0.5000	0.4998	0.9710
$M(O)_2^T$	0.0216	-0.9205[a]	—	0.7604	0.4999	1.6386
$M(O_2)^T$	0.0118	0.0125	—	0.4972	0.4972	0.9813
$MO\cdot(O_2)^T$	-0.0069	-0.0019	1.0097	0.4988	0.0237	0.4766
$M(\eta^2\text{-}O_3)^T$	0.0116	0.0182	—	0.4966	0.4965	0.9772
$M(\eta^3\text{-}O_3)^T$	0.0090	0.0103	—	0.4973	0.4889	0.9946
$M\cdot(O_2)_2^T$	-0.0545	—	2.0096[b]	0.4816	-0.4770	0.0404
$MO\cdot(\eta^2\text{-}O_3)^T$	0.0105	0.0083	0.9794	0.5018	0.0016	0.4984
$MO\cdot(\eta^3\text{-}O_3)^T$	-0.0201	0.0287	0.9459	0.4954	-0.0084	0.5585
$M(\eta^2\text{-}O_3)\cdot(O_2)^T$	-0.0158	0.0030	1.0038	0.4948	0.0128	0.5015
$M(\eta^3\text{-}O_3)\cdot(O_2)^T$	-0.0136	0.0004	1.0006	0.4843	0.0351	0.4932
$M\cdot(\eta^2\text{-}O_3)_2^T$	-0.0037	—	1.9430[c]	0.4799	-0.4910	0.0718
$M(\eta^3\text{-}O_3)\cdot(\eta^2\text{-}O_3)^T$	0.0076	0.0102	0.9789	0.4920	0.0014	0.5098
$M(O_2)\cdot(O_2)^T_{butterfly}$	-0.0264	-0.0057	1.0013	0.4604	0.0218	0.5486

[a] Two strongly adsorbed oxygen atoms have ASMs of 0.0097 and -0.9302; the summation is -0.9205. [b] Two weakly adsorbed peroxo groups have ASMs of 1.0048 and 1.0048; the summation is 2.0096. [c] Two weakly adsorbed ozone groups have ASMs of 0.9723 and 0.9707; the summation is 1.9430.

Table S8: Assigned spin magnetic moments (ASMs) for the DMZB triplet conformations with adsorbed Me_2Py, Me_2PyO, or EO molecule.

Species	Zr	Non-ligand Oxygens		Nitrogens		Other Atoms
		Strongly Ads.	Weakly Ads.	Ligand 1	Ligand 2	
$M(O_2)\cdot Me_2Py^T$	0.0114	0.0053	—	0.4893	0.4888	1.0053
$M(\eta^3\text{-}O_3)\cdot Me_2Py^T$	0.0124	0.0102	—	0.5025	0.4831	0.9918
$MO\cdot Me_2PyO^T$	0.0122	0.0099	-0.0004	0.4906	0.4901	0.9975
$M(O_2)\cdot Me_2PyO^T$	0.0121	0.0084	0.0000	0.4890	0.4795	1.0110
$M(\eta^3\text{-}O_3)\cdot Me_2PyO^T$	-0.0007	0.0040	0.0033	0.5059	0.4721	1.0154
$MO\cdot EO^T$	0.0183	0.0055	0.0017	0.4887	0.4837	1.0021
$M(O_2)\cdot EO^T$	0.0131	0.0116	0.0007	0.4914	0.4833	0.9999
$M(\eta^2\text{-}O_3)\cdot EO^T$	0.0054	0.0102	0.0025	0.5214	0.4894	0.9710
$M(\eta^3\text{-}O_3)\cdot EO^T$	0.0057	0.0048	0.0026	0.5208	0.4821	0.9841

Table S9: Assigned spin magnetic moments (ASMs) for the RuTDCPP triplet conformations

Species	Ru	N & O Atoms in Ads. Group	Nitrogens		Other Atoms
			Tethering Group	Porphyrin ring	
$RuTDCPP^{T}$	1.9407	—	0.1109	0.0877	-0.1393
$RuTDCPP(O)^{T}$	0.9001	1.0091	0.0037	-0.0039	0.0911
$RuTDCPP(Me_2Py)^{T}$	0.8356	0.0006	-0.0057	0.2092	0.9603
$RuTDCPP(Me_2PyO)^{T}$	0.8412	0.0520	-0.0014	0.1870	0.9211
$RuTDCPP(P)^{T}$	0.7903	—	0.0005	0.2252	0.9839
$RuTDCPP(PO)^{T}$	0.9036	-0.0050	-0.0131	0.2486	0.8659

1.5. Computed Reaction Cycles and Energy Profiles

We use notation M to represent the $Zr(O–N(Ar)–C_6H_4–N(Ar)–O)_2$ [Ar = $–C_6H_3–2,6–Me_2$] (aka DMZB) bare structure and M' to represent the $Zr(O–N(Ar')–C_6H_4–N(Ar')–O)_2$ [Ar' = $–C_6H_3–2,6–^iPr_2$] (aka DIZB) bare structure. The bisperoxo structures in this section are the spiro conformation.

ethylene epoxidation using molecular O_2 as the oxidant over the DMZB catalyst (Reaction cycle 2 is presented in Fig. S4 below. Reaction cycle 1 is presented in the main text.)

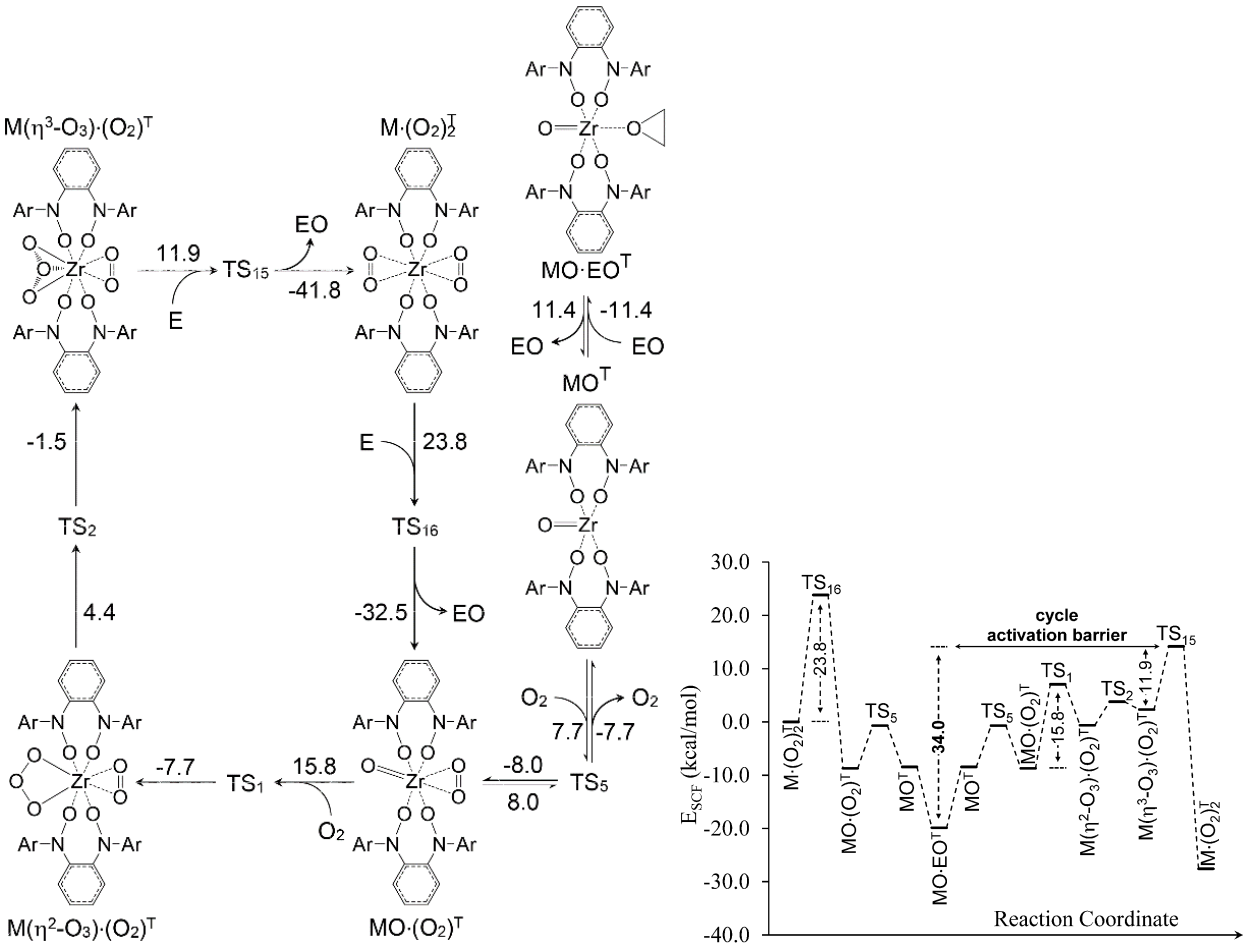

Fig. S4: (left panel) Triplet peroxo η^3-ozone intermediate ($M(\eta^3\text{-}O_3)\cdot(O_2)^T$) involved catalytic cycle for the ethylene epoxidation using the DMZB catalyst. For each step, the energies are labeled in kcal/mol. (right panel) SCF energy profile for this cycle. The triplet spiro bisperoxo form of the DMZB complex ($M\cdot(O_2)_2^T$) is the reference state. Activation barriers for major reaction steps and the whole catalytic cycle are presented in kcal/mol.

2,6-dimethylpyridine oxidation using molecular O_2 as the oxidant over the DIZB catalyst (reaction cycle 1)

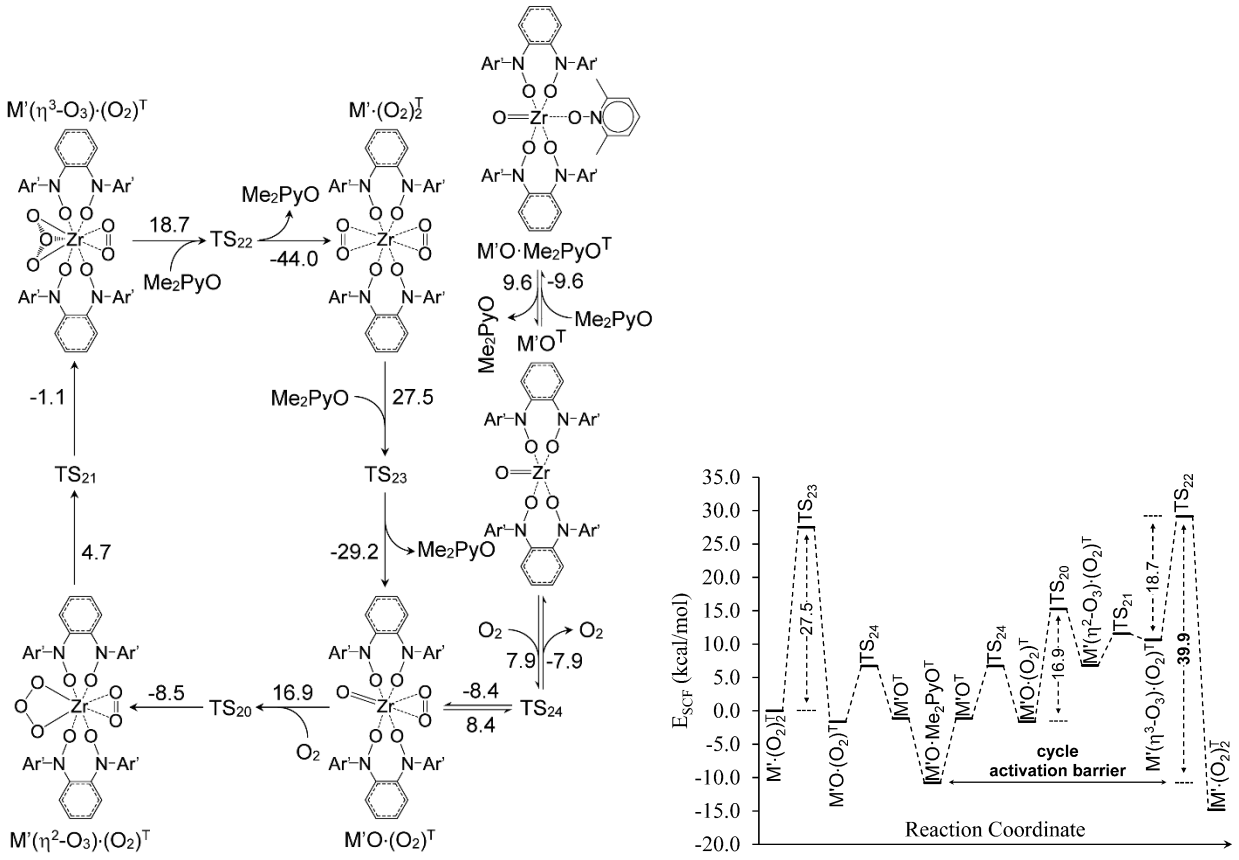

Fig. S5: (left panel) Triplet peroxo η^3-ozone intermediate ($M'(\eta^3\text{-}O_3)\cdot(O_2)^T$) involved catalytic cycle for the 2,6-dimethylpyridine oxidation using the DIZB catalyst. For each step, the energies are labeled in kcal/mol. (right panel) SCF energy profile for this cycle. The triplet spiro bisperoxo form of the DIZB complex ($M'\cdot(O_2)_2^T$) is the reference state. Activation barriers for major reaction steps and the whole catalytic cycle are presented in kcal/mol.

2,6-dimethylpyridine oxidation using molecular O_2 as the oxidant over the DIZB catalyst (reaction cycle 2)

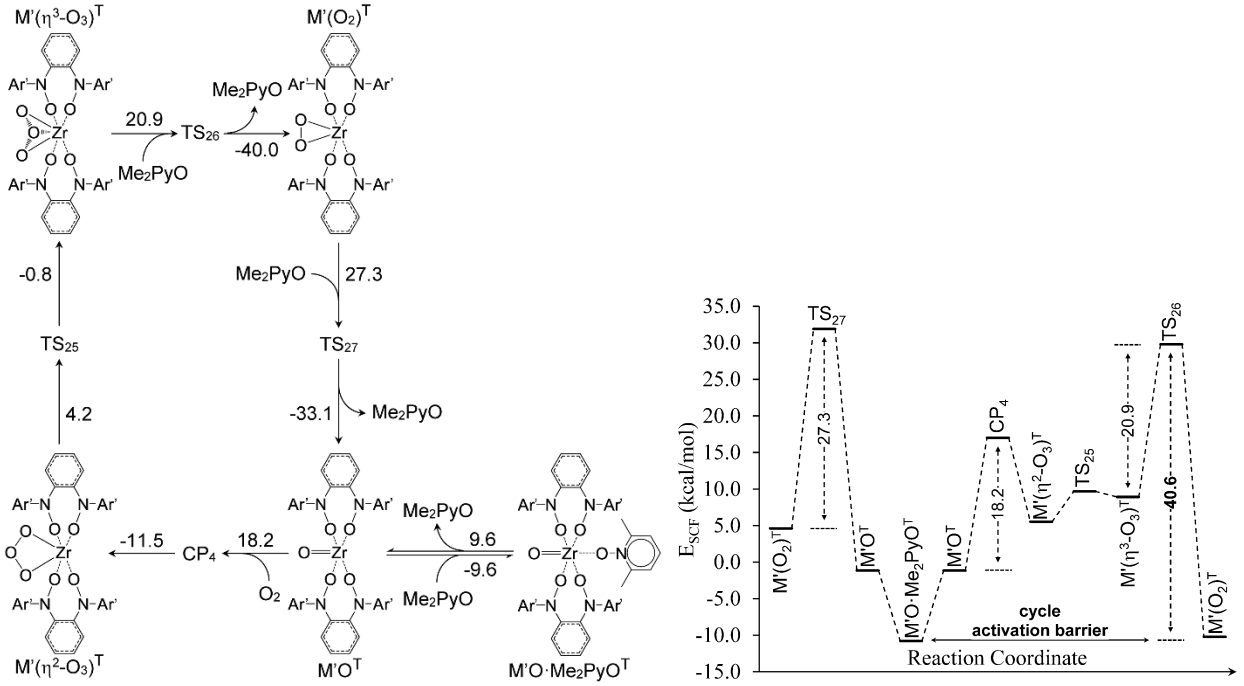

Fig. S6: (left panel) Triplet η^3-ozone intermediate (M'(η^3-O_3)^T) involved catalytic cycle for the 2,6-dimethylpyridine oxidation using the DIZB catalyst. For each step, the energies are labeled in kcal/mol. (right panel) SCF energy profile for this cycle. The triplet spiro bisperoxo form of the DIZB complex (M'·$(O_2)_2^T$) is the reference state. Activation barriers for major reaction steps and the whole catalytic cycle are presented in kcal/mol.

2,6-dichrolopyridine oxidation using molecular O_2 as the oxidant over the DIZB catalyst (reaction cycle 1)

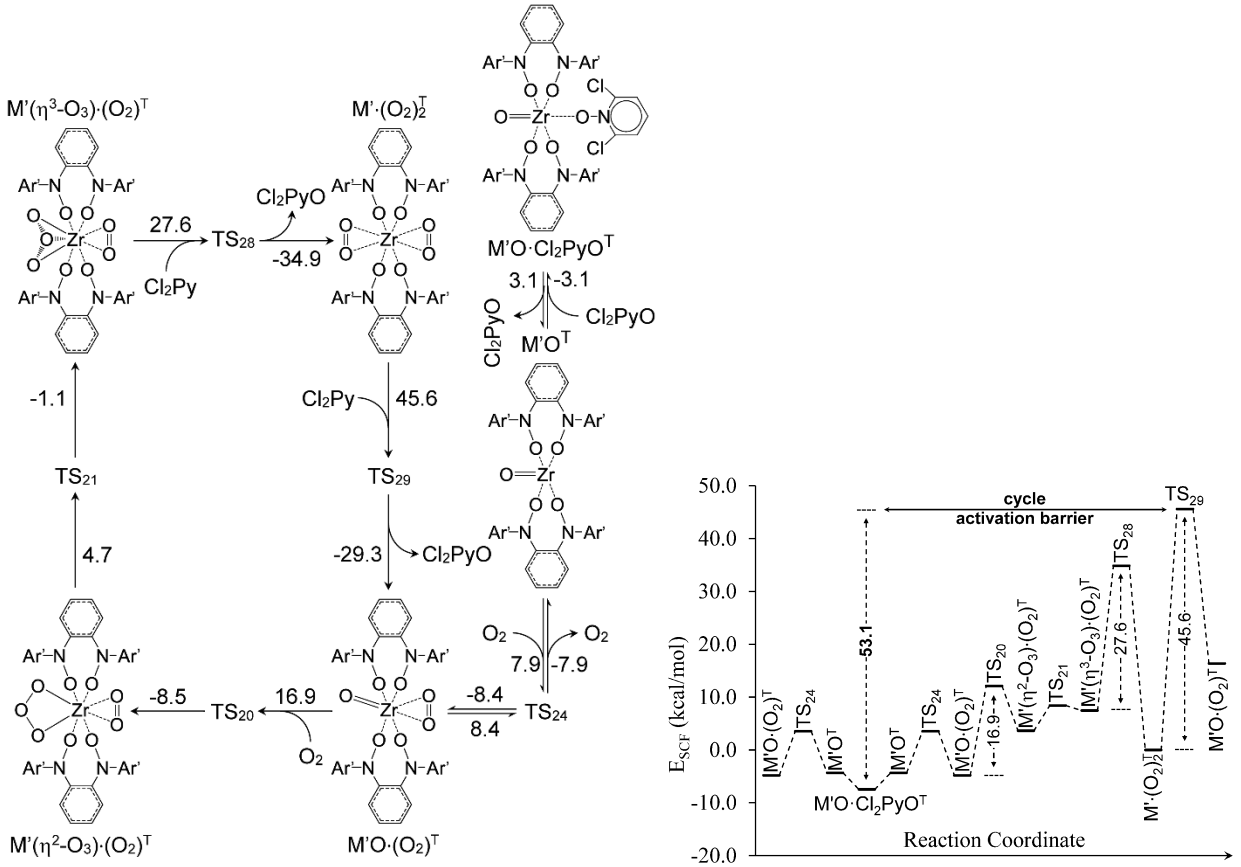

Fig. S7: (left panel) Triplet peroxo η^3-ozone intermediate ($M'(\eta^3\text{-}O_3)\cdot(O_2)^T$) involved catalytic cycle for the 2,6-dichloropyridine oxidation using the DIZB catalyst. For each step, the energies are labeled in kcal/mol. (right panel) SCF energy profile for this cycle. The triplet spiro bisperoxo form of the DIZB complex ($M'\cdot(O_2)_2^T$) is the reference state. Activation barriers for major reaction steps and the whole catalytic cycle are presented in kcal/mol.

2,6-dichrolopyridine oxidation using molecular O_2 as the oxidant over the DIZB catalyst (reaction cycle 2)

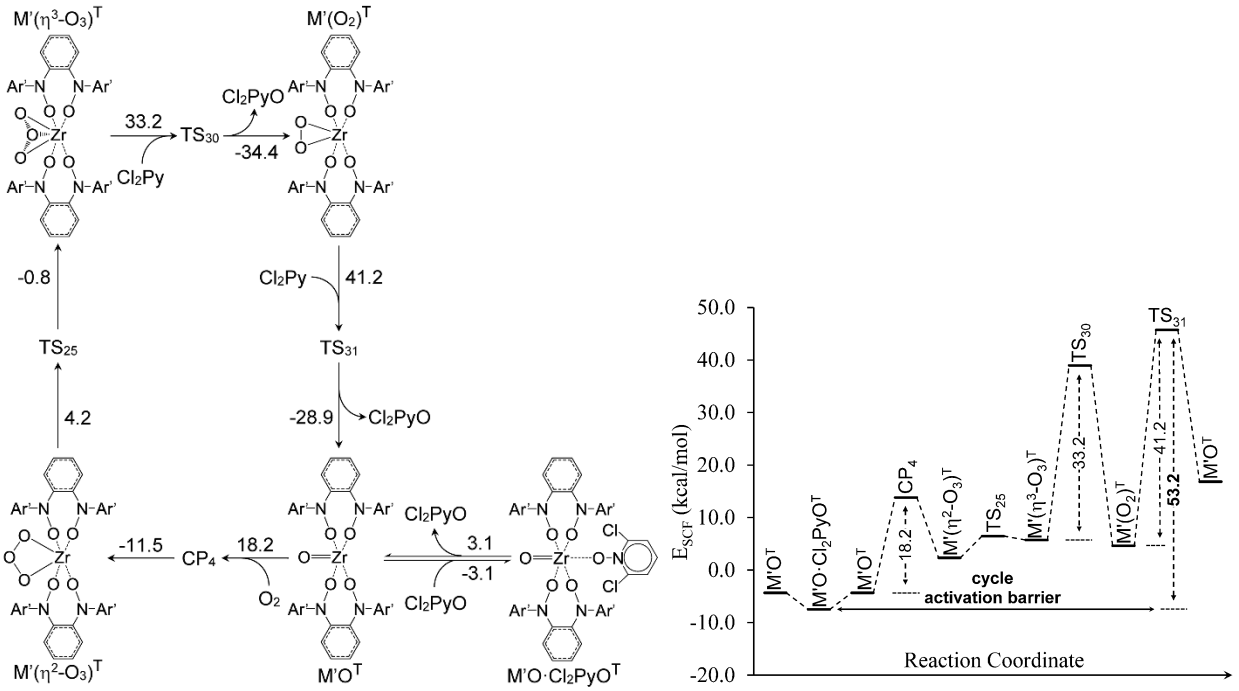

Fig. S8: (left panel) Triplet η^3-ozone intermediate ($M'(\eta^3\text{-}O_3)^T$) involved catalytic cycle for the 2,6-dichloropyridine oxidation using the DIZB catalyst. For each step, the energies are labeled in kcal/mol. (right panel) SCF energy profile for this cycle. The triplet spiro bisperoxo form of the DIZB complex ($M'\cdot(O_2)_2^T$) is the reference state. Activation barriers for major reaction steps and the whole catalytic cycle are presented in kcal/mol.

pyridine oxidation using molecular O_2 as the oxidant over the DIZB catalyst (reaction cycle 1)

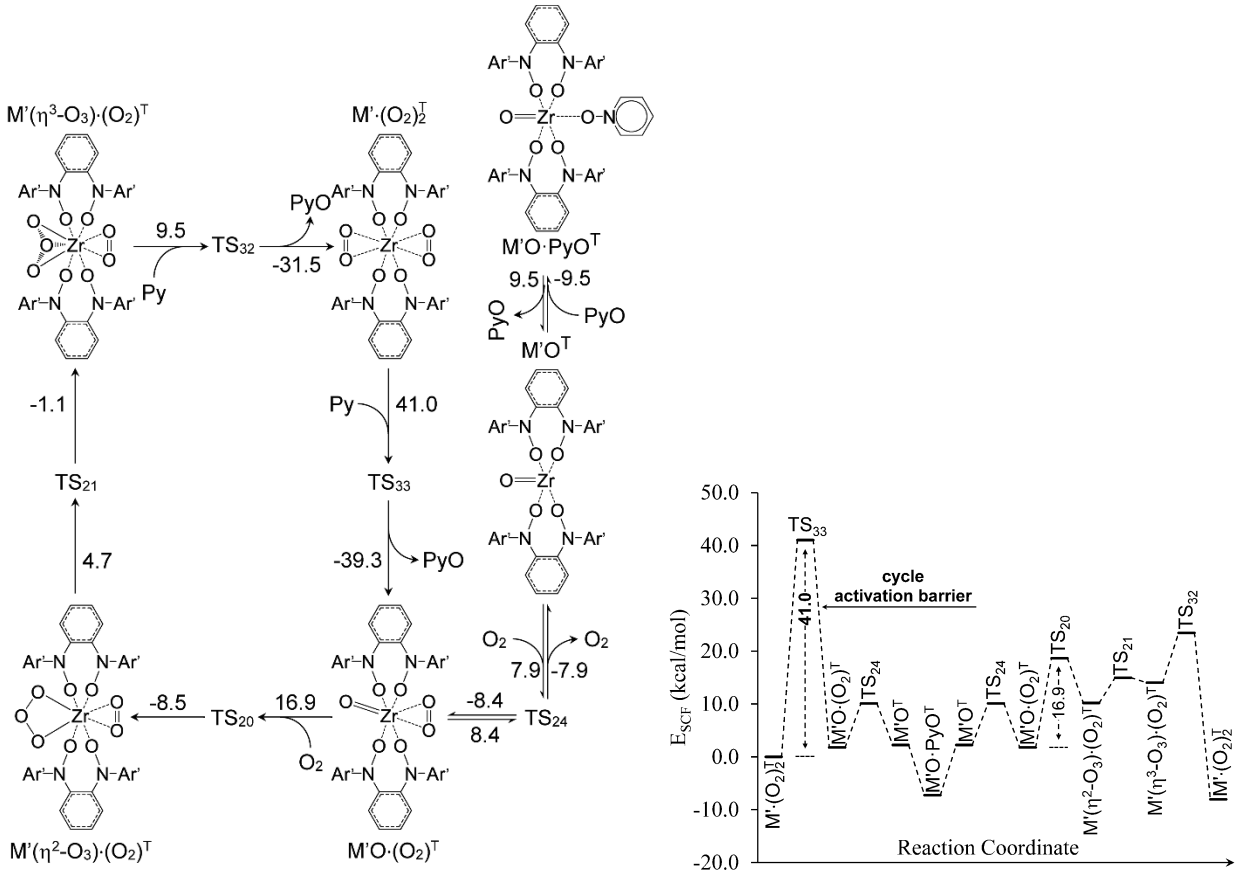

Fig. S9: (left panel) Triplet peroxo η^3-ozone intermediate ($M'(\eta^3\text{-}O_3)\cdot(O_2)^T$) involved catalytic cycle for the pyridine oxidation using the DIZB catalyst. For each step, the energies are labeled in kcal/mol. (right panel) SCF energy profile for this cycle. The triplet spiro bisperoxo form of the DIZB complex ($M'\cdot(O_2)_2^T$) is the reference state. Activation barriers for major reaction steps and the whole catalytic cycle are presented in kcal/mol.

pyridine oxidation using molecular O_2 as the oxidant over the DIZB catalyst (reaction cycle 2)

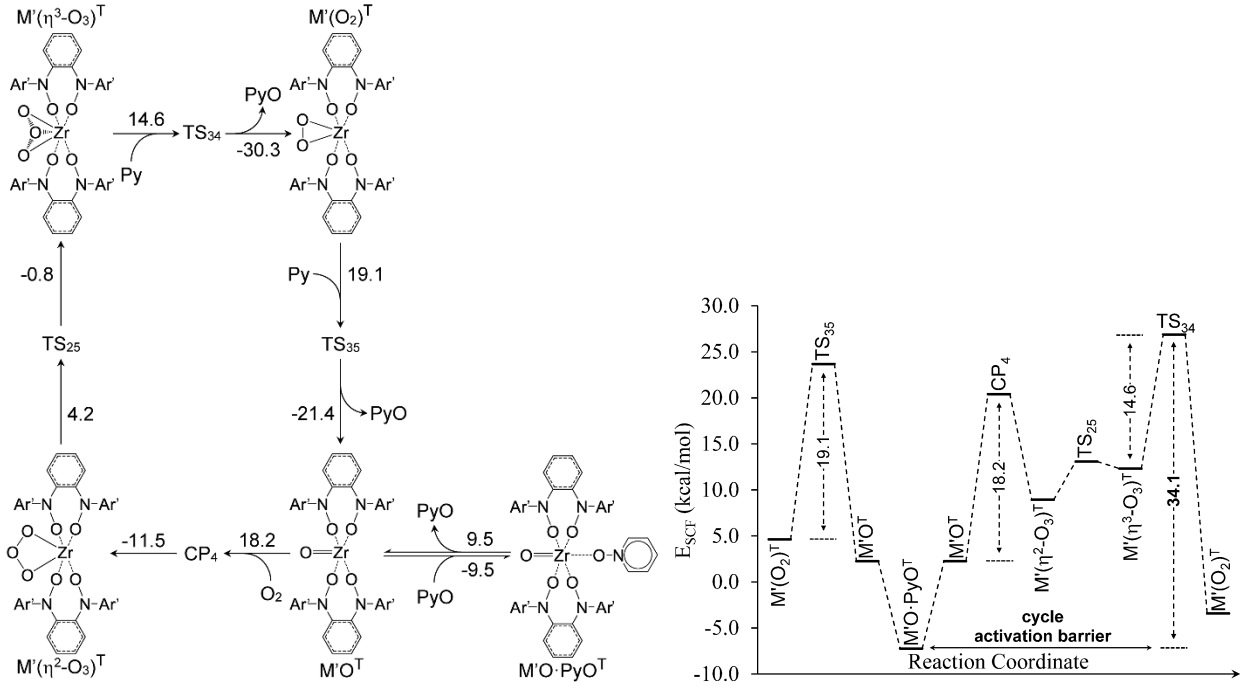

Fig. S10: (left panel) Triplet η^3-ozone intermediate (M'(η^3-O_3)^T) involved catalytic cycle for the pyridine oxidation using the DIZB catalyst. For each step, the energies are labeled in kcal/mol. (right panel) SCF energy profile for this cycle. The triplet spiro bisperoxo form of the DIZB complex (M'·$(O_2)_2^T$) is the reference state. Activation barriers for major reaction steps and the whole catalytic cycle are presented in kcal/mol.

4-nitroquinoline oxidation using molecular O_2 as the oxidant over the DIZB catalyst (reaction cycle 1)

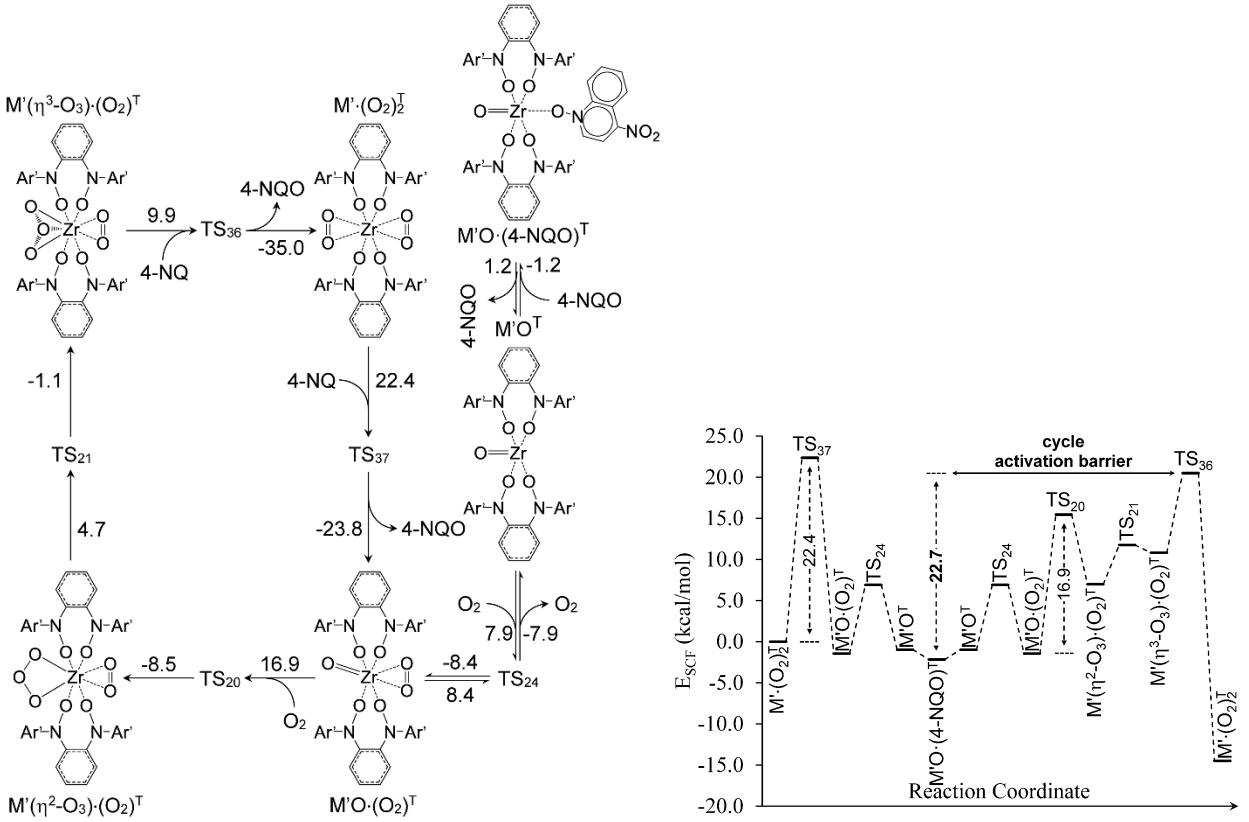

Fig. S11: (left panel) Triplet peroxo η^3-ozone intermediate (M'(η^3-O_3)·$(O_2)^T$) involved catalytic cycle for the 4-nitroquinoline oxidation using the DIZB catalyst. For each step, the energies are labeled in kcal/mol. (right panel) SCF energy profile for this cycle. The triplet spiro bisperoxo form of the DIZB complex (M'·$(O_2)^T_2$) is the reference state. Activation barriers for major reaction steps and the whole catalytic cycle are presented in kcal/mol.

4-nitroquinoline oxidation using molecular O_2 as the oxidant over the DIZB catalyst (reaction cycle 2)

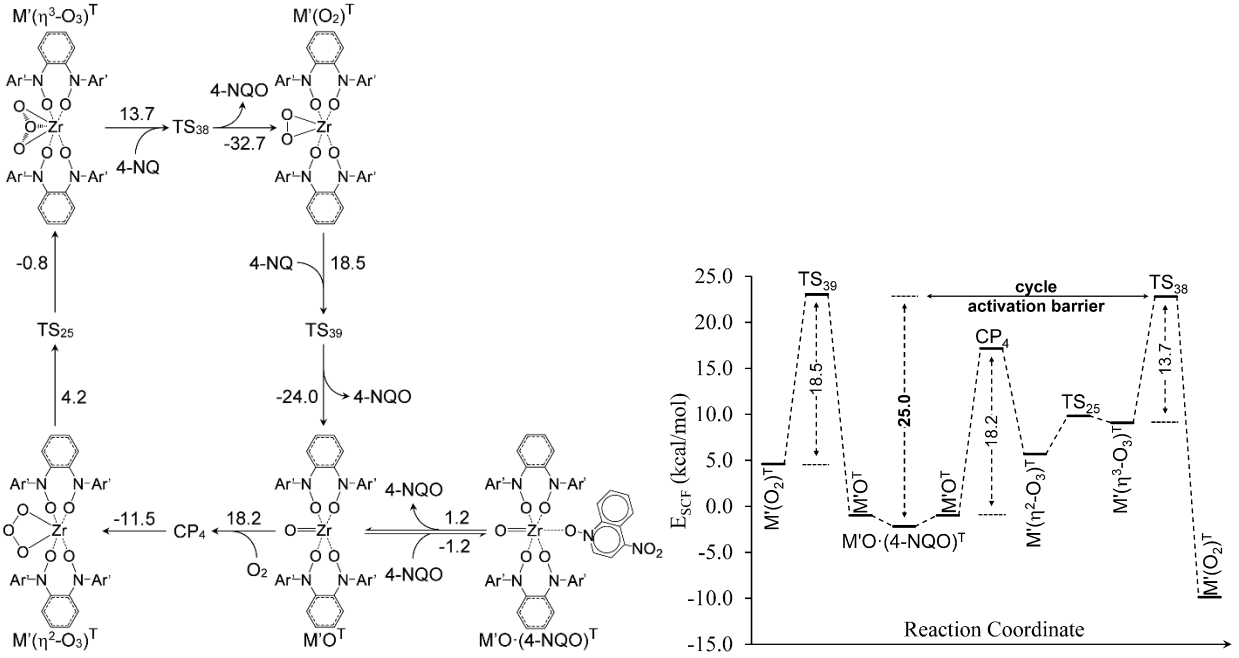

Fig. S12: (left panel) Triplet η^3-ozone intermediate (M'(η^3-O_3)^T) involved catalytic cycle for the 4-nitroquinoline oxidation using the DIZB catalyst. For each step, the energies are labeled in kcal/mol. (right panel) SCF energy profile for this cycle. The triplet spiro bisperoxo form of the DIZB complex (M'·$(O_2)_2^T$) is the reference state. Activation barriers for major reaction steps and the whole catalytic cycle are presented in kcal/mol.

2-chloropyridine oxidation using molecular O_2 as the oxidant over the DIZB catalyst (reaction cycle 1)

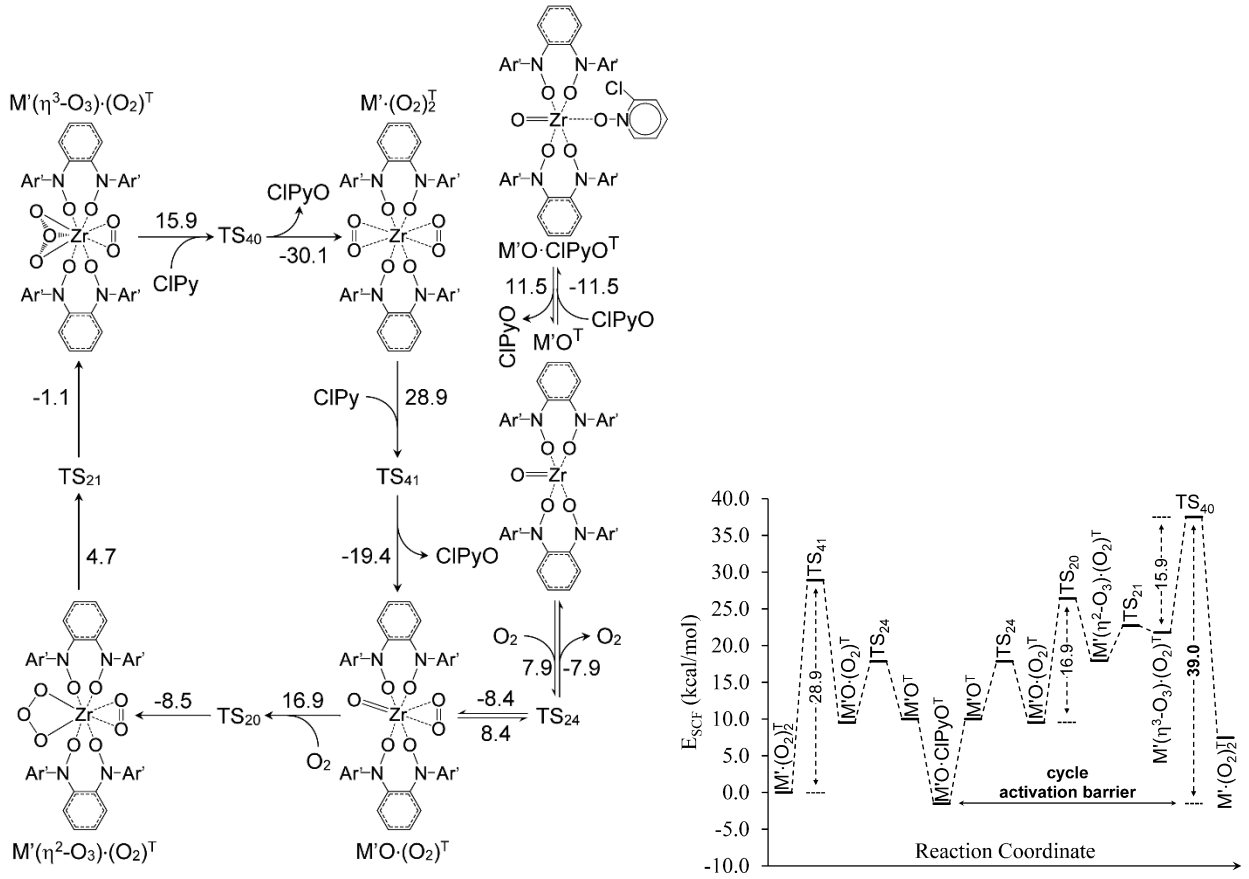

Fig. S13: (left panel) Triplet peroxo η^3-ozone intermediate (M'(η^3-O_3)·$(O_2)^T$) involved catalytic cycle for the 2-chloropyridine oxidation using the DIZB catalyst. For each step, the energies are labeled in kcal/mol. (right panel) SCF energy profile for this cycle. The triplet spiro bisperoxo form of the DIZB complex (M'·$(O_2)_2^T$) is the reference state. Activation barriers for major reaction steps and the whole catalytic cycle are presented in kcal/mol.

2-chloropyridine oxidation using molecular O_2 as the oxidant over the DIZB catalyst (reaction cycle 2)

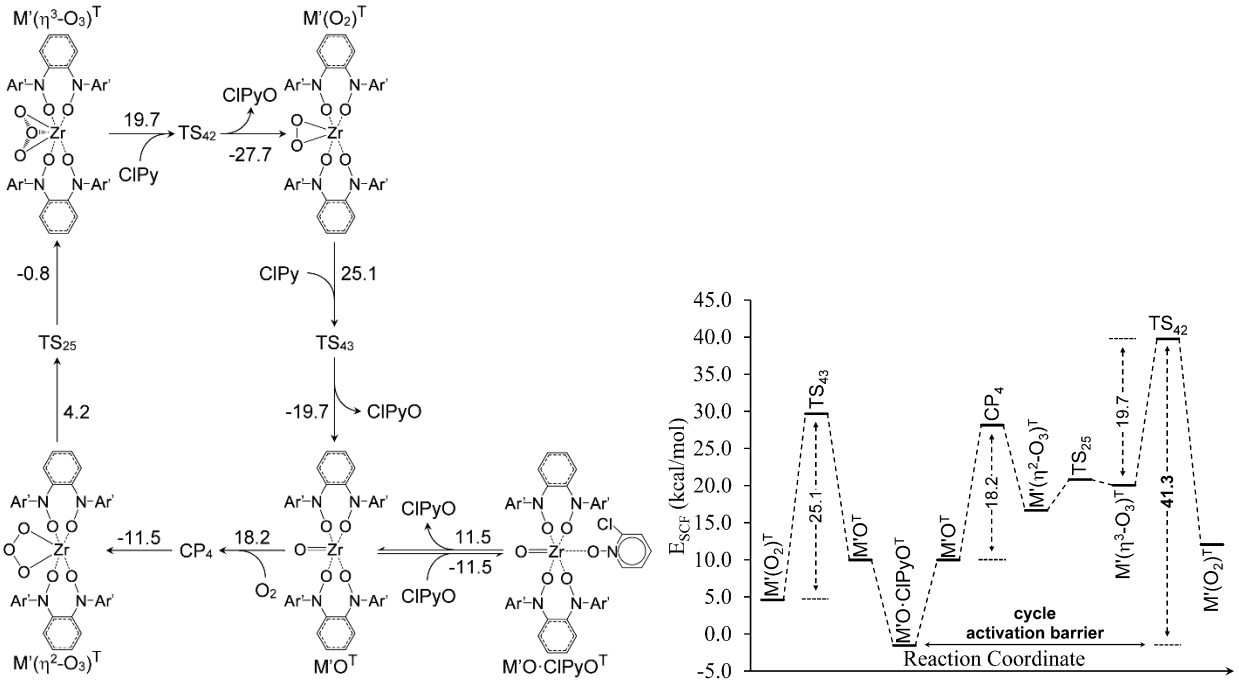

Fig. S14: (left panel) Triplet η^3-ozone intermediate (M'(η^3-O_3)^T) involved catalytic cycle for the 2-chloropyridine oxidation using the DIZB catalyst. For each step, the energies are labeled in kcal/mol. (right panel) SCF energy profile for this cycle. The triplet spiro bisperoxo form of the DIZB complex (M'·$(O_2)_2^T$) is the reference state. Activation barriers for major reaction steps and the whole catalytic cycle are presented in kcal/mol.

2. DFT-Optimized Geometries

2.1 DMZB Catalytic System (B3LYP/LANL2DZ)

2.1.1 Singlet Ground States

bare complex

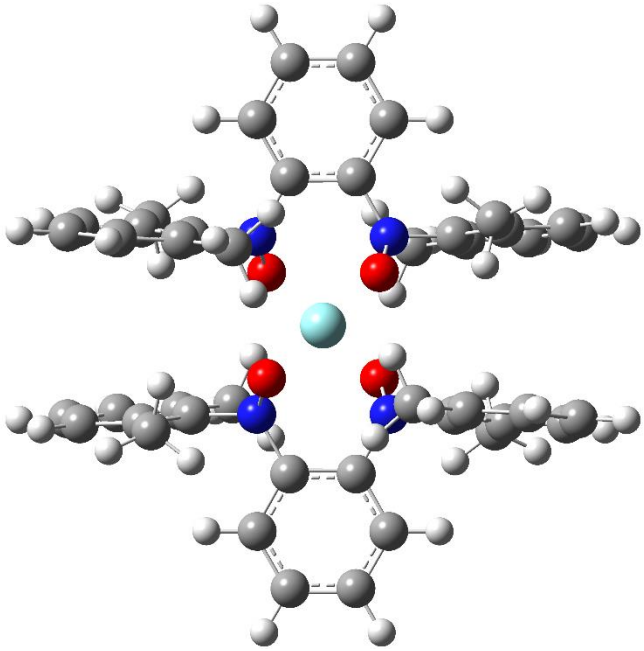

Fig. S15: bare complex

E_{SCF}	E_{ZP}	H	G
-2269.428306	-2268.639497	-2268.589492	-2268.719878

oxo complex

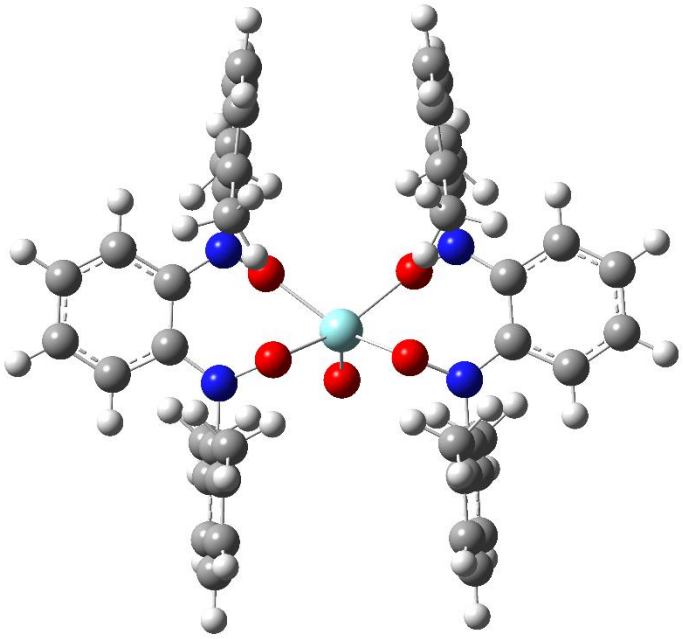

Fig. S16: oxo complex

E_{SCF}	E_{ZP}	H	G
-2344.587395	-2343.798097	-2343.745654	-2343.885215

dioxo complex

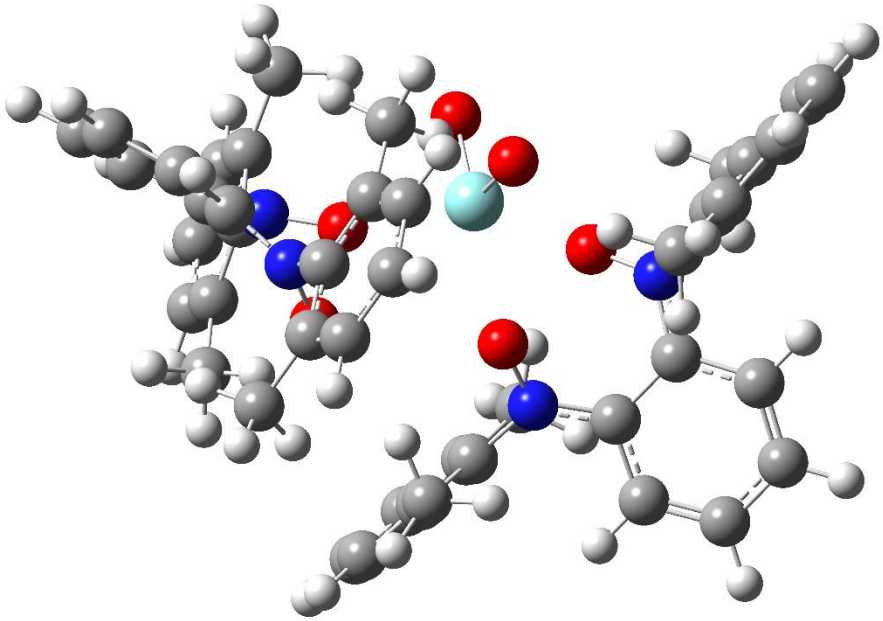

Fig. S17: dioxo complex

E_{SCF}	E_{ZP}	H	G
-2419.722737	-2418.929009	-2418.874659	-2419.019705

peroxo complex

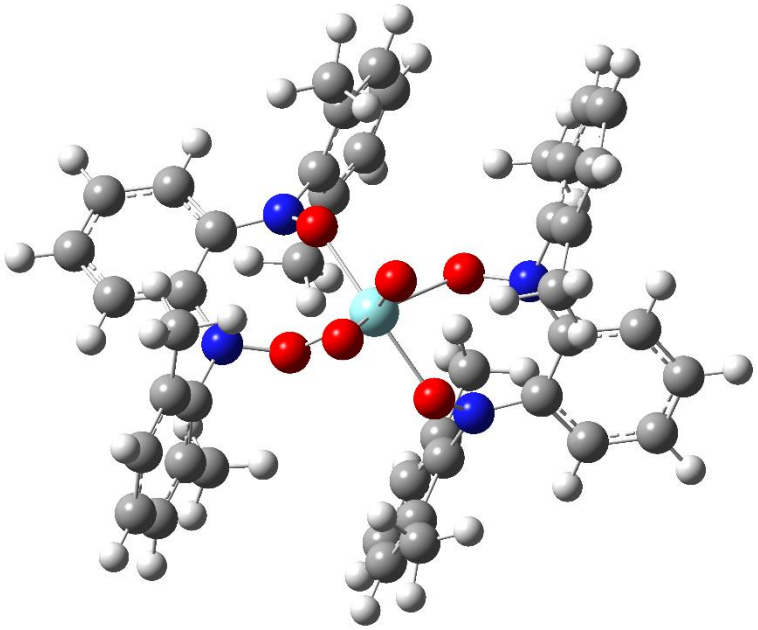

Fig. S18: peroxo complex

E_{SCF}	E_{ZP}	H	G
-2419.744884	-2418.952246	-2418.898069	-2419.041470

oxo peroxo complex

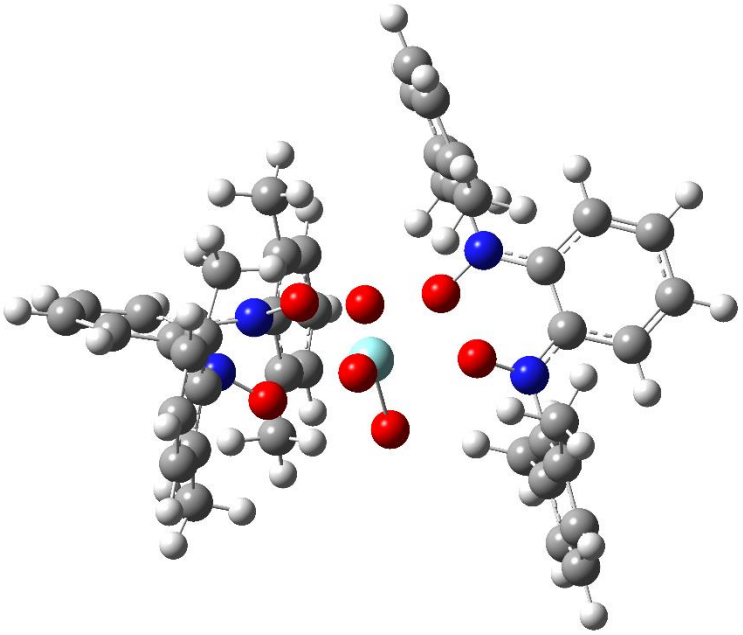

Fig. S19: oxo peroxo complex

E_{SCF}	E_{ZP}	H	G
-2494.892149	-2494.096344	-2494.040590	-2494.187293

η^2-ozone complex

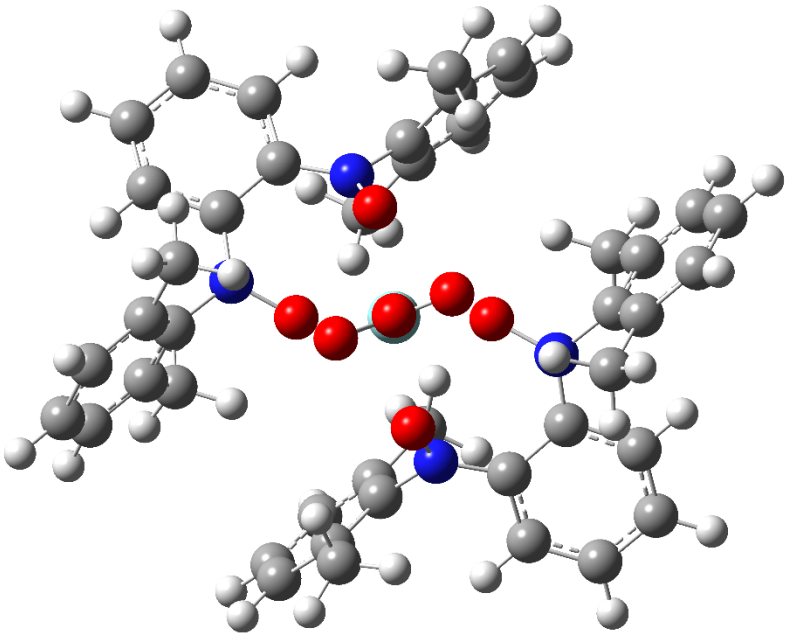

Fig. S20: η^2-ozone complex

E_{SCF}	E_{ZP}	H	G
-2494.893052	-2494.097156	-2494.041891	-2494.187483

η^3-ozone complex

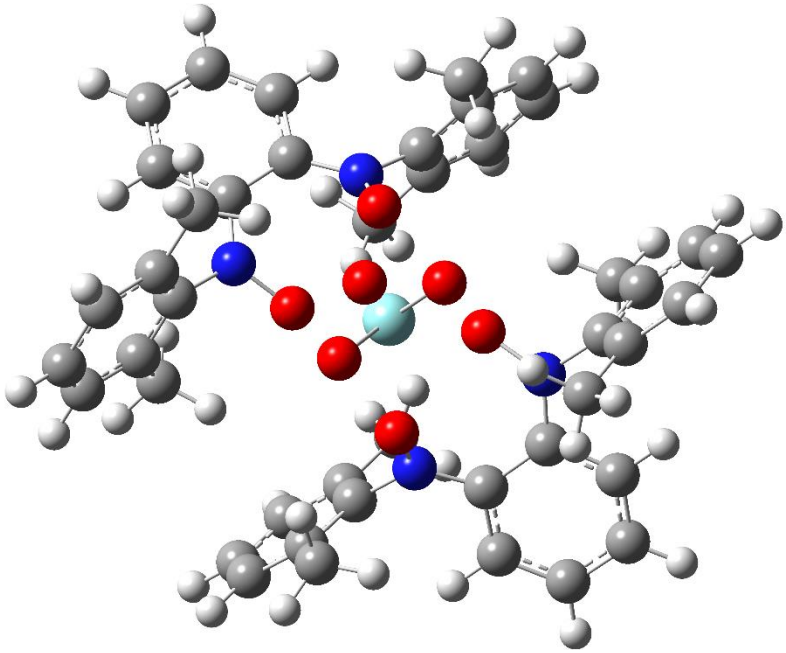

Fig. S21: η^3-ozone complex

E_{SCF}	E_{ZP}	H	G
-2494.886148	-2494.090695	-2494.035258	-2494.181677

spiro bisperoxo complex

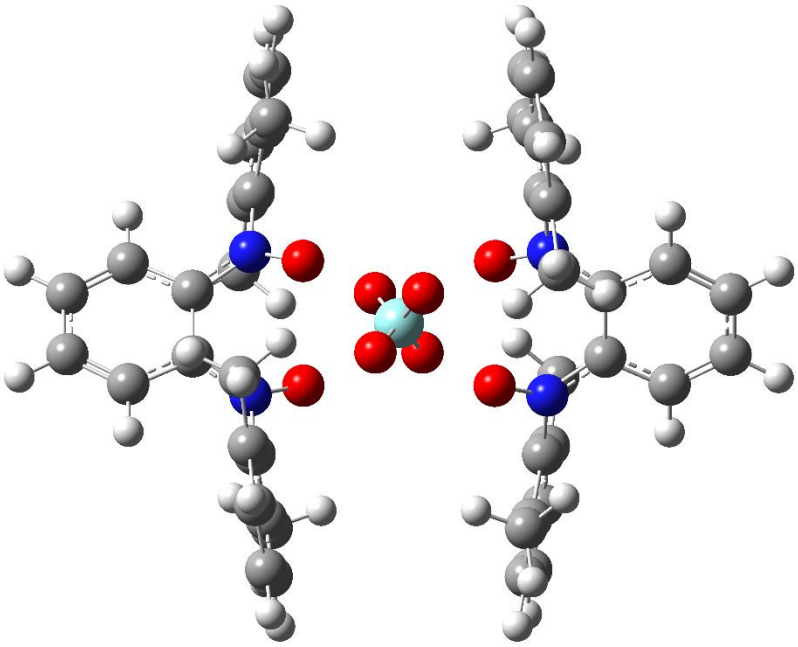

Fig. S22: spiro bisperoxo complex

E_{SCF}	E_{ZP}	H	G
-2570.046698	-2569.248030	-2569.191491	-2569.340038

oxo η^2-ozone complex

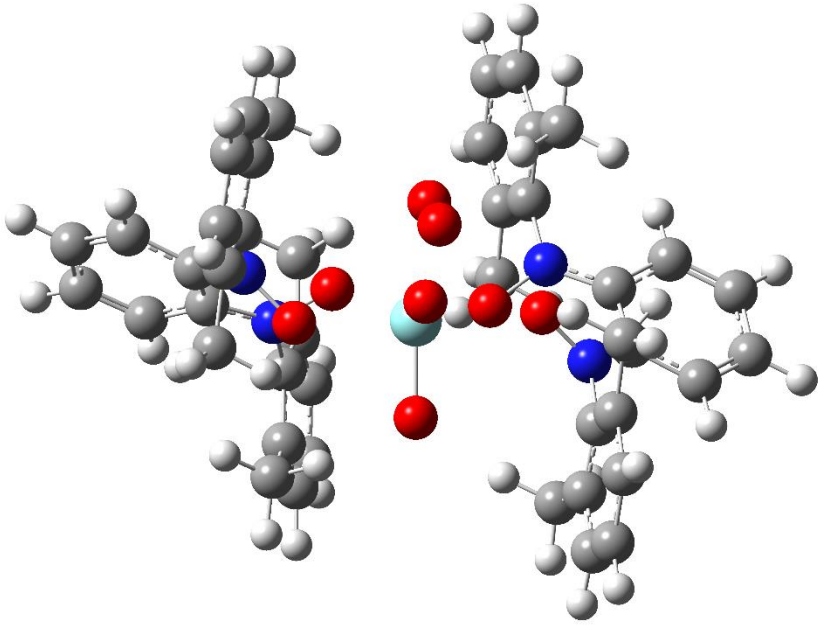

Fig. S23: oxo η^2-ozone complex

E_{SCF}	E_{ZP}	H	G
-2570.050098	-2569.251105	-2569.194075	-2569.344777

peroxo η^2-ozone complex

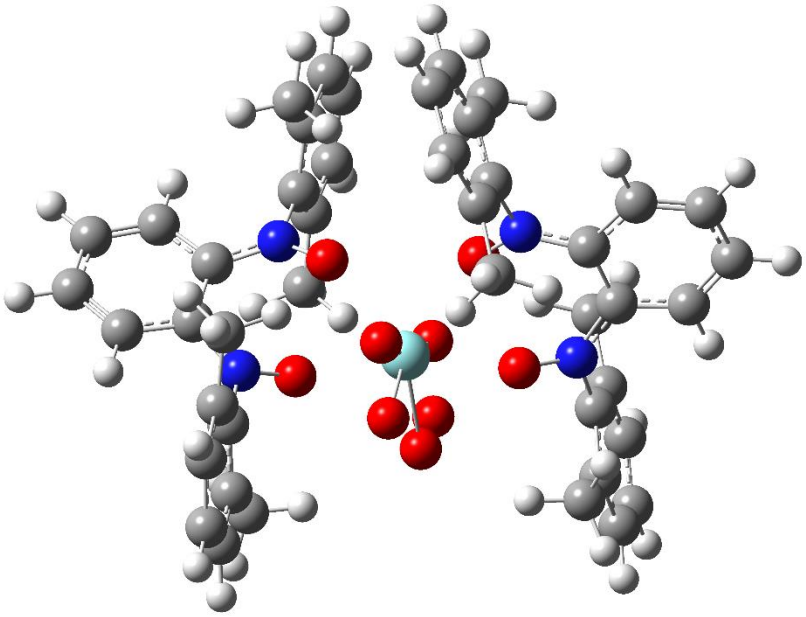

Fig. S24: peroxo η^2-ozone complex

E_{SCF}	E_{ZP}	H	G
-2645.210754	-2644.408219	-2644.350476	-2644.501189

peroxo η^3-ozone complex

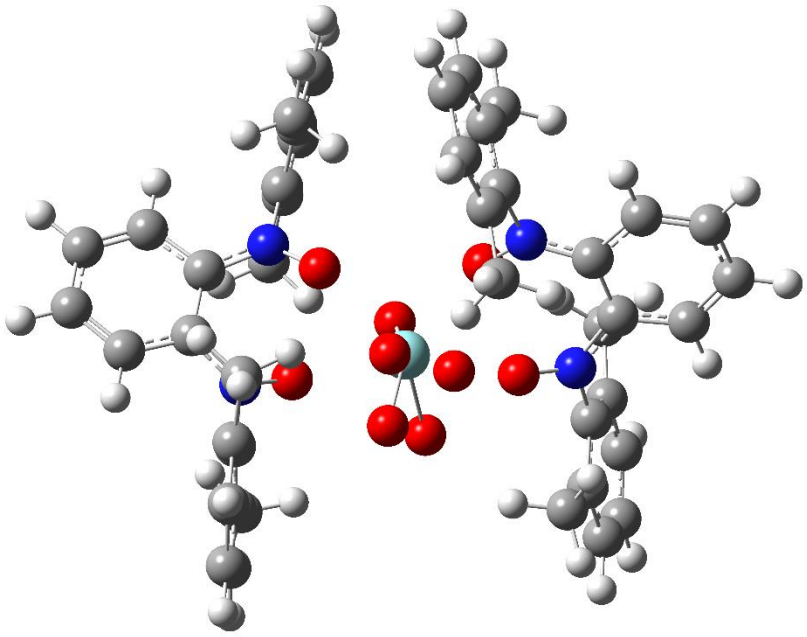

Fig. S25: peroxo η^3-ozone complex

E_{SCF}	E_{ZP}	H	G
-2645.202113	-2644.399109	-2644.341748	-2644.490827

bis-η^2-ozone complex

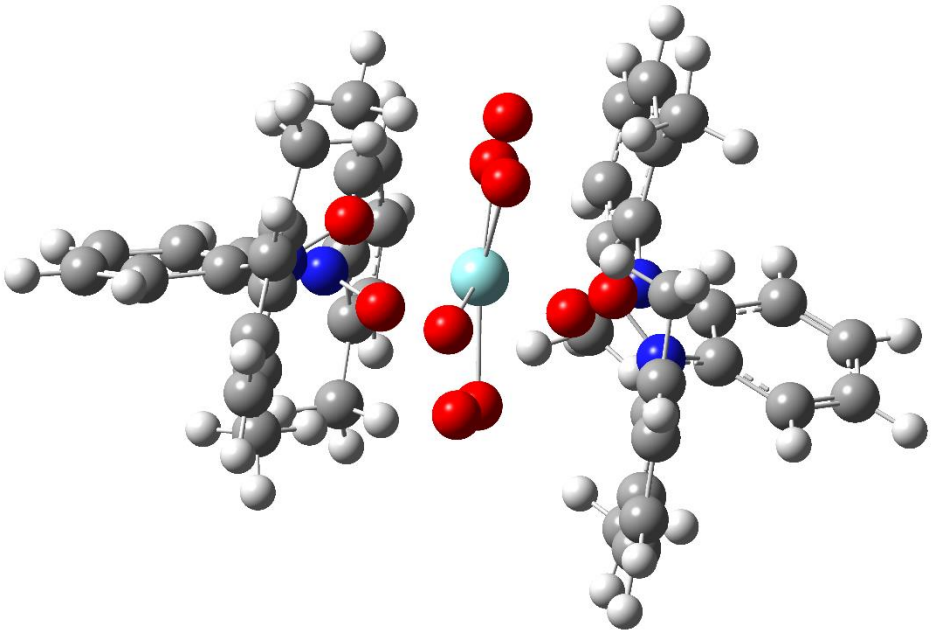

Fig. S26: bis-η^2-ozone complex

E_{SCF}	E_{ZP}	H	G
-2720.355084	-2719.549135	-2719.490268	-2719.644067

η^2-ozone η^3-ozone complex

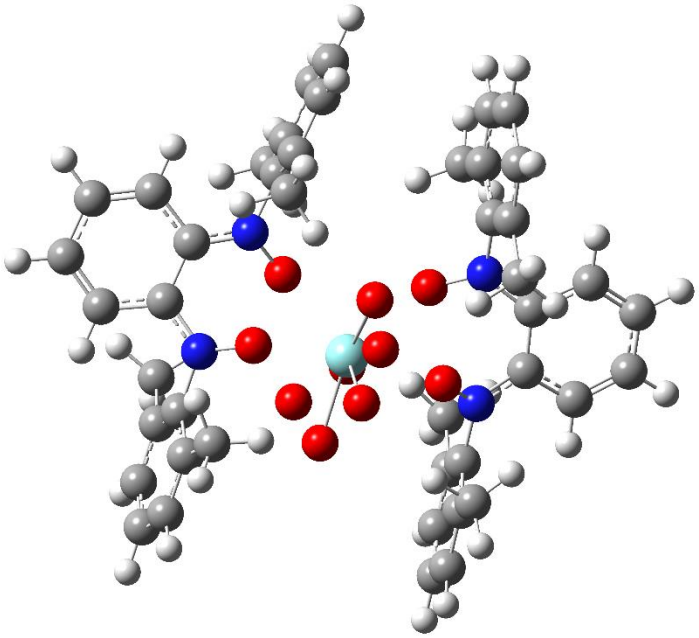

Fig. S27: η^2-ozone η^3-ozone complex

E_{SCF}	E_{ZP}	H	G
-2720.350002	-2719.544047	-2719.485430	-2719.637132

oxo complex with adsorbed 2,6-dimethylpyridine molecule

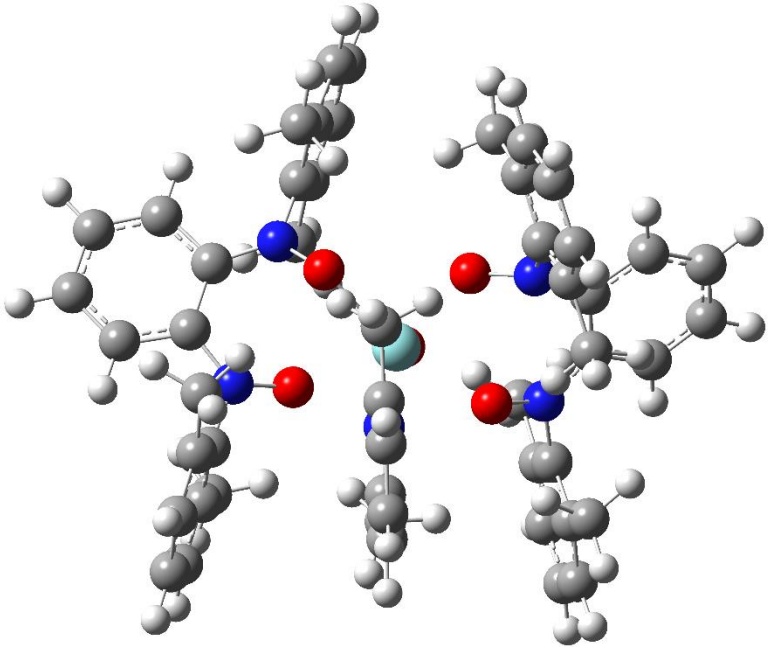

Fig. S28: oxo complex with adsorbed 2,6-dimethylpyridine molecule

E_{SCF}	E_{ZP}	H	G
-2671.460050	-2670.523491	-2670.461463	-2670.621939

peroxo complex with adsorbed 2,6-dimethylpyridine molecule

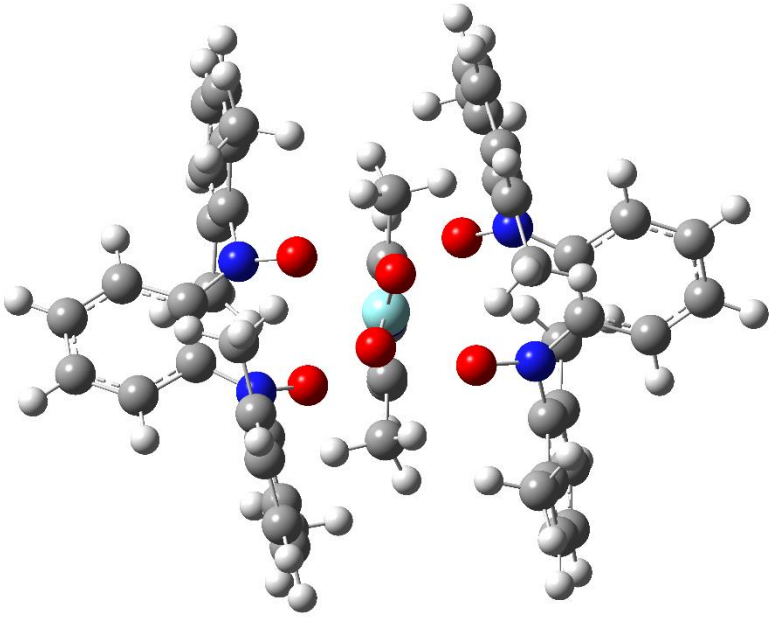

Fig. S29: peroxo complex with adsorbed 2,6-dimethylpyridine molecule

E_{SCF}	E_{ZP}	H	G
-2746.605077	-2745.664790	-2745.602214	-2745.761662

η^2-ozone complex with adsorbed 2,6-dimethylpyridine molecule

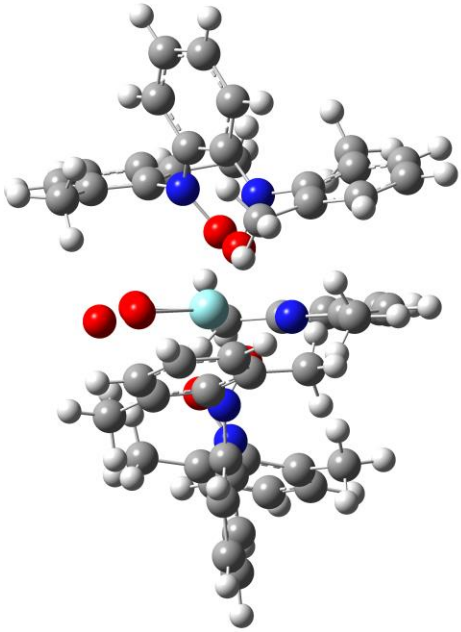

Fig. S30: η^2-ozone complex with adsorbed 2,6-dimethylpyridine molecule

E_{SCF}	E_{ZP}	H	G
-2821.750903	-2820.808148	-2820.744783	-2820.906280

η^3-ozone complex with adsorbed 2,6-dimethylpyridine molecule

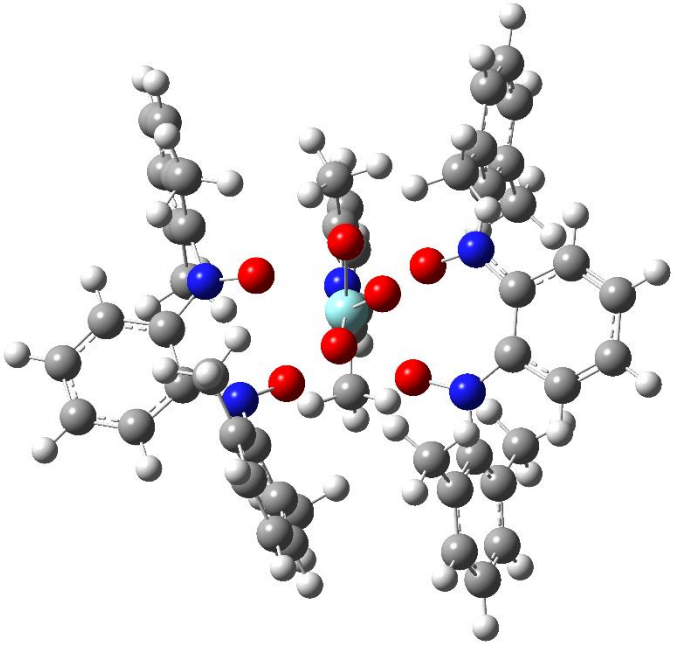

Fig. S31: η^3-ozone complex with adsorbed 2,6-dimethylpyridine molecule

E_{SCF}	E_{ZP}	H	G
-2821.736803	-2820.794579	-2820.730422	-2820.893729

oxo complex with adsorbed 2,6-dimethylpyridine *N*-oxide molecule

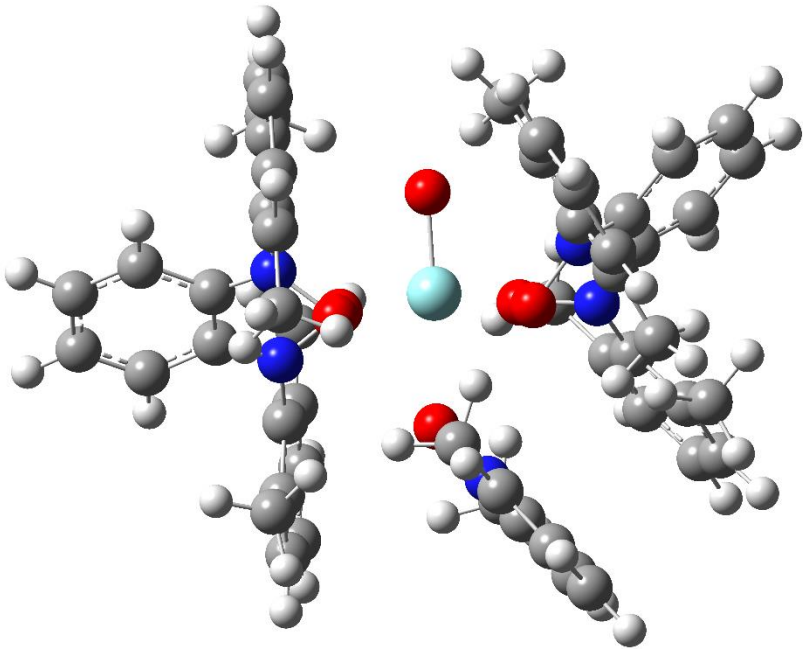

Fig. S32: oxo complex with adsorbed 2,6-dimethylpyridine *N*-oxide molecule

E_{SCF}	E_{ZP}	H	G
-2746.639238	-2745.698586	-2745.635989	-2745.797669

peroxo complex with adsorbed 2,6-dimethylpyridine *N*-oxide molecule

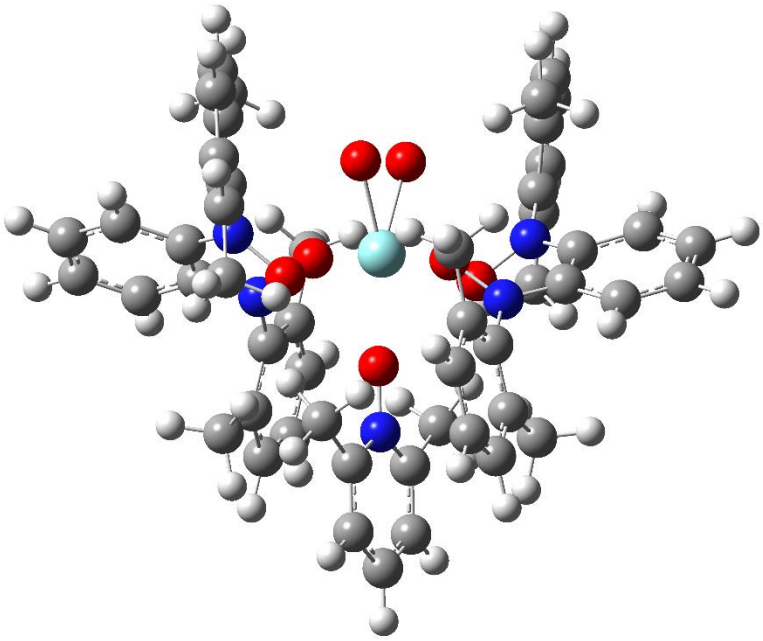

Fig. S33: peroxo complex with adsorbed 2,6-dimethylpyridine *N*-oxide molecule

E_{SCF}	E_{ZP}	H	G
-2821.793190	-2820.849172	-2820.785749	-2820.948143

η^2-ozone complex with adsorbed 2,6-dimethylpyridine *N*-oxide molecule

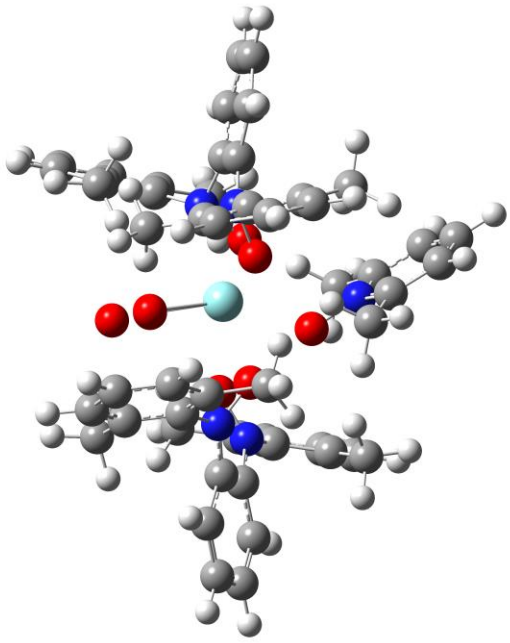

Fig. S34: η^2-ozone complex with adsorbed 2,6-dimethylpyridine *N*-oxide molecule

E_{SCF}	E_{ZP}	H	G
-2896.937596	-2895.989102	-2895.925161	-2896.086626

η^3-ozone complex with adsorbed 2,6-dimethylpyridine *N*-oxide molecule

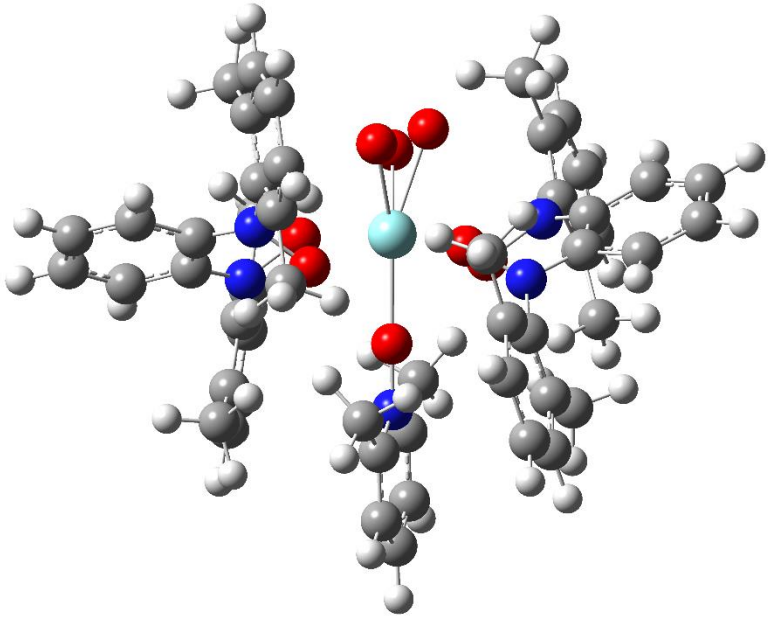

Fig. S35: η^3-ozone complex with adsorbed 2,6-dimethylpyridine *N*-oxide molecule

E_{SCF}	E_{ZP}	H	G
-2896.925843	-2895.979006	-2895.915313	-2896.076563

oxo complex with adsorbed ethylene oxide molecule

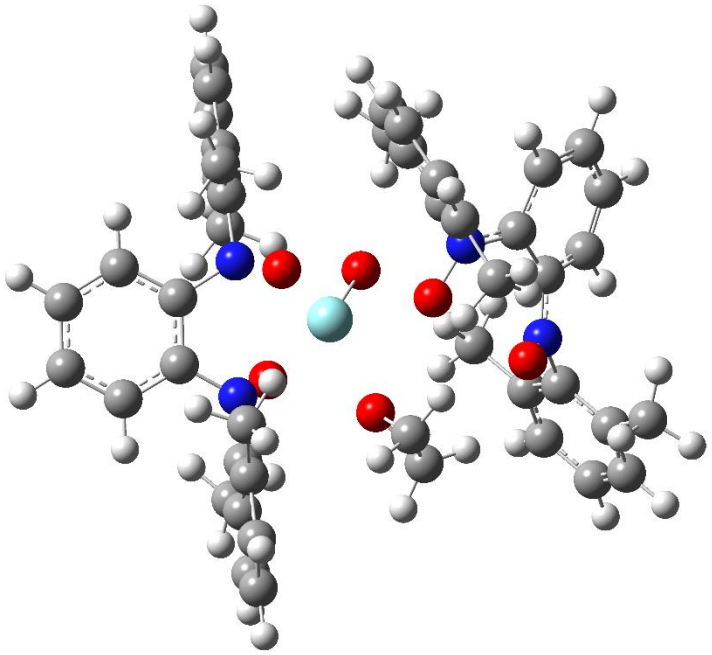

Fig. S36: oxo complex with adsorbed ethylene oxide molecule

E_{SCF}	E_{ZP}	H	G
-2498.344972	-2497.494453	-2497.437695	-2497.585797

peroxo complex with adsorbed ethylene oxide molecule

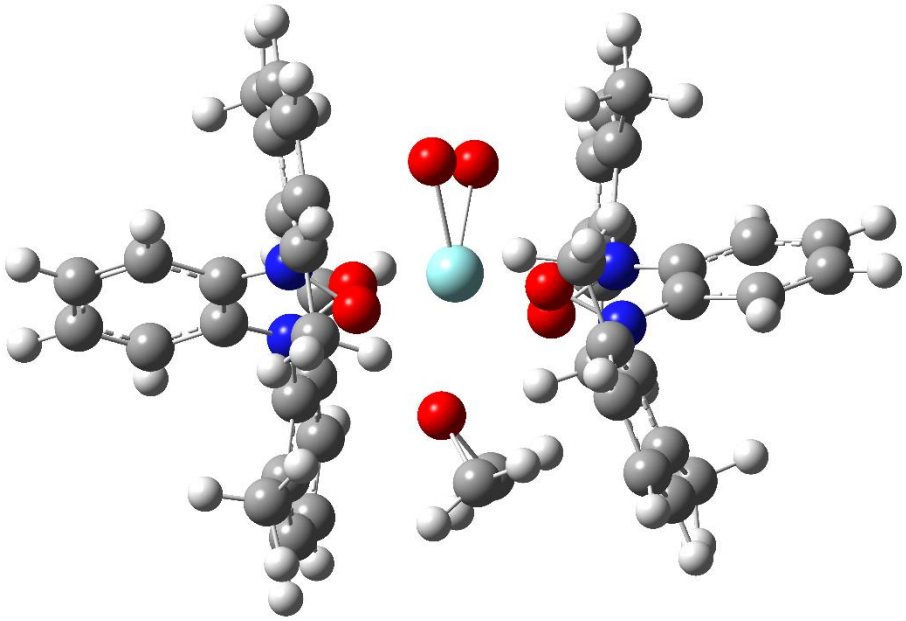

Fig. S37: peroxo complex with adsorbed ethylene oxide molecule

E_{SCF}	E_{ZP}	H	G
-2573.510489	-2572.657821	-2572.599858	-2572.750577

η^2-ozone complex with adsorbed ethylene oxide molecule

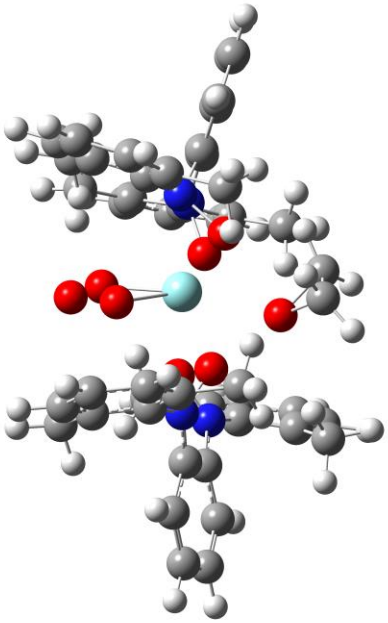

Fig. S38: η^2-ozone complex with adsorbed ethylene oxide molecule

E_{SCF}	E_{ZP}	H	G
-2648.657832	-2647.801521	-2647.742607	-2647.894730

η^3-ozone complex with adsorbed ethylene oxide molecule

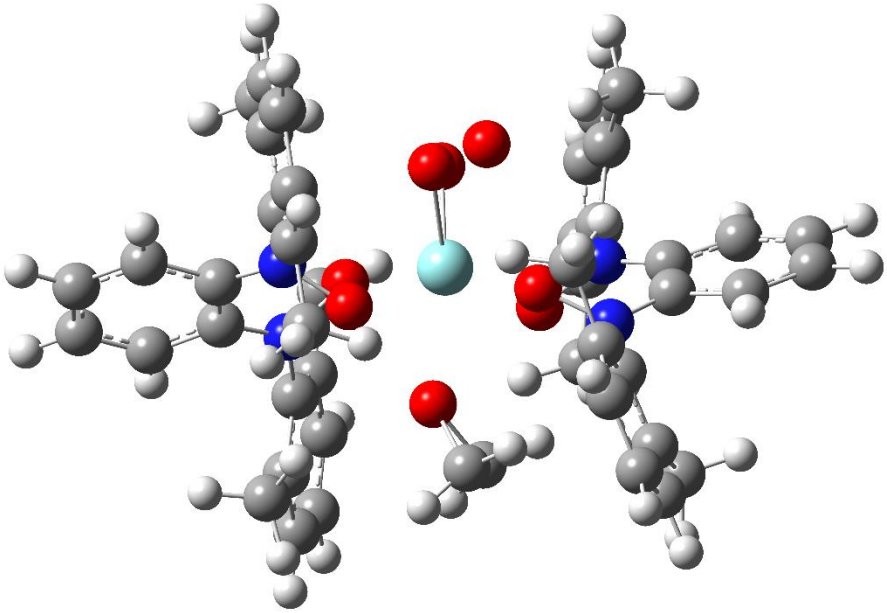

Fig. S39: η^3-ozone complex with adsorbed ethylene oxide molecule

E_{SCF}	E_{ZP}	H	G
-2648.647354	-2647.791685	-2647.732730	-2647.884592

butterfly bisperoxo complex

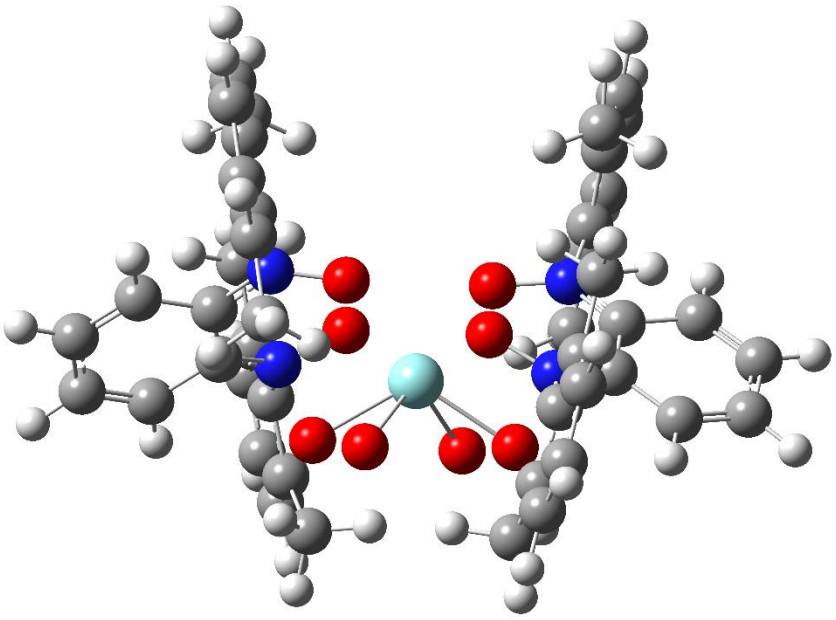

Fig. S40: butterfly bisperoxo complex

E_{SCF}	E_{ZP}	H	G
-2570.038145	-2569.240157	-2569.182904	-2569.334142

planar bisperoxo complex

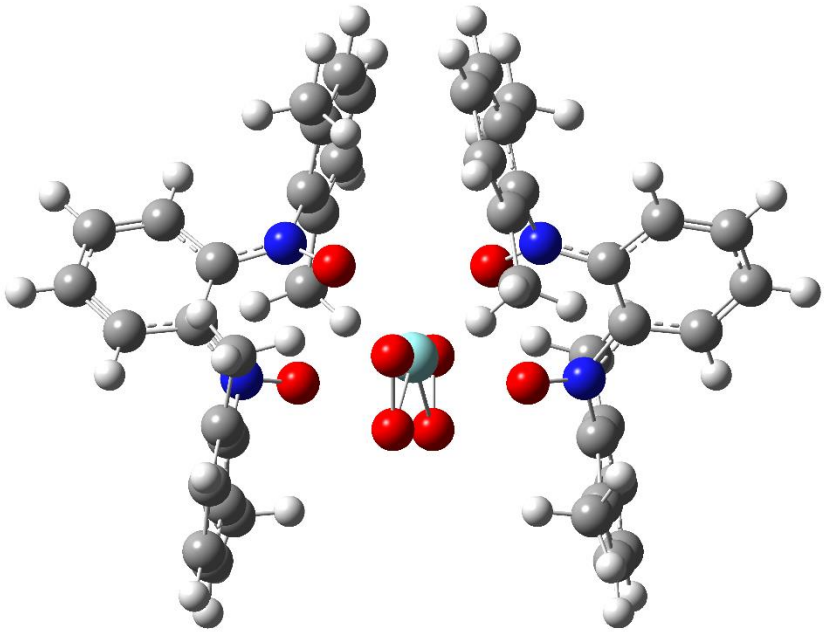

Fig. S41: planar bisperoxo complex

E_{SCF}	E_{ZP}	H	G
-2570.056004	-2569.257121	-2569.200468	-2569.348660

2.1.2 Triplet Ground States

bare complex

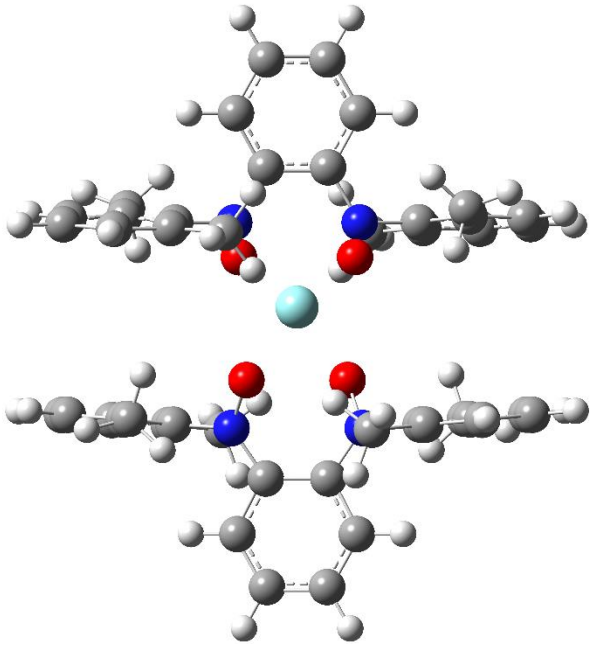

Fig. S42: bare complex

E_{SCF}	E_{ZP}	H	G
-2269.342198	-2268.557133	-2268.505484	-2268.645720

oxo complex

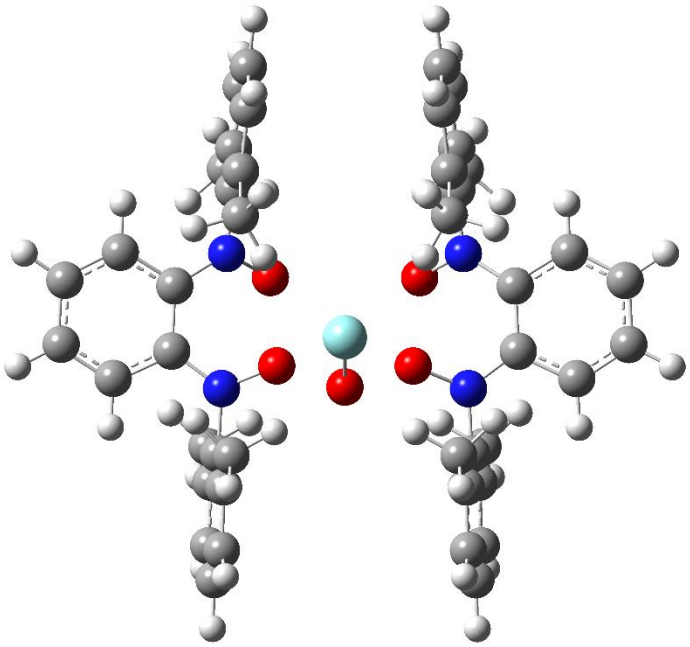

Fig. S43: oxo complex

E_{SCF}	E_{ZP}	H	G
-2344.606390	-2343.817488	-2343.764886	-2343.906190

dioxo complex

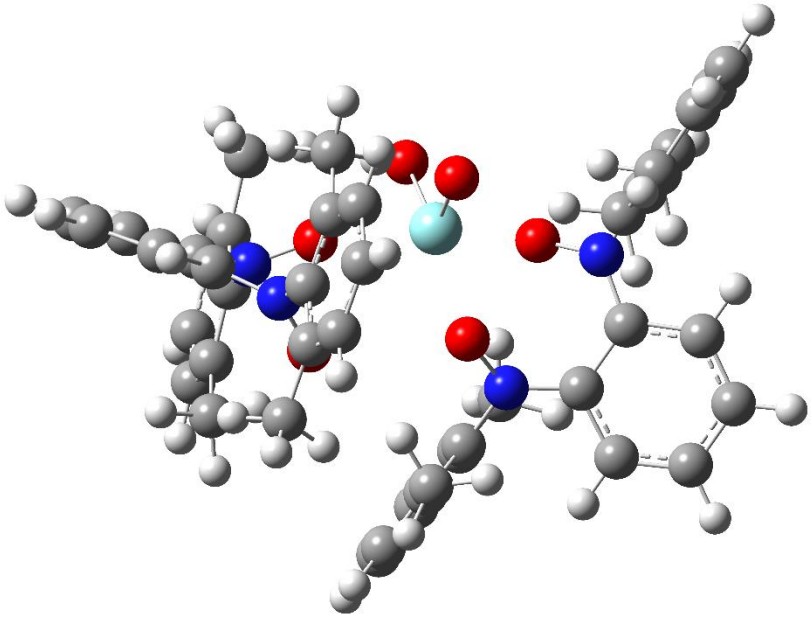

Fig. S44: dioxo complex

E_{SCF}	E_{ZP}	H	G
-2419.718452	-2418.927052	-2418.871988	-2419.019945

peroxo complex

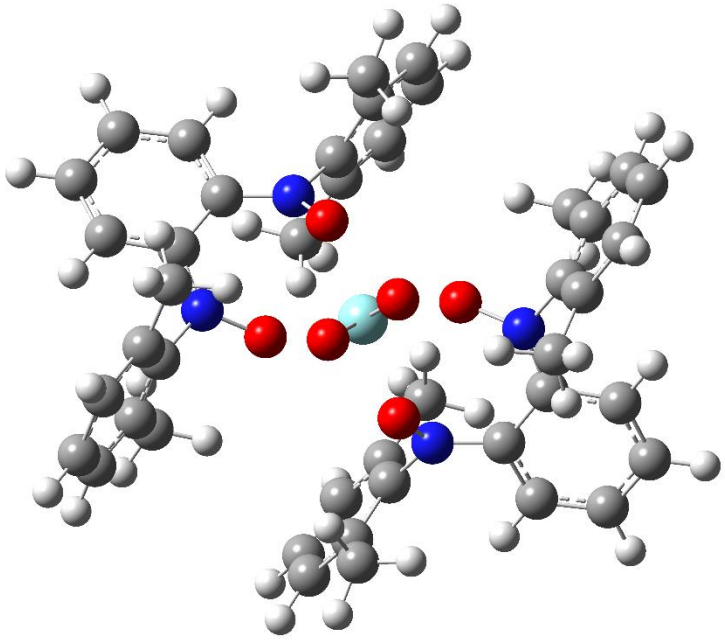

Fig. S45: peroxo complex

E_{SCF}	E_{ZP}	H	G
-2419.761241	-2418.969208	-2418.915717	-2419.058182

oxo peroxo complex

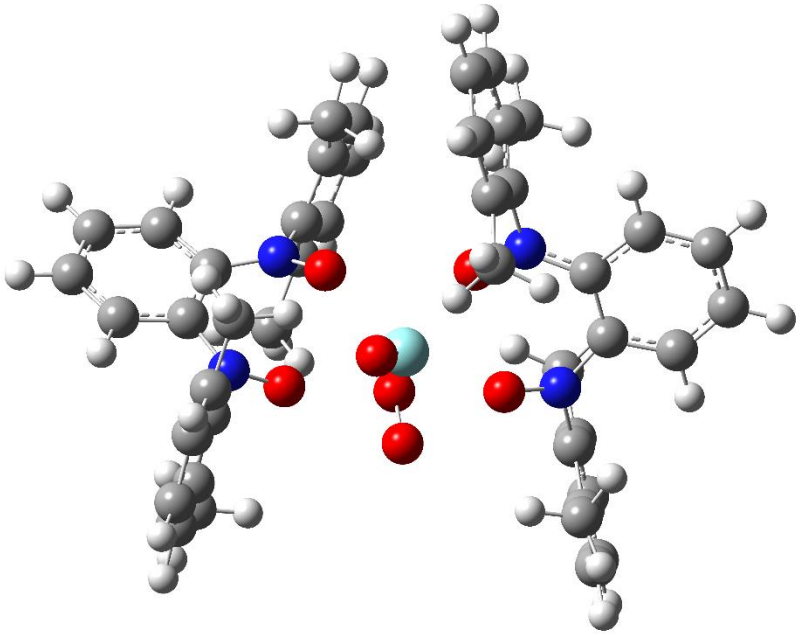

Fig. S46: oxo peroxo complex

E_{SCF}	E_{ZP}	H	G
-2494.921548	-2494.127226	-2494.070724	-2494.222045

η^2-ozone complex

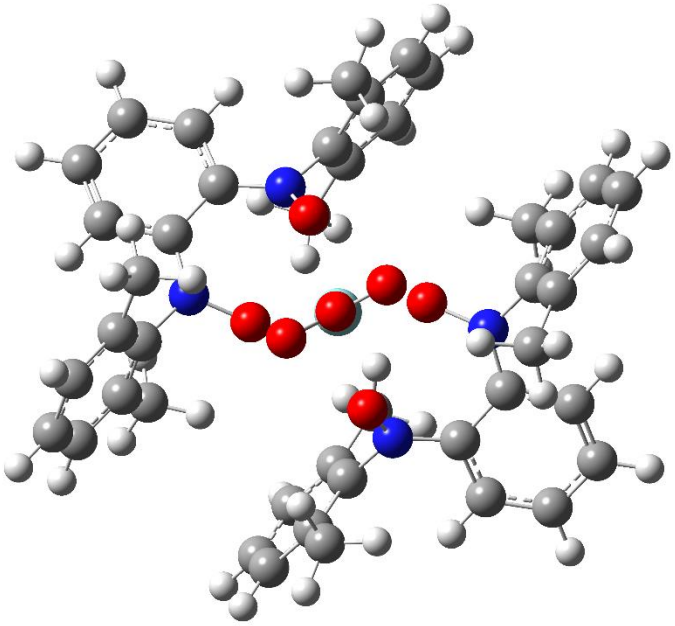

Fig. S47: η^2-ozone complex

E_{SCF}	E_{ZP}	H	G
-2494.908355	-2494.112813	-2494.057373	-2494.204573

η^3-ozone complex

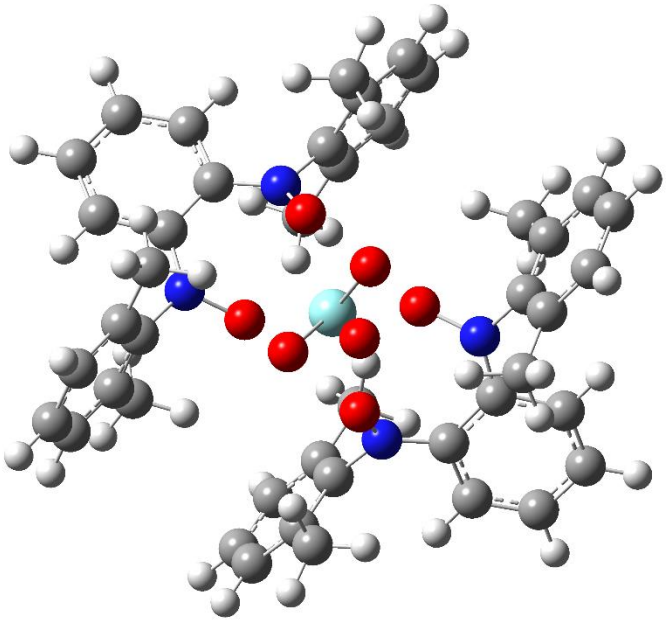

Fig. S48: η^3-ozone complex

E_{SCF}	E_{ZP}	H	G
-2494.902426	-2494.107785	-2494.051953	-2494.200864

spiro bisperoxo complex

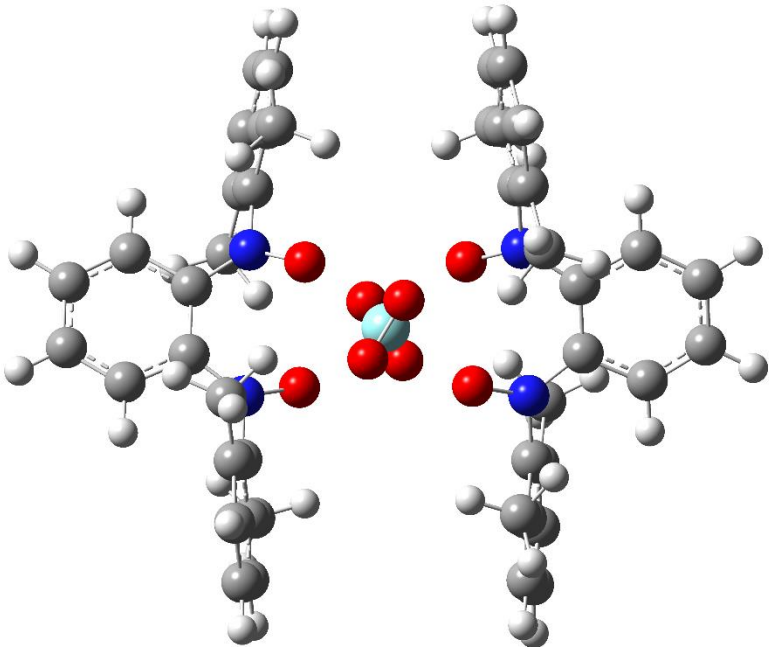

Fig. S49: spiro bisperoxo complex

E_{SCF}	E_{ZP}	H	G
-2570.087004	-2569.289408	-2569.232309	-2569.383422

oxo η^2-ozone complex

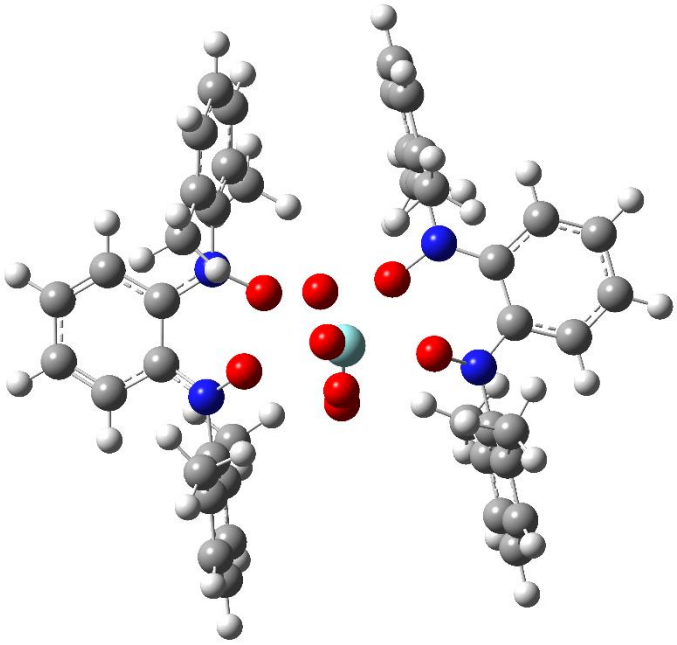

Fig. S50: oxo η^2-ozone complex

E_{SCF}	E_{ZP}	H	G
-2570.066935	-2569.268483	-2569.211152	-2569.362831

oxo η^3-ozone complex

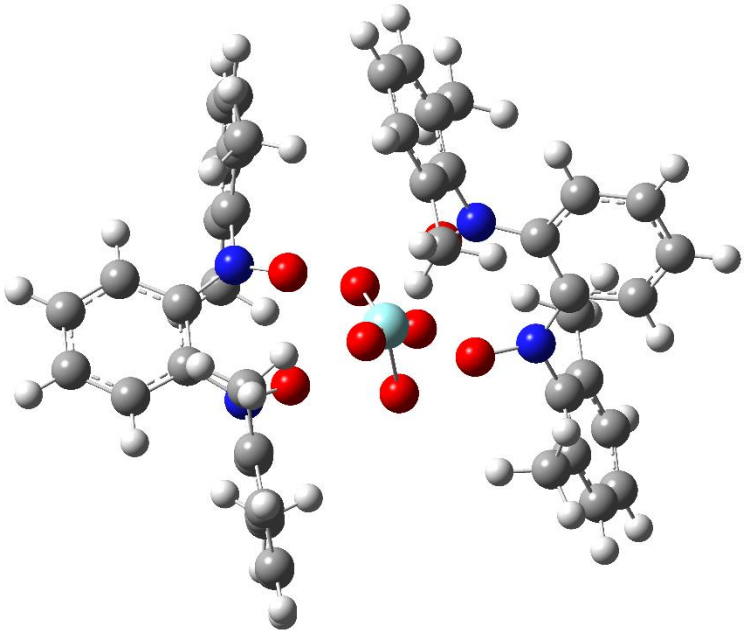

Fig. S51: oxo η^3-ozone complex

E_{SCF}	E_{ZP}	H	G
-2570.033726	-2569.236438	-2569.179473	-2569.330353

peroxo η^2-ozone complex

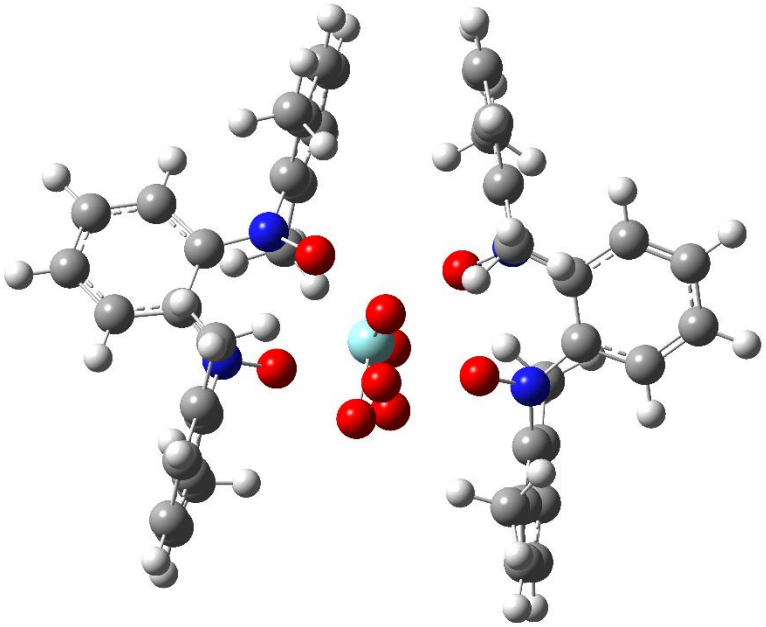

Fig. S52: peroxo η^2-ozone complex

E_{SCF}	E_{ZP}	H	G
-2645.223403	-2644.422665	-2644.364303	-2644.518130

peroxo η^3-ozone complex

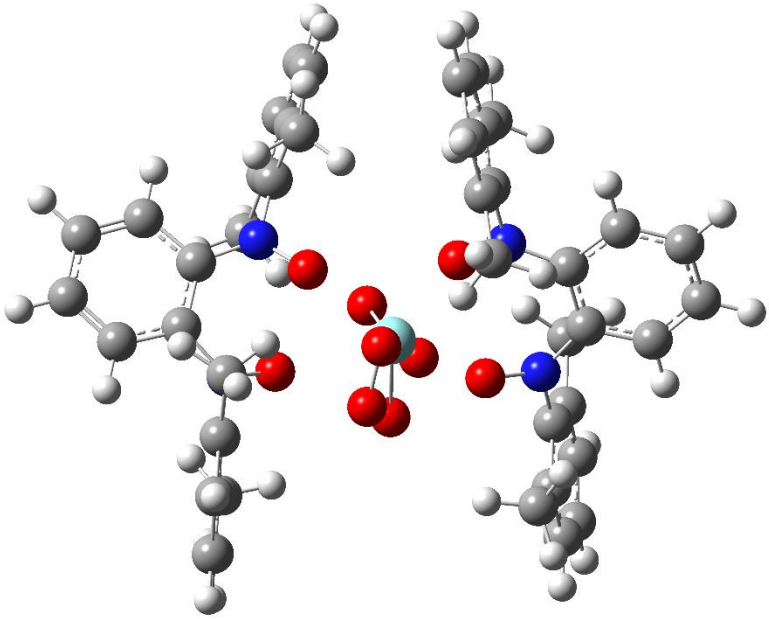

Fig. S53: peroxo η^3-ozone complex

E_{SCF}	E_{ZP}	H	G
-2645.218708	-2644.417808	-2644.359741	-2644.512188

bis-η^2-ozone complex

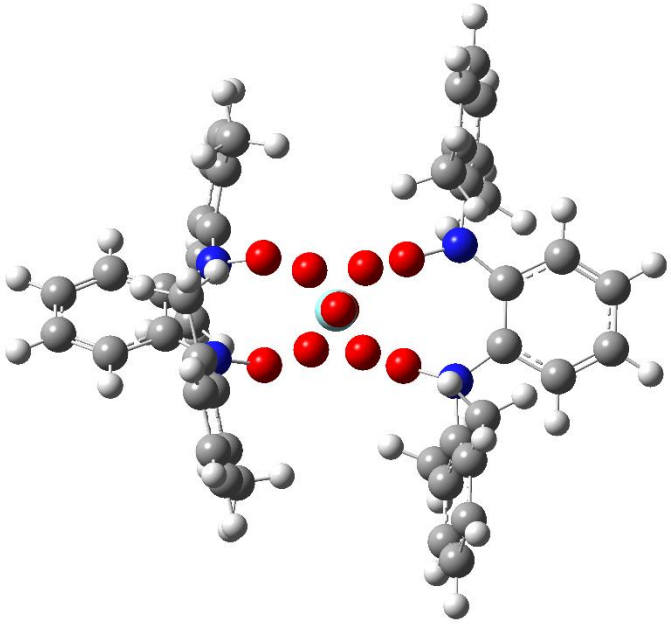

Fig. S54: bis-η^2-ozone complex

E_{SCF}	E_{ZP}	H	G
-2720.358353	-2719.554319	-2719.495168	-2719.650382

η^2-ozone η^3-ozone complex

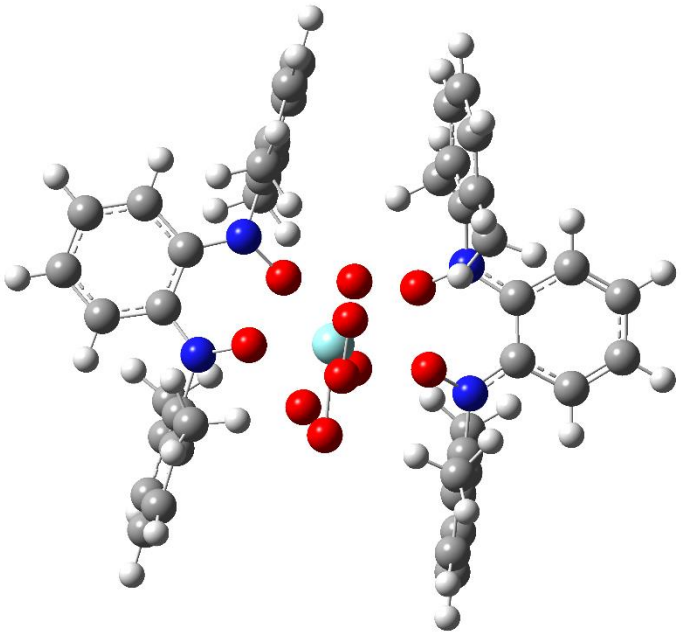

Fig. S55: η^2-ozone η^3-ozone complex

E_{SCF}	E_{ZP}	H	G
-2720.357268	-2719.552528	-2719.493458	-2719.647454

peroxo complex with adsorbed 2,6-dimethylpyridine molecule

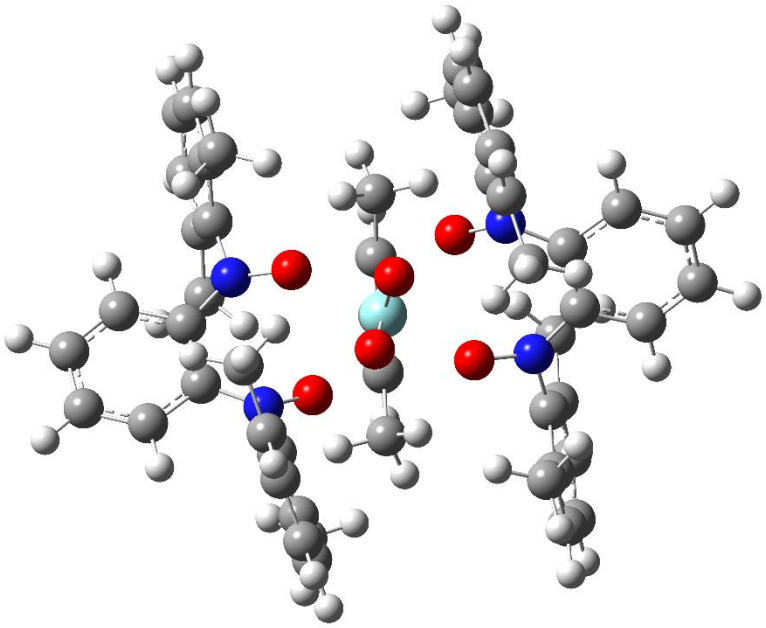

Fig. S56: peroxo complex with adsorbed 2,6-dimethylpyridine molecule

E_{SCF}	E_{ZP}	H	G
-2746.624144	-2745.684365	-2745.621467	-2745.783309

η^2-ozone complex with adsorbed 2,6-dimethylpyridine molecule

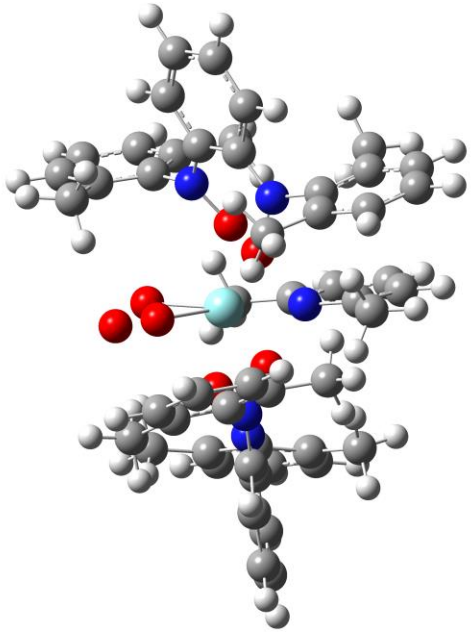

Fig. S57: η^2-ozone complex with adsorbed 2,6-dimethylpyridine molecule

E_{SCF}	E_{ZP}	H	G
-2821.769170	-2820.826698	-2820.762456	-2820.927571

η^3-ozone complex with adsorbed 2,6-dimethylpyridine molecule

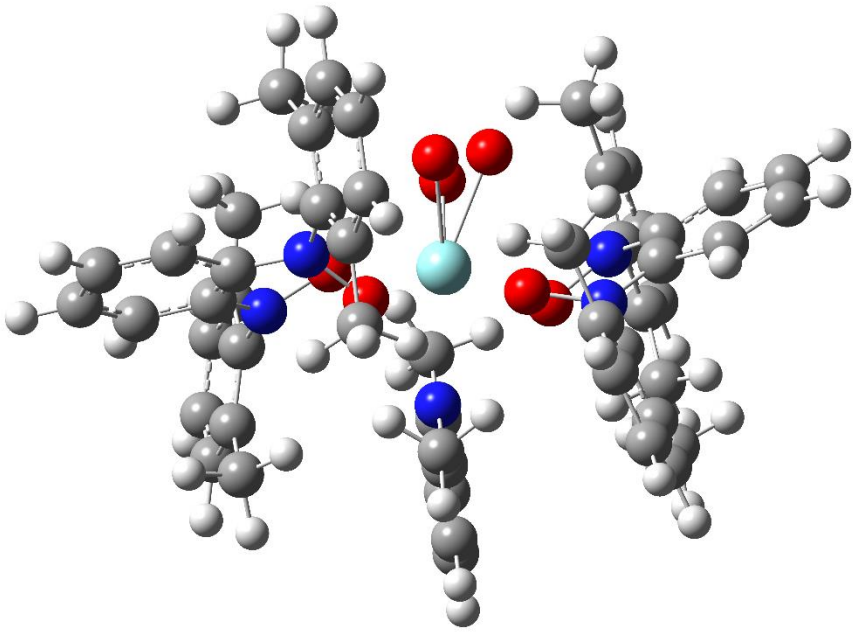

Fig. S58: η^3-ozone complex with adsorbed 2,6-dimethylpyridine molecule

E_{SCF}	E_{ZP}	H	G
-2821.764101	-2820.822013	-2820.757768	-2820.922739

oxo complex with adsorbed 2,6-dimethylpyridine *N*-oxide molecule

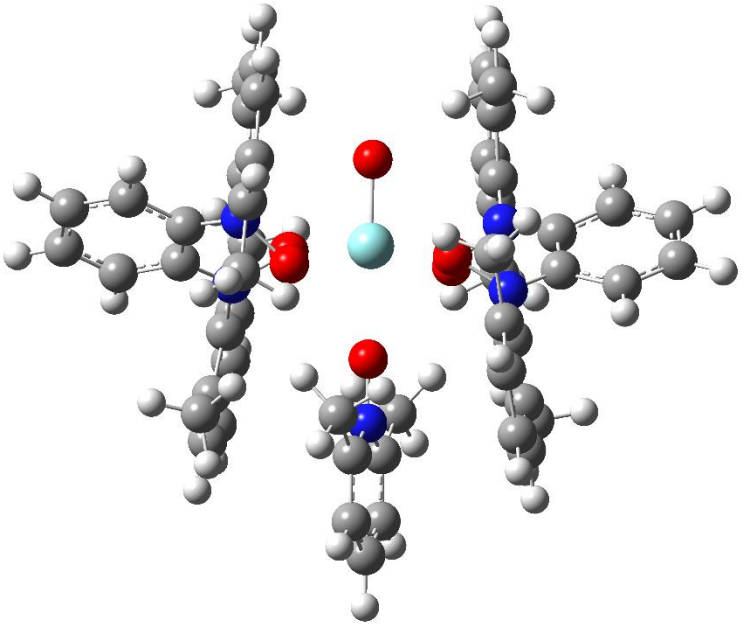

Fig. S59: oxo complex with adsorbed 2,6-dimethylpyridine *N*-oxide molecule

E_{SCF}	E_{ZP}	H	G
-2746.658259	-2745.718090	-2745.655284	-2745.818166

peroxo complex with adsorbed 2,6-dimethylpyridine *N*-oxide molecule

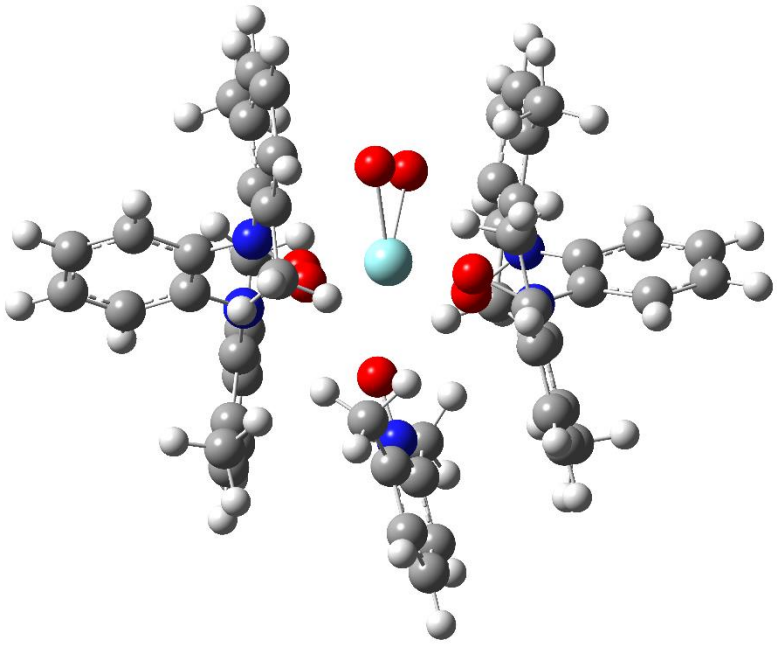

Fig. S60: peroxo complex with adsorbed 2,6-dimethylpyridine *N*-oxide molecule

E_{SCF}	E_{ZP}	H	G
-2821.809970	-2820.866500	-2820.802850	-2820.966603

η^2-ozone complex with adsorbed 2,6-dimethylpyridine *N*-oxide molecule

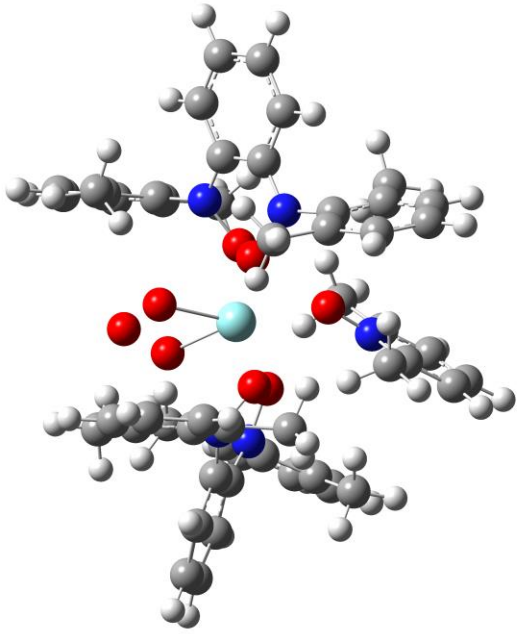

Fig. S61: η^2-ozone complex with adsorbed 2,6-dimethylpyridine *N*-oxide molecule

E_{SCF}	E_{ZP}	H	G
-2896.950954	-2896.003893	-2895.939422	-2896.104823

η^3-ozone complex with adsorbed 2,6-dimethylpyridine *N*-oxide molecule

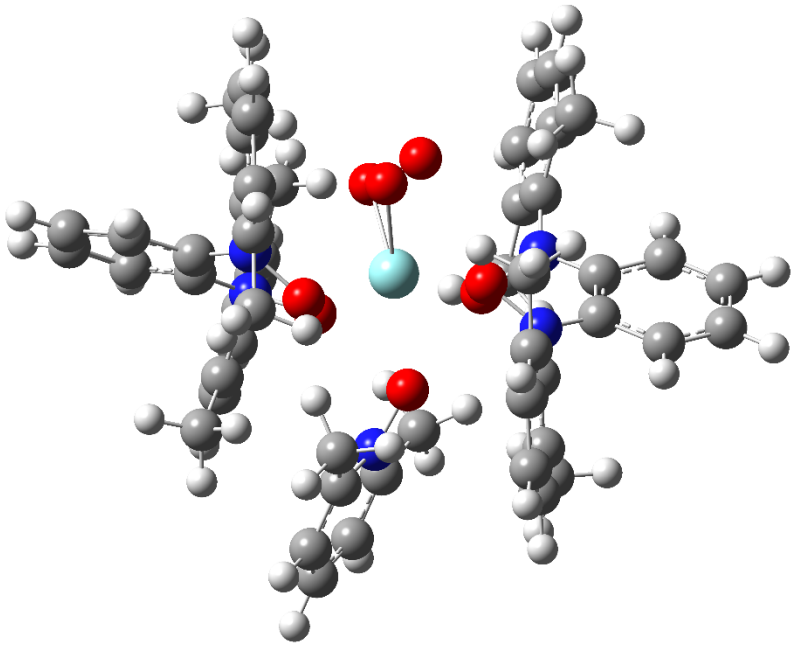

Fig. S62: η^3-ozone complex with adsorbed 2,6-dimethylpyridine *N*-oxide molecule

E_{SCF}	E_{ZP}	H	G
-2896.946948	-2896.000408	-2895.935937	-2896.100510

oxo complex with adsorbed ethylene oxide molecule

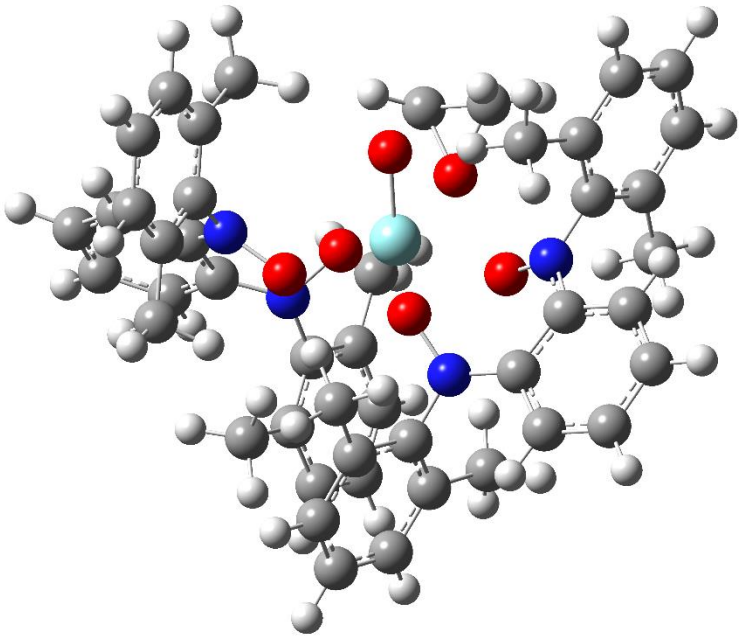

Fig. S63: oxo complex with adsorbed ethylene oxide molecule

E_{SCF}	E_{ZP}	H	G
-2498.382118	-2497.533308	-2497.475927	-2497.627302

peroxo complex with adsorbed ethylene oxide molecule

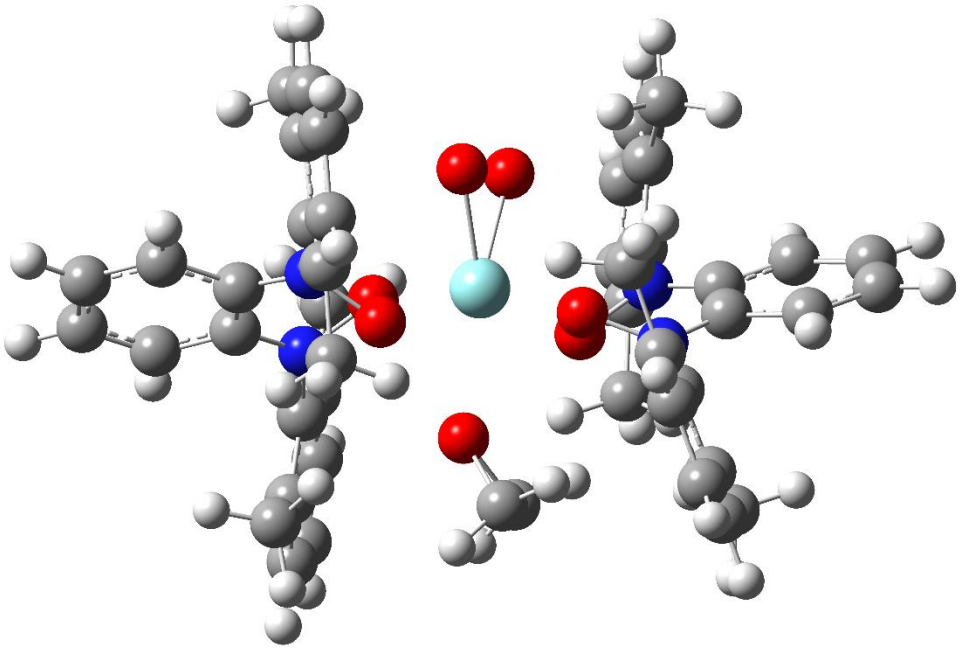

Fig. S64: peroxo complex with adsorbed ethylene oxide molecule

E_{SCF}	E_{ZP}	H	G
-2573.527775	-2572.675738	-2572.617506	-2572.770094

η^2-ozone complex with adsorbed ethylene oxide molecule

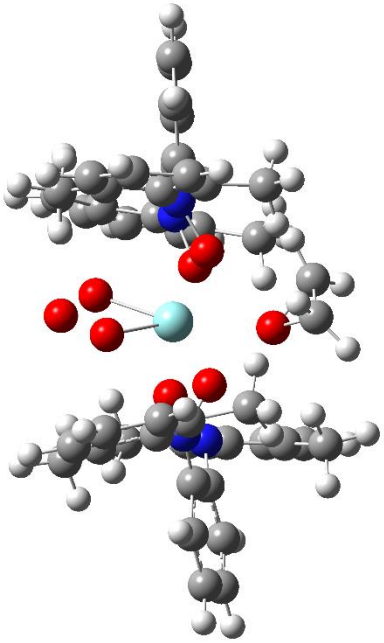

Fig. S65: η^2-ozone complex with adsorbed ethylene oxide molecule

E_{SCF}	E_{ZP}	H	G
-2648.671752	-2647.816929	-2647.758257	-2647.911604

η^3-ozone complex with adsorbed ethylene oxide molecule

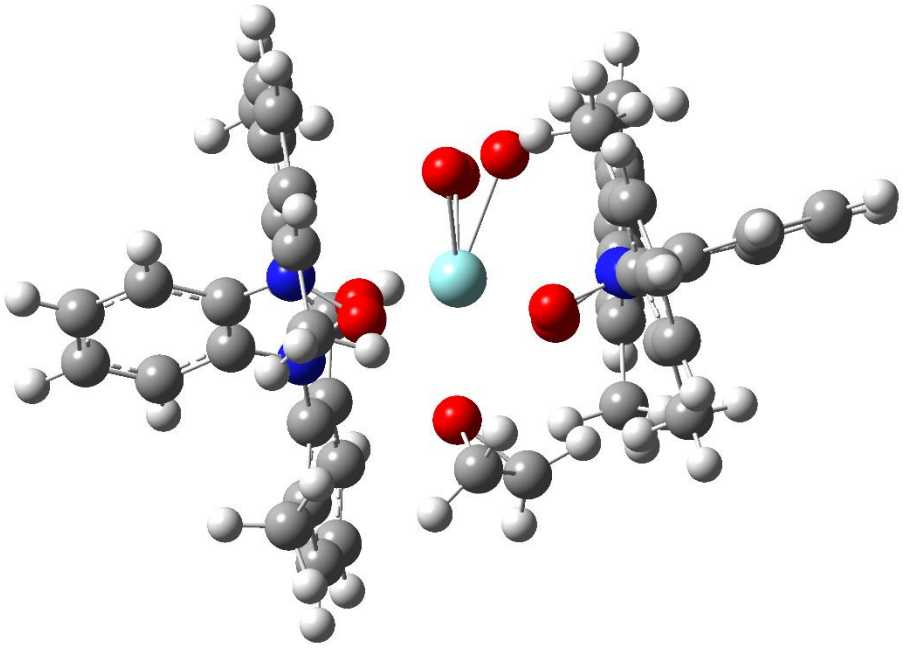

Fig. S66: η^3-ozone complex with adsorbed ethylene oxide molecule

E_{SCF}	E_{ZP}	H	G
-2648.665966	-2647.811292	-2647.751802	-2647.908745

butterfly bisperoxo complex

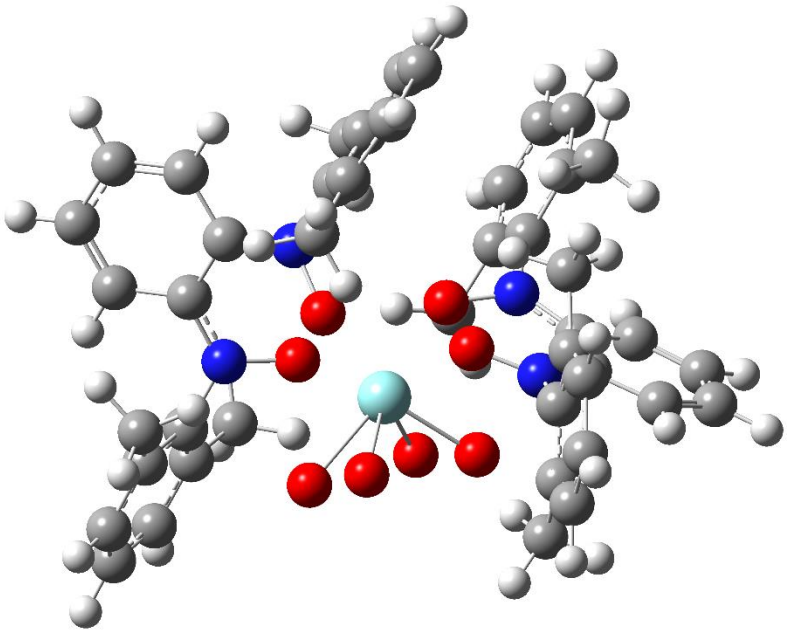

Fig. S67: butterfly bisperoxo complex

E_{SCF}	E_{ZP}	H	G
-2570.069497	-2569.272592	-2569.215238	-2569.367529

2.1.3 Triplet Transition States (2,6-dimethylpyridine involved structures)

TS(3): peroxo η^3-ozone complex to spiro bisperoxo complex

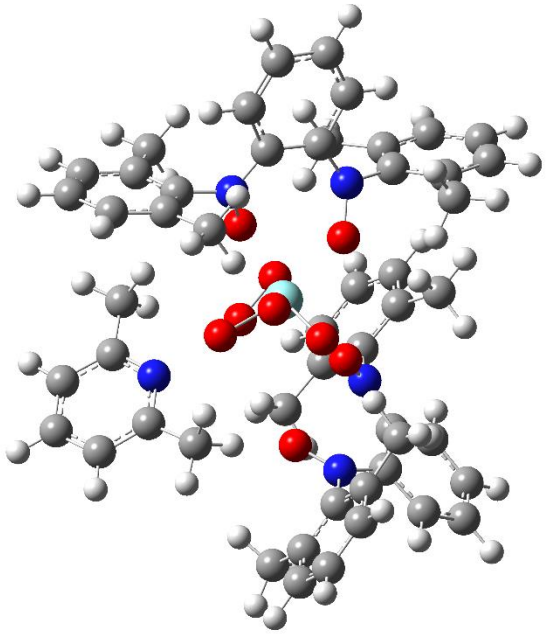

Fig. S68: peroxo η^3-ozone complex to spiro bisperoxo complex

E_{SCF}	E_{ZP}	H	G	*f*
-2972.067602	-2971.121521	-2971.054402	-2971.228074	-210

TS(4): spiro bisperoxo complex to oxo peroxo complex

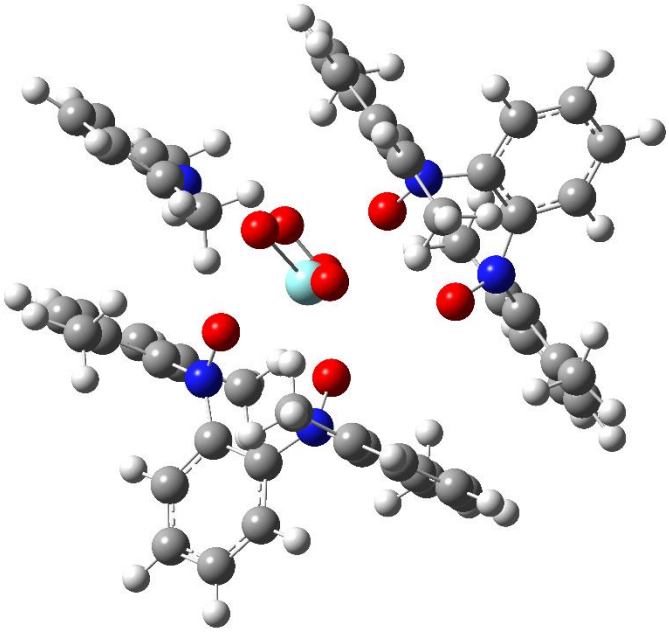

Fig. S69: spiro bisperoxo complex to oxo peroxo complex

E_{SCF}	E_{ZP}	H	G	*f*
-2896.915704	-2895.972865	-2895.906821	-2896.079385	-354

TS(8): η^3-ozone complex to peroxo complex

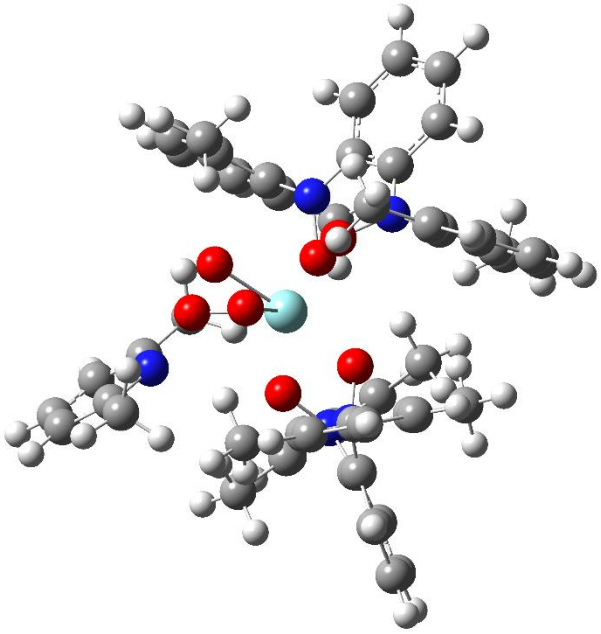

Fig. S70: η^3-ozone complex to peroxo complex

E_{SCF}	E_{ZP}	H	G	*f*
-2821.749736	-2820.808875	-2820.744890	-2820.909587	-255

TS(9): peroxo complex to oxo complex

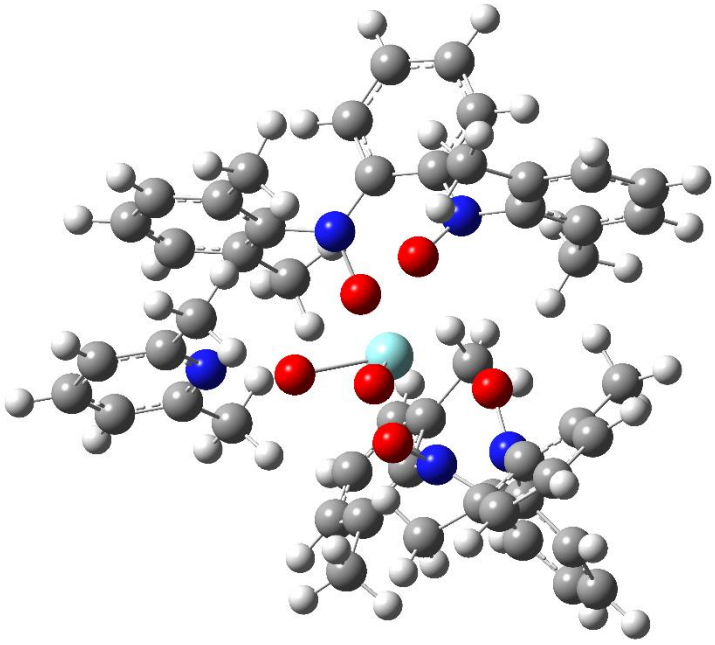

Fig. S71: peroxo complex to oxo complex

E_{SCF}	E_{ZP}	H	G	*f*
-2746.598892	-2745.661445	-2745.598284	-2745.762890	-358

oxo peroxo complex to dioxo complex

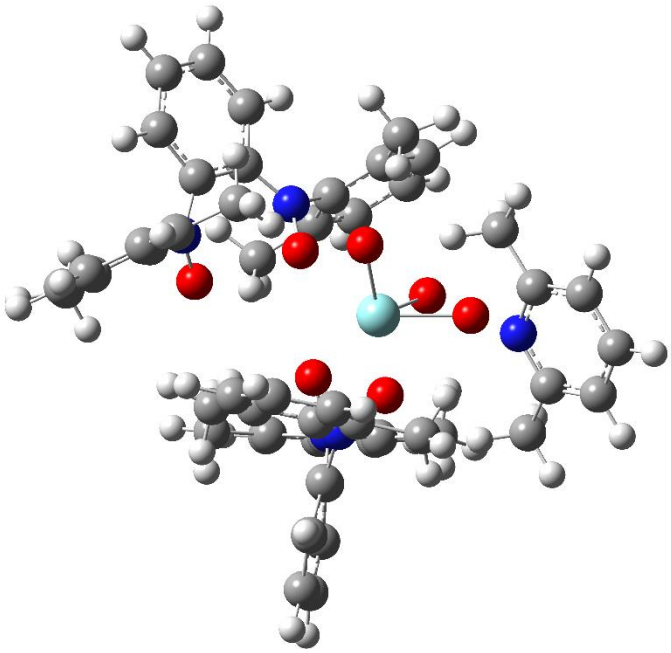

Fig. S72: oxo peroxo complex to dioxo complex

E_{SCF}	E_{ZP}	H	G	*f*
-2821.732240	-2820.792979	-2820.727988	-2820.898102	-350

η^2-ozone η^3-ozone complex to peroxo η^2-ozone complex

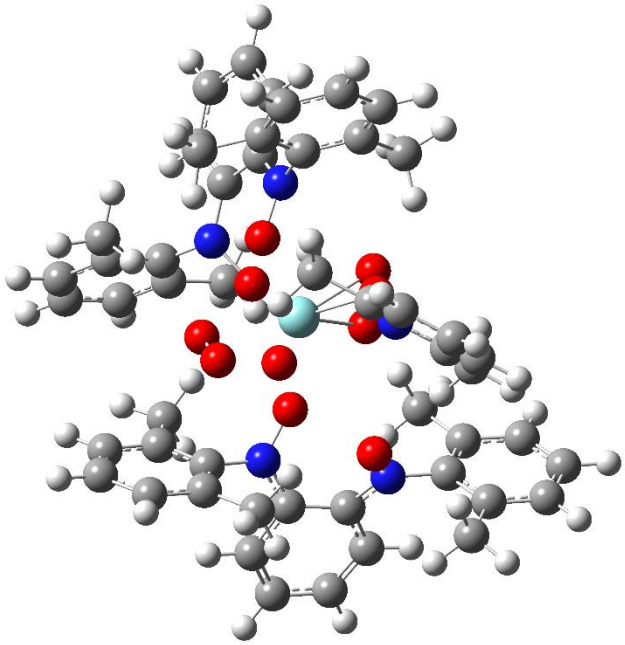

Fig. S73: η^2-ozone η^3-ozone complex to peroxo η^2-ozone complex

E_{SCF}	E_{ZP}	H	G	*f*
-3047.204502	-3046.254709	-3046.186583	-3046.361765	-199

oxo η^3-ozone complex to oxo peroxo complex

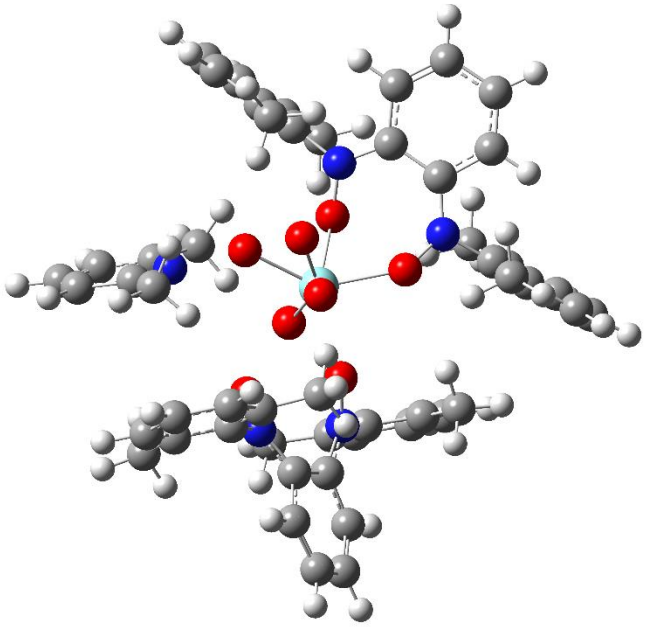

Fig. S74: oxo η^3-ozone complex to oxo peroxo complex

E_{SCF}	E_{ZP}	H	G	*f*
-2896.879670	-2895.936620	-2895.870760	-2896.042713	-224

2.1.4 Triplet Transition States (ethylene involved structures)

TS(15): peroxo η^3-ozone complex to spiro bisperoxo complex

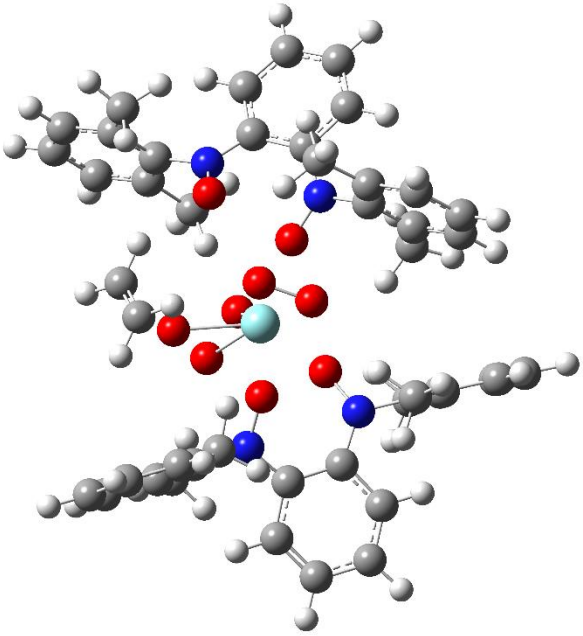

Fig. S75: peroxo η^3-ozone complex to spiro bisperoxo complex

E_{SCF}	E_{ZP}	H	G	*f*
-2723.778011	-2722.924759	-2722.862791	-2723.025009	-346

TS(16): spiro bisperoxo complex to oxo peroxo complex

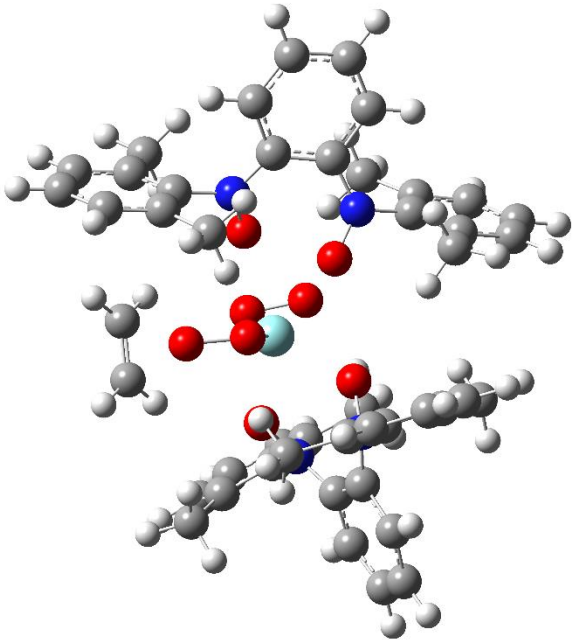

Fig. S76: spiro bisperoxo complex to oxo peroxo complex

E_{SCF}	E_{ZP}	H	G	*f*
-2648.627235	-2647.777006	-2647.716276	-2647.875622	-446

TS(11): oxo complex with adsorbed EO molecule to η^2-ozone complex with adsorbed EO molecule

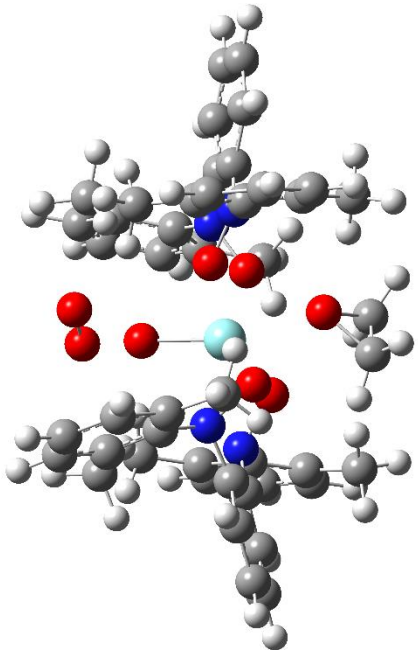

Fig. S77: oxo complex with adsorbed EO molecule to η^2-ozone complex with adsorbed EO molecule

E_{SCF}	E_{ZP}	H	G	*f*
-2648.655914	-2647.801357	-2647.742409	-2647.897209	-10

TS(12): η^2-ozone complex with adsorbed EO molecule to η^3-ozone complex with adsorbed EO molecule

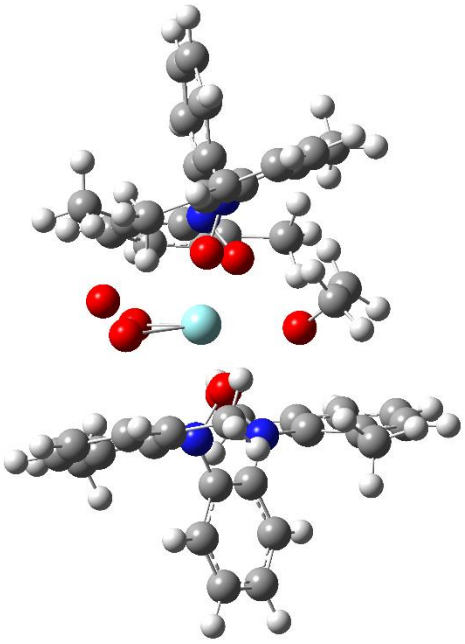

Fig. S78: η^2-ozone complex with adsorbed EO molecule to η^3-ozone complex with adsorbed EO molecule

E_{SCF}	E_{ZP}	H	G	*f*
-2648.663861	-2647.809599	-2647.750749	-2647.905040	-144

TS(13): η^3-ozone complex with adsorbed EO molecule to peroxo complex with adsorbed EO molecule

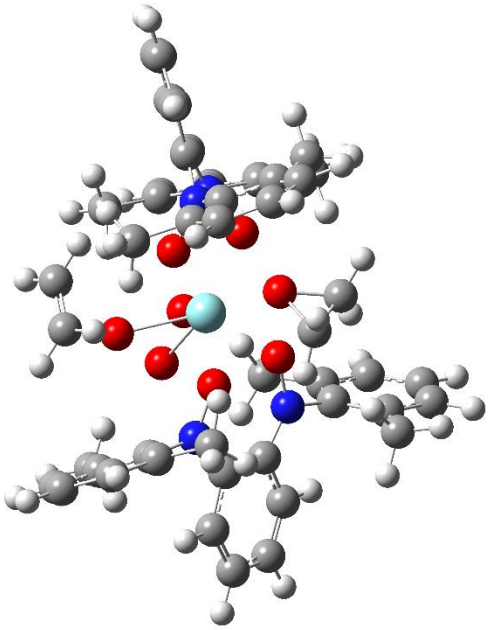

Fig. S79: η^3-ozone complex with adsorbed EO molecule to peroxo complex with adsorbed EO molecule

E_{SCF}	E_{ZP}	H	G	*f*
-2727.220678	-2726.313089	-2726.251401	-2726.409662	-383

TS(14): peroxo complex with adsorbed EO molecule to oxo complex with adsorbed EO molecule

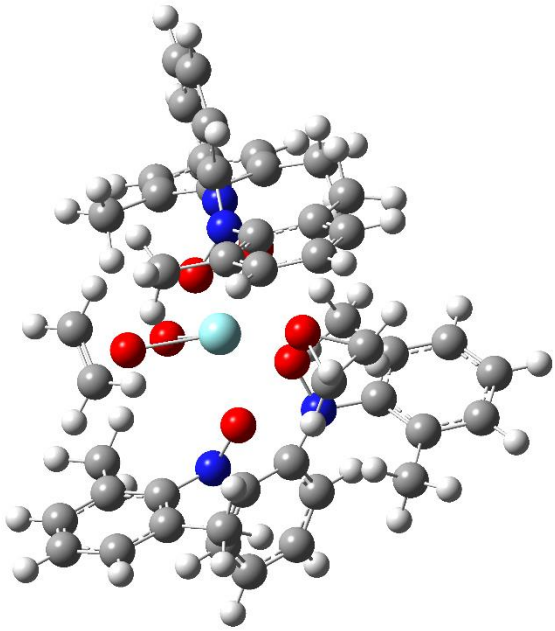

Fig. S80: peroxo complex with adsorbed EO molecule to oxo complex with adsorbed EO molecule

E_{SCF}	E_{ZP}	H	G	*f*
-2652.071454	-2651.167033	-2651.105354	-2651.264425	-462

η^3-ozone complex to peroxo complex

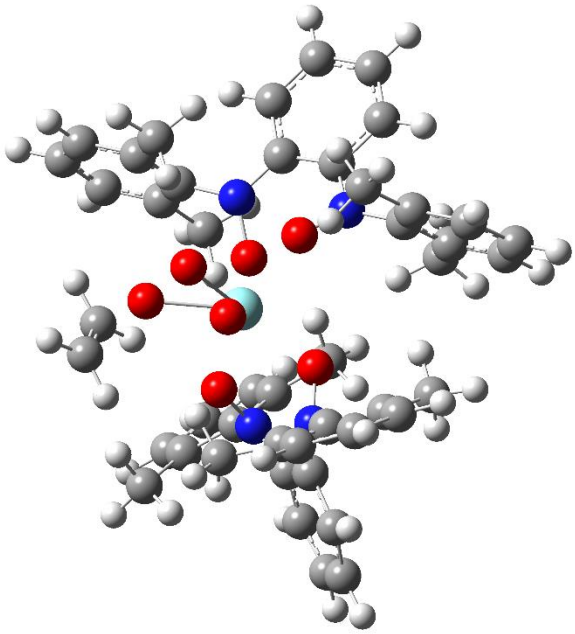

Fig. S81: η^3-ozone complex to peroxo complex

E_{SCF}	E_{ZP}	H	G	*f*
-2573.459738	-2572.612241	-2572.553941	-2572.706284	-366

oxo peroxo complex to dioxo complex

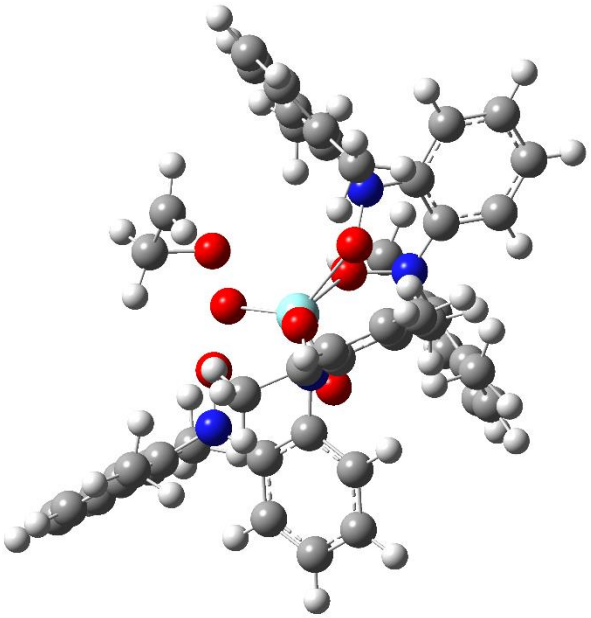

Fig. S82: oxo peroxo complex to dioxo complex

E_{SCF}	E_{ZP}	H	G	*f*
-2573.456126	-2572.608602	-2572.549339	-2572.705258	-642

2.1.5 Triplet Transition States (other structures)

TS(1): oxo peroxo complex to peroxo η^2-ozone complex

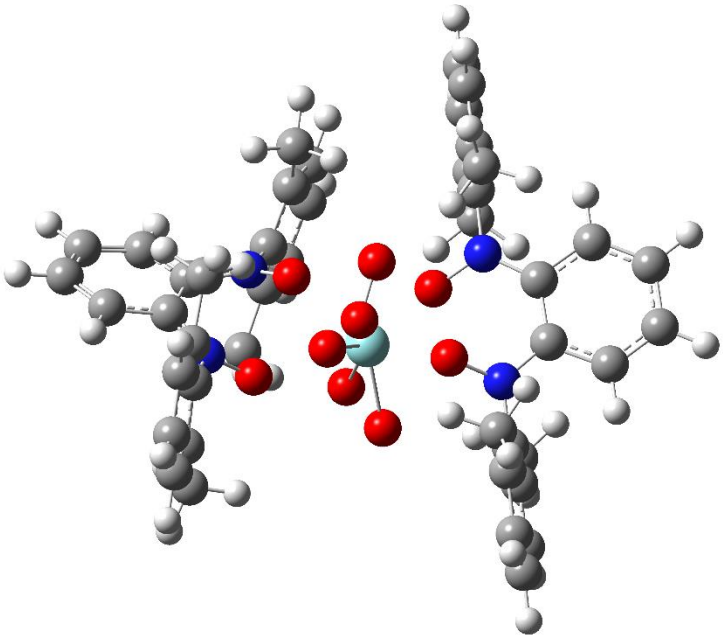

Fig. S83: oxo peroxo complex to peroxo η^2-ozone complex

E_{SCF}	E_{ZP}	H	G	*f*
-2645.211141	-2644.409757	-2644.352235	-2644.504049	-35

TS(2): peroxo η^2-ozone complex to peroxo η^3-ozone complex

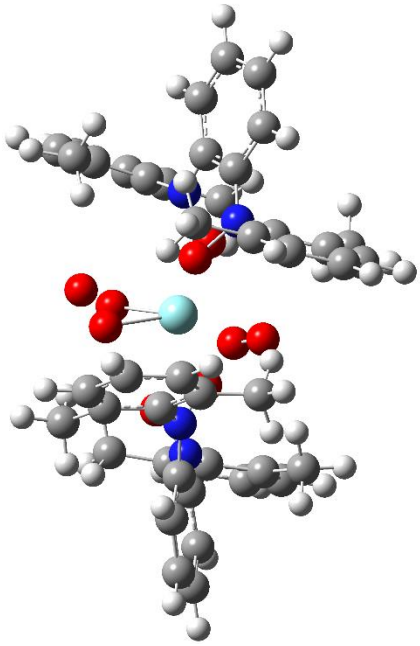

Fig. S84: peroxo η^2-ozone complex to peroxo η^3-ozone complex

E_{SCF}	E_{ZP}	H	G	*f*
-2645.216369	-2644.416113	-2644.358454	-2644.510736	-168

TS(5): oxo complex to oxo peroxo complex

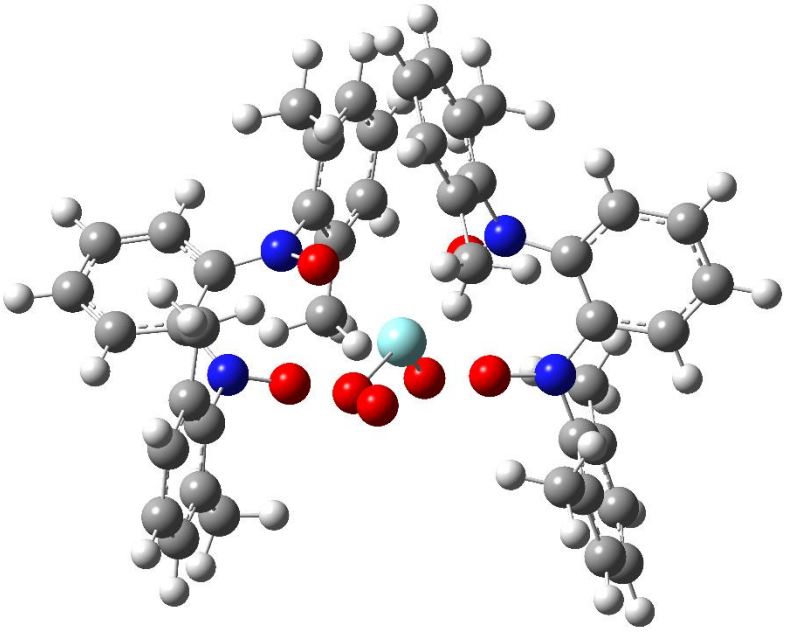

Fig. S85: oxo complex to oxo peroxo complex

E_{SCF}	E_{ZP}	H	G	*f*
-2494.908781	-2494.115258	-2494.059286	-2494.209244	-48

TS(7): η^2-ozone complex to η^3-ozone complex

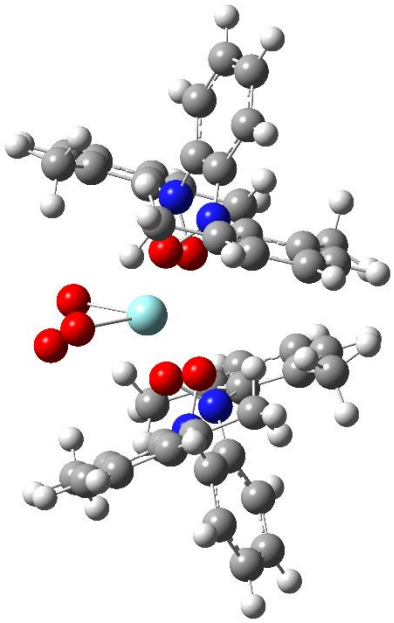

Fig. S86: η^2-ozone complex to η^3-ozone complex

E_{SCF}	E_{ZP}	H	G	*f*
-2494.902091	-2494.107641	-2494.052510	-2494.199600	-135

2.1.6 Approximate Crossing Point Geometry

Approximate CP(1): oxo complex to η^2-ozone complex (triplet geometry)

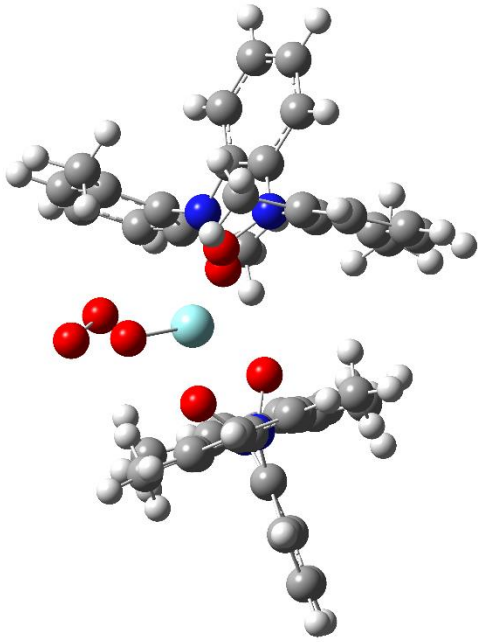

Fig. S87: oxo complex to η^2-ozone complex (triplet geometry)

	E_{SCF}	E_{ZP}	H	G
Triplet	-2494.882652	-2494.089846	-2494.034750	-2494.180502
Quintet	-2494.885459	n/a	n/a	n/a

C	0.250944	3.450674	-1.100828
C	1.007355	4.404751	-0.369516
C	2.011625	5.112959	-1.061098
C	2.254563	4.883830	-2.426761
C	1.496563	3.928858	-3.125796
C	0.485555	3.191353	-2.476774
C	-4.010443	-0.171752	0.690825
C	-4.499173	0.059440	2.001165
C	-5.497367	-0.808978	2.488375
C	-5.983043	-1.868565	1.703786
C	-5.480915	-2.073327	0.406674
C	-4.485377	-1.229497	-0.124704
C	-0.101841	-3.454029	-1.182857
C	-0.282036	-3.189100	-2.566224
C	-1.268423	-3.923939	-3.255067
C	-2.053117	-4.880461	-2.588529
C	-1.865445	-5.111721	-1.214638
C	-0.890718	-4.404557	-0.481053
C	3.931759	0.269356	0.847750
C	4.309590	0.067324	2.199790
C	5.249738	0.961829	2.754254
C	5.785167	2.016243	1.995622
C	5.397777	2.188534	0.654959

C	4.466772	1.317078	0.055567
H	2.597417	5.854132	-0.522493
H	3.031286	5.444254	-2.941879
H	1.693167	3.742472	-4.179125
H	-5.878700	-0.659121	3.495393
H	-6.748595	-2.531053	2.101109
H	-5.863309	-2.888465	-0.203346
H	-1.425394	-3.733171	-4.314217
H	-2.809655	-5.438770	-3.134949
H	-2.474920	-5.850897	-0.700363
H	5.547805	0.832808	3.791790
H	6.503305	2.697866	2.445791
H	5.820587	2.997976	0.064379
C	2.269459	-2.845509	-0.670264
C	3.253719	-1.882988	-0.220756
C	2.724341	-4.036728	-1.320829
C	4.637331	-2.254711	-0.304299
C	4.074142	-4.335535	-1.437002
H	1.980921	-4.742951	-1.674551
C	5.040654	-3.442279	-0.896713
H	5.379508	-1.557901	0.068014
H	4.386167	-5.262549	-1.909531
H	6.099428	-3.677618	-0.962381
C	-3.188688	1.978421	-0.283391
C	-2.143274	2.907486	-0.664226
C	-4.552758	2.400541	-0.432828
C	-2.528604	4.130970	-1.302597
C	-4.885396	3.614097	-1.014508
H	-5.336687	1.719335	-0.122466
C	-3.859097	4.483092	-1.477546
H	-1.745834	4.817587	-1.605791
H	-5.930269	3.888130	-1.130695
H	-4.111007	5.433082	-1.940595
O	1.757357	0.018728	-0.142679
N	2.950755	-0.616039	0.248199
O	0.437972	-2.045098	0.658559
O	-0.368327	2.022392	0.709476
O	-1.770775	0.036867	-0.125097
N	0.900816	-2.704033	-0.461308
N	-2.963818	0.685112	0.164549
N	-0.787578	2.704652	-0.428994
O	0.708832	0.334936	2.891407
O	-0.518331	-0.819855	3.687521
O	-1.472183	-0.988963	2.691119
Zr	0.019226	-0.013240	1.094496
C	3.723160	-1.043067	3.048173
H	2.652827	-0.867152	3.212025
H	3.836806	-2.028539	2.579317
H	4.215919	-1.075694	4.026031
C	4.069068	1.495528	-1.395202
H	4.132115	0.549281	-1.948187
H	3.033318	1.840260	-1.475595
H	4.718702	2.227193	-1.887533
C	-0.317203	2.159724	-3.245655
H	-0.491379	1.257681	-2.649130
H	-1.304477	2.550608	-3.529643

H	0.205354	1.875935	-4.165743
C	0.749195	4.685206	1.097070
H	-0.323409	4.765682	1.311101
H	1.125005	3.869469	1.724415
H	1.237259	5.617962	1.401020
C	-3.969656	1.178157	2.874940
H	-2.894286	1.054919	3.042425
H	-4.130817	2.167185	2.427251
H	-4.464131	1.165686	3.851893
C	-3.960489	-1.450494	-1.528723
H	-3.922682	-0.512534	-2.097574
H	-2.939812	-1.846502	-1.505316
H	-4.596041	-2.158649	-2.071497
C	0.542507	-2.150113	-3.302559
H	0.042091	-1.855342	-4.231389
H	0.704049	-1.254103	-2.693336
H	1.535346	-2.539438	-3.568058
C	-0.705446	-4.677447	0.997978
H	0.354854	-4.745015	1.269594
H	-1.124721	-3.863344	1.600006
H	-1.198581	-5.614922	1.278523

2.2. DIZB Catalytic System (B3LYP/LANL2DZ)

2.2.1 Triplet Ground States

oxo complex with adsorbed 2,6-dimethylpyridine *N*-oxide

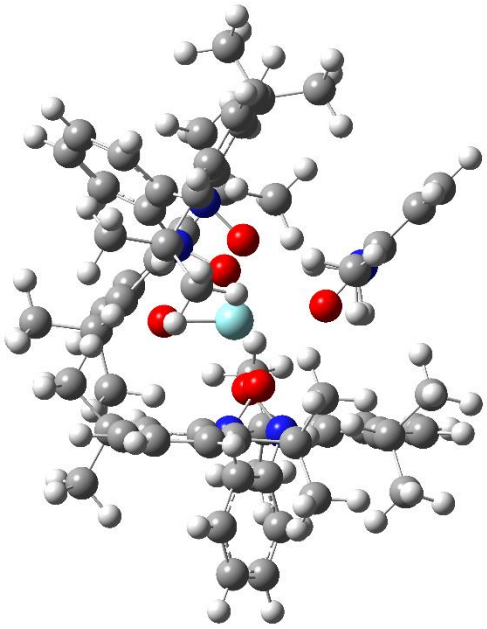

Fig. S88: oxo complex with adsorbed 2,6-dimethylpyridine *N*-oxide

E_{SCF}	E_{ZP}	H	G
-3375.545197	-3374.148123	-3374.063466	-3374.271513

oxo complex with adsorbed 2,6-dichrolopyridine *N*-oxide

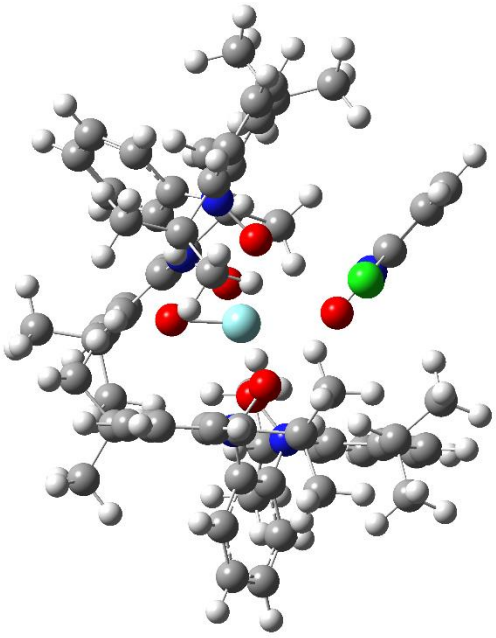

Fig. S89: oxo complex with adsorbed 2,6-dichrolopyridine *N*-oxide

E_{SCF}	E_{ZP}	H	G
-3325.550459	-3324.229600	-3324.145504	-3324.353280

oxo complex with adsorbed 2-chloropyridine *N*-oxide

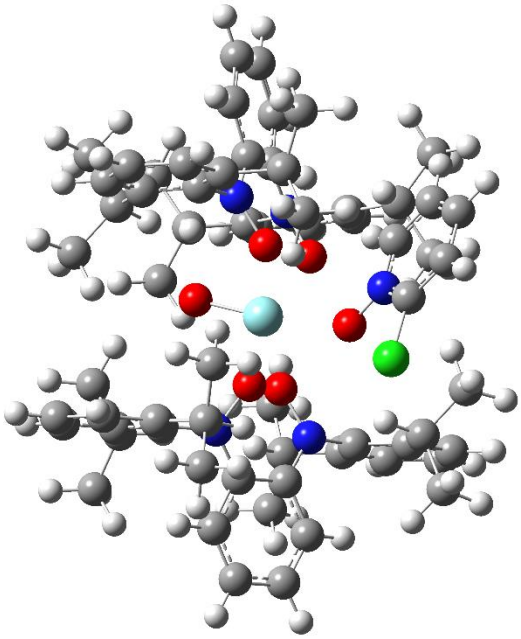

Fig. S90: oxo complex with adsorbed 2-chloropyridine *N*-oxide

E_{SCF}	E_{ZP}	H	G
-3311.238980	-3309.908897	-3309.825684	-3310.033667

oxo complex with adsorbed pyridine *N*-oxide

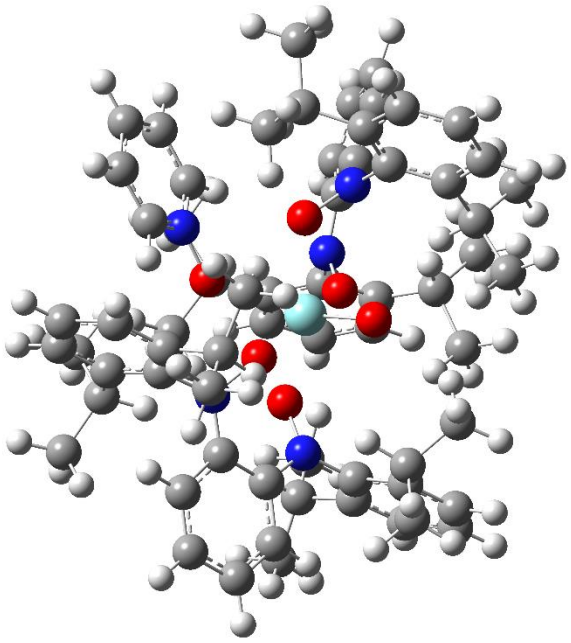

Fig. S91: oxo complex with adsorbed pyridine *N*-oxide

E_{SCF}	E_{ZP}	H	G
-3296.909724	-3295.568984	-3295.487069	-3295.691733

oxo complex with adsorbed 4-nitroquinoline *N*-oxide

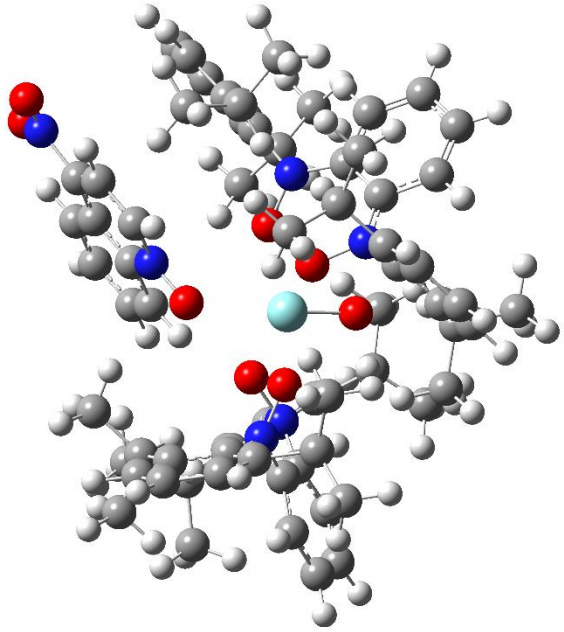

Fig. S92: oxo complex with adsorbed 4-nitroquinoline *N*-oxide

E_{SCF}	E_{ZP}	H	G
-3654.984464	-3653.595280	-3653.508087	-3653.723742

2.2.2 Triplet Transition States (2,6-dimethylpyridine involved structures)

TS(22): peroxo η^3-ozone complex to spiro bisperoxo complex

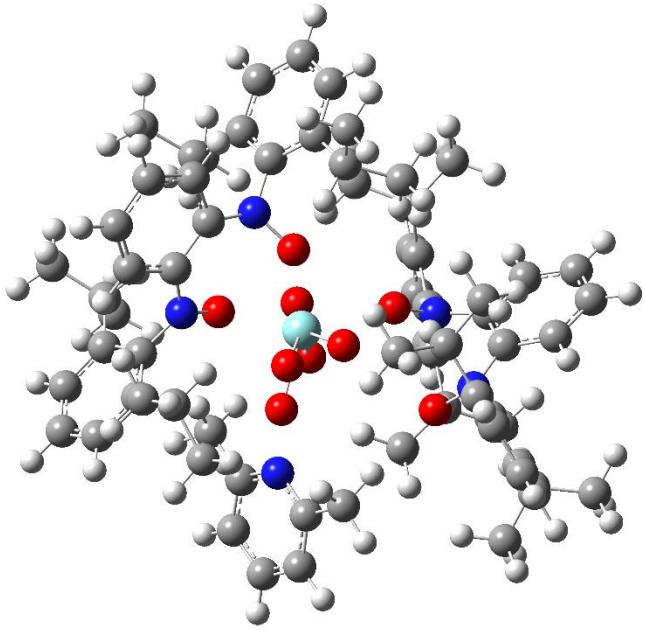

Fig. S93: peroxo η^3-ozone complex to spiro bisperoxo complex

E_{SCF}	E_{ZP}	H	G	*f*
-3600.941844	-3599.539192	-3599.449997	-3599.670332	-198

TS(23): spiro bisperoxo complex to oxo peroxo complex

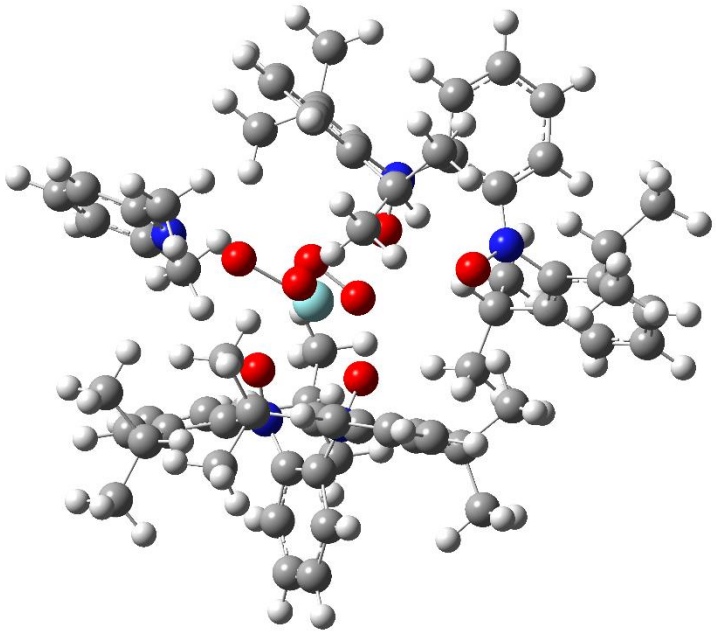

Fig. S94: spiro bisperoxo complex to oxo peroxo complex

E_{SCF}	E_{ZP}	H	G	*f*
-3525.798859	-3524.398527	-3524.310764	-3524.526998	-356

TS(26): η^3-ozone complex to peroxo complex

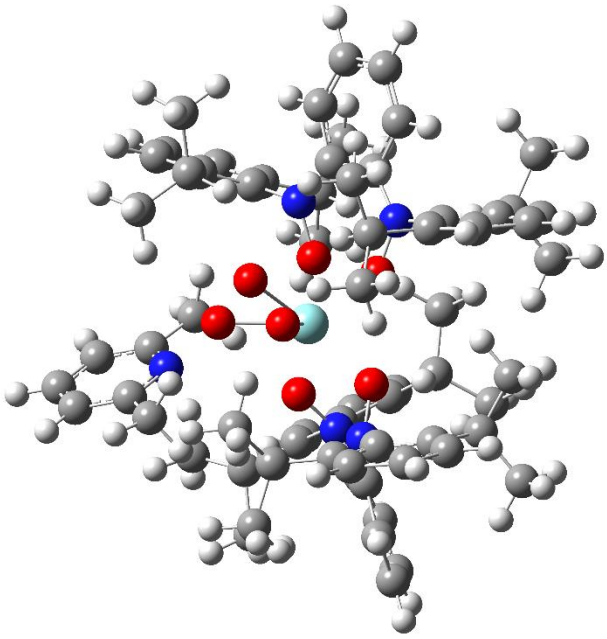

Fig. S95: η^3-ozone complex to peroxo complex

E_{SCF}	E_{ZP}	H	G	*f*
-3450.626079	-3449.228421	-3449.142574	-3449.353945	-260

TS(27): peroxo complex to oxo complex

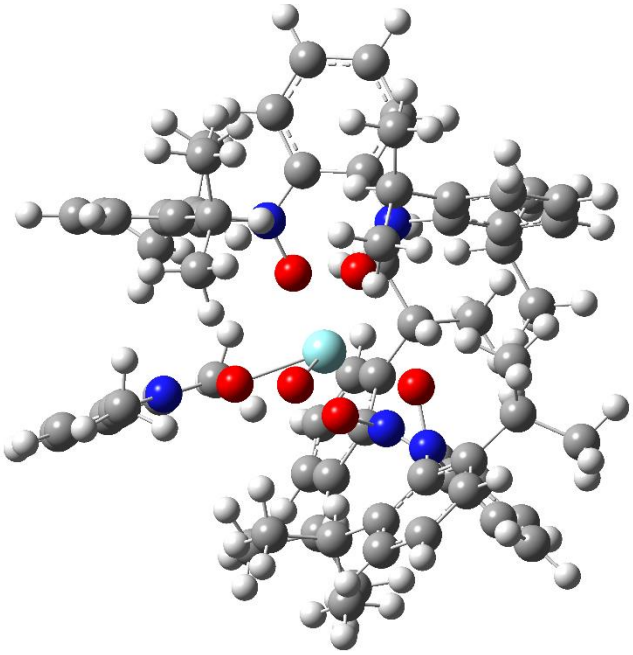

Fig. S96: peroxo complex to oxo complex

E_{SCF}	E_{ZP}	H	G	*f*
-3375.477177	-3374.081597	-3373.997370	-3374.204113	-357

2.2.3 Triplet Transition States (2,6-dichloropyridine involved structures)

TS(28): peroxo η^3-ozone complex to spiro bisperoxo complex

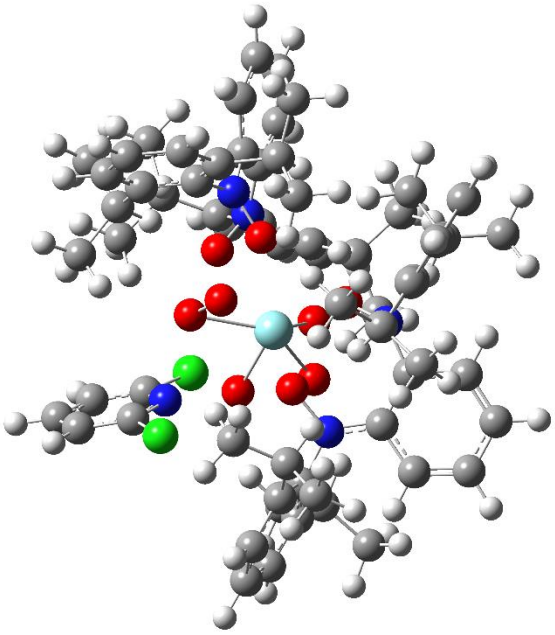

Fig. S97: peroxo η^3-ozone complex to spiro bisperoxo complex

E_{SCF}	E_{ZP}	H	G	*f*
-3550.971984	-3549.645104	-3549.557847	-3549.772099	-367

TS(29): spiro bisperoxo complex to oxo peroxo complex

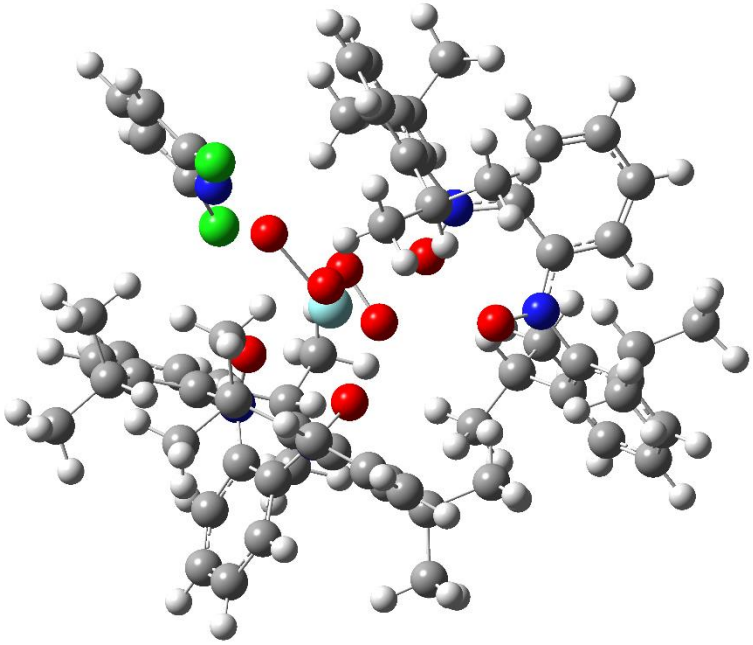

Fig. S98: spiro bisperoxo complex to oxo peroxo complex

E_{SCF}	E_{ZP}	H	G	*f*
-3475.814362	-3474.489577	-3474.402543	-3474.618879	-491

TS(30): η^3-ozone complex to peroxo complex

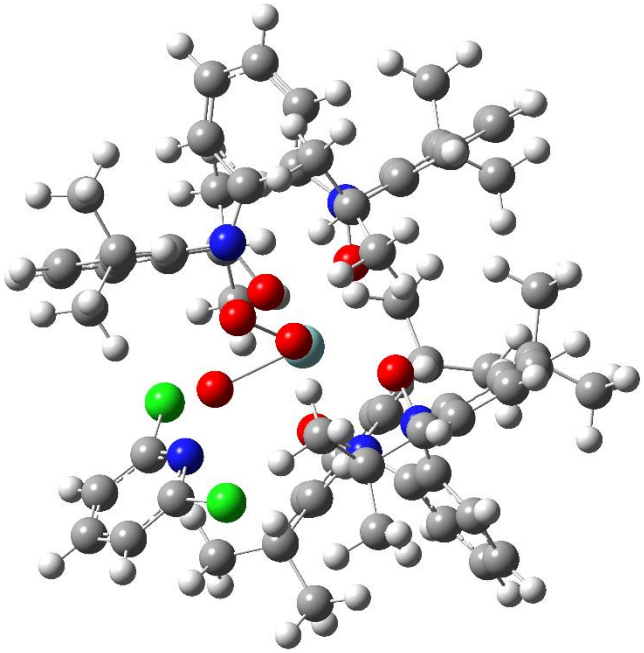

Fig. S99: η^3-ozone complex to peroxo complex

E_{SCF}	E_{ZP}	H	G	*f*
-3400.650685	-3399.328998	-3399.243993	-3399.453404	-408

TS(31): peroxo complex to oxo complex

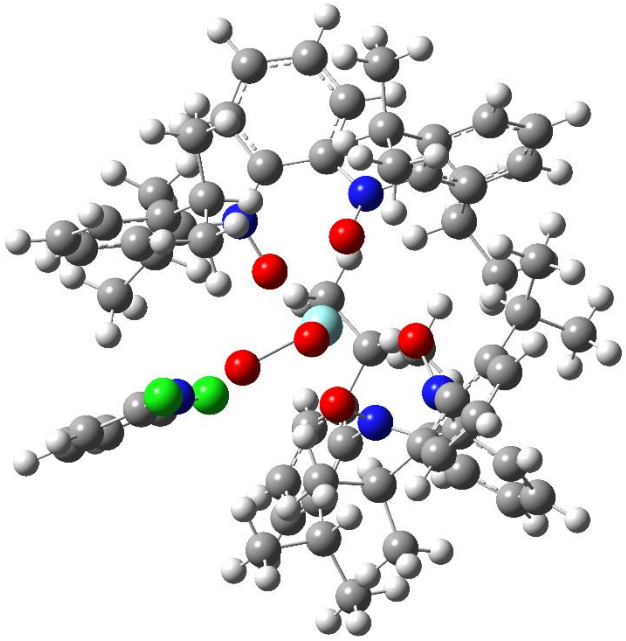

Fig. S100: peroxo complex to oxo complex

E_{SCF}	E_{ZP}	H	G	*f*
-3325.499391	-3324.180152	-3324.096584	-3324.302481	-481

2.2.4 Triplet Transition States (2-chloropyridine involved structures)

TS(40): peroxo η^3-ozone complex to spiro bisperoxo complex

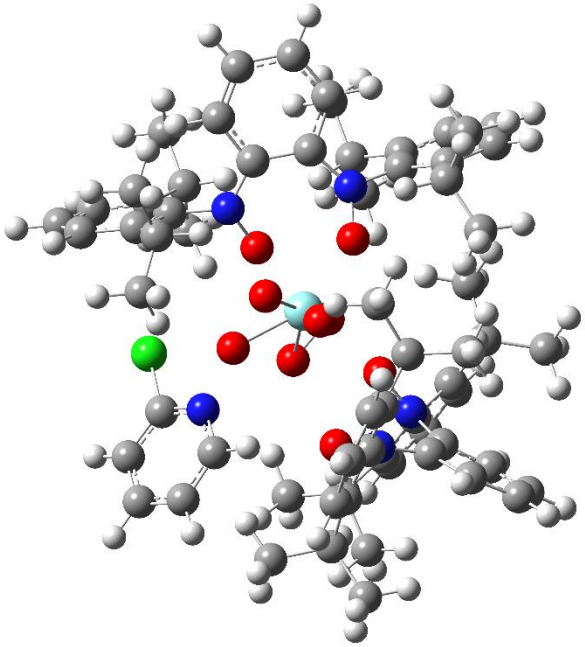

Fig. S101: peroxo η^3-ozone complex to spiro bisperoxo complex

E_{SCF}	E_{ZP}	H	G	*f*
-3536.654823	-3535.317085	-3535.230481	-3535.443442	-299

TS(41): spiro bisperoxo complex to oxo peroxo complex

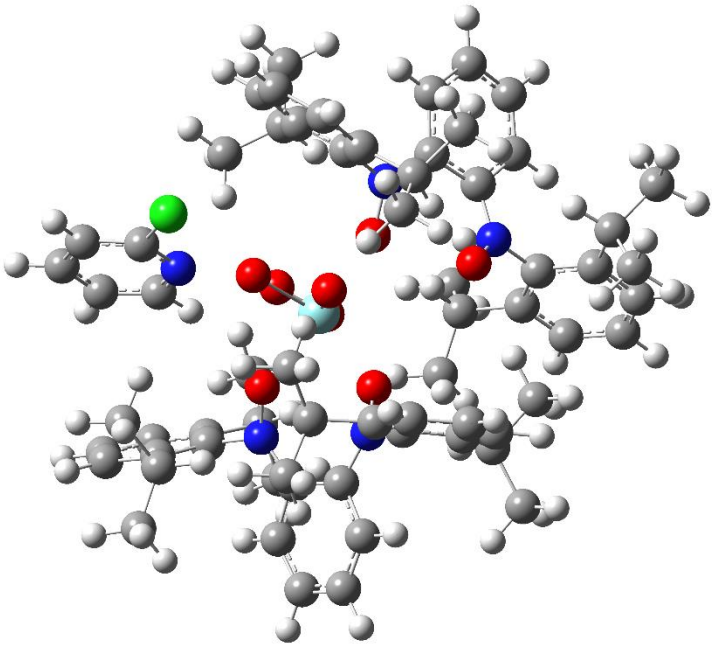

Fig. S102: spiro bisperoxo complex to oxo peroxo complex

E_{SCF}	E_{ZP}	H	G	*f*
-3461.505222	-3460.171103	-3460.085140	-3460.299216	-399

TS(42): η^3-ozone complex to peroxo complex

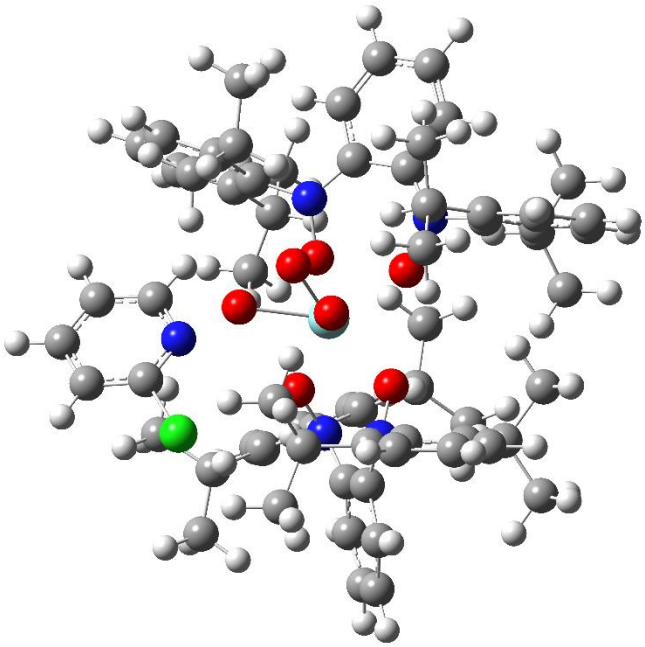

Fig. S103: η^3-ozone complex to peroxo complex

E_{SCF}	E_{ZP}	H	G	*f*
-3386.336472	-3385.004399	-3384.920719	-3385.127533	-342

TS(43): peroxo complex to oxo complex

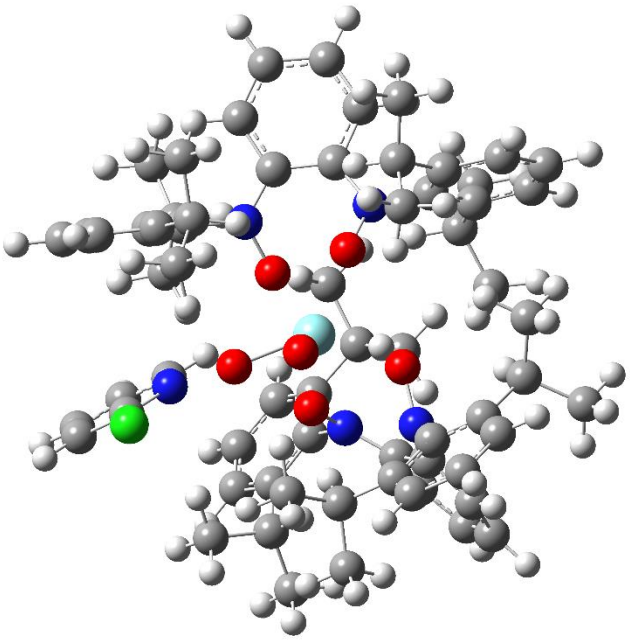

Fig. S104: peroxo complex to oxo complex

E_{SCF}	E_{ZP}	H	G	*f*
-3311.189228	-3309.860013	-3309.777534	-3309.980573	-398

2.2.5 Triplet Transition States (pyridine involved structures)

TS(32): peroxo η^3-ozone complex to spiro bisperoxo complex

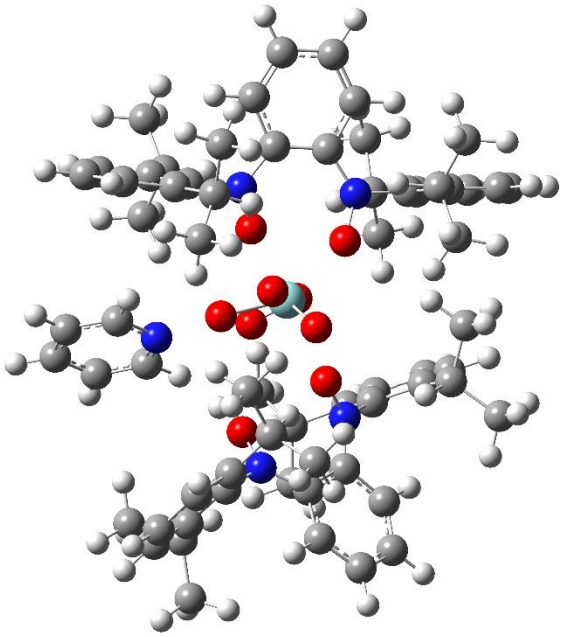

Fig. S105: peroxo η^3-ozone complex to spiro bisperoxo complex

E_{SCF}	E_{ZP}	H	G	*f*
-3522.326489	-3520.979071	-3520.893398	-3521.105781	-227

TS(33): spiro bisperoxo complex to oxo peroxo complex

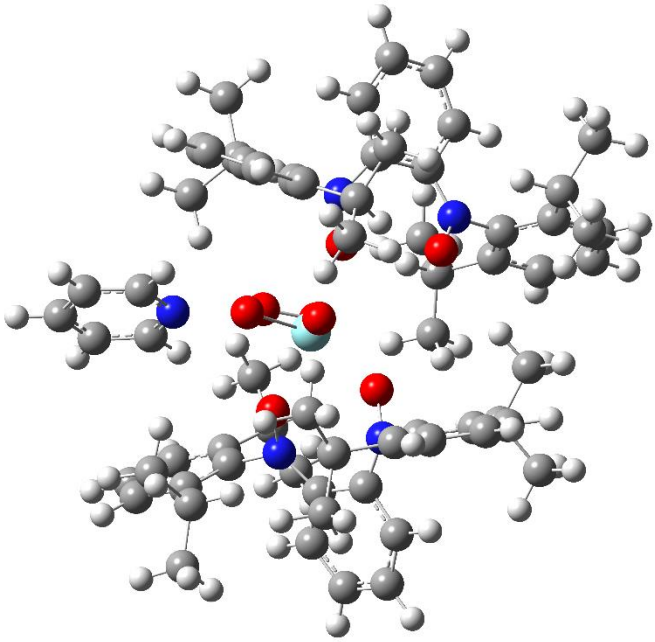

Fig. S106: spiro bisperoxo complex to oxo peroxo complex

E_{SCF}	E_{ZP}	H	G	*f*
-3447.147533	-3445.804139	-3445.720751	-3445.928145	-368

TS(34): η^3-ozone complex to peroxo complex

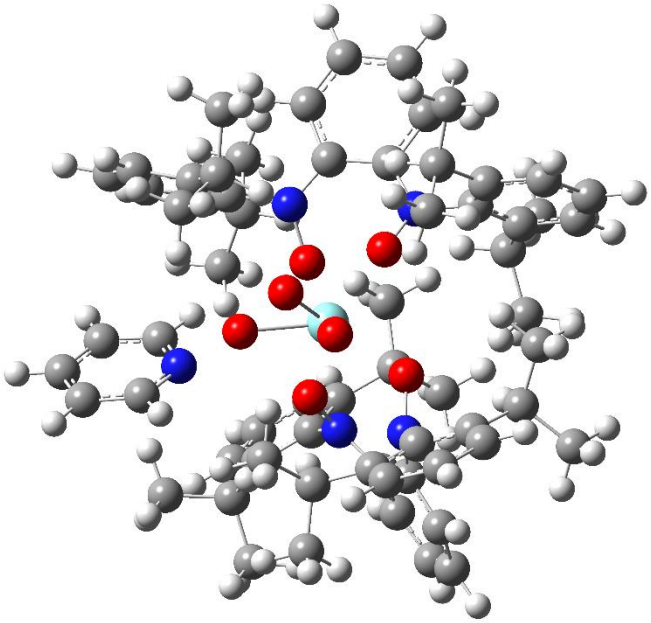

Fig. S107: η^3-ozone complex to peroxo complex

E_{SCF}	E_{ZP}	H	G	*f*
-3372.006297	-3370.664463	-3370.581950	-3370.786228	-262

TS(35): peroxo complex to oxo complex

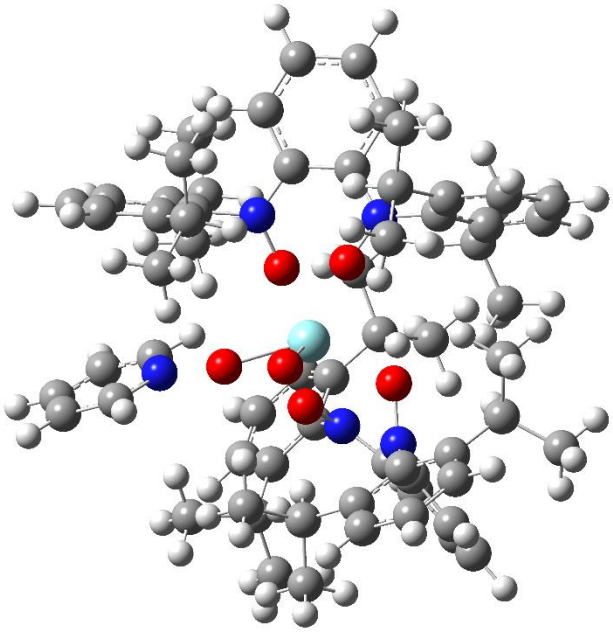

Fig. S108: peroxo complex to oxo complex

E_{SCF}	E_{ZP}	H	G	*f*
-3296.860443	-3295.521318	-3295.439885	-3295.641564	-341

2.2.6 Triplet Transition States (4-nitroquinoline involved structures)

TS(36): peroxo η^3-ozone complex to spiro bisperoxo complex

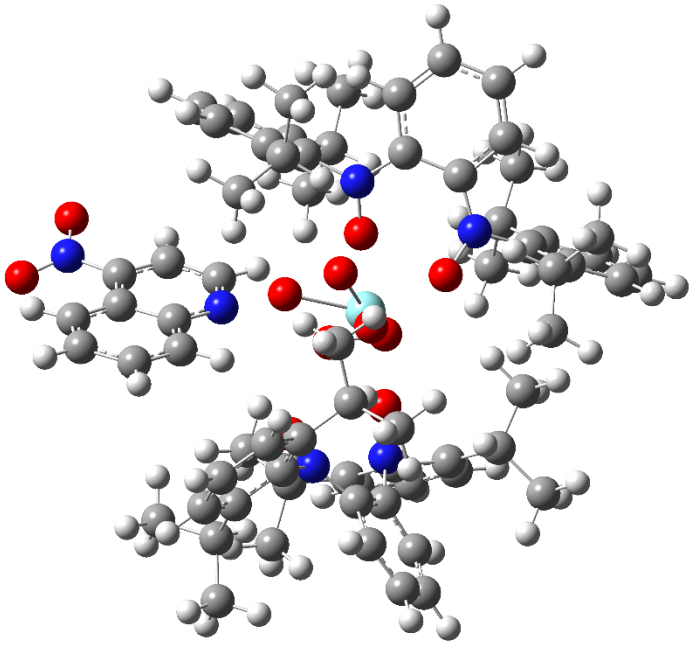

Fig. S109: peroxo η^3-ozone complex to spiro bisperoxo complex

E_{SCF}	E_{ZP}	H	G	*f*
-3880.408940	-3879.013444	-3878.922410	-3879.147678	-283

TS(37): spiro bisperoxo complex to oxo peroxo complex

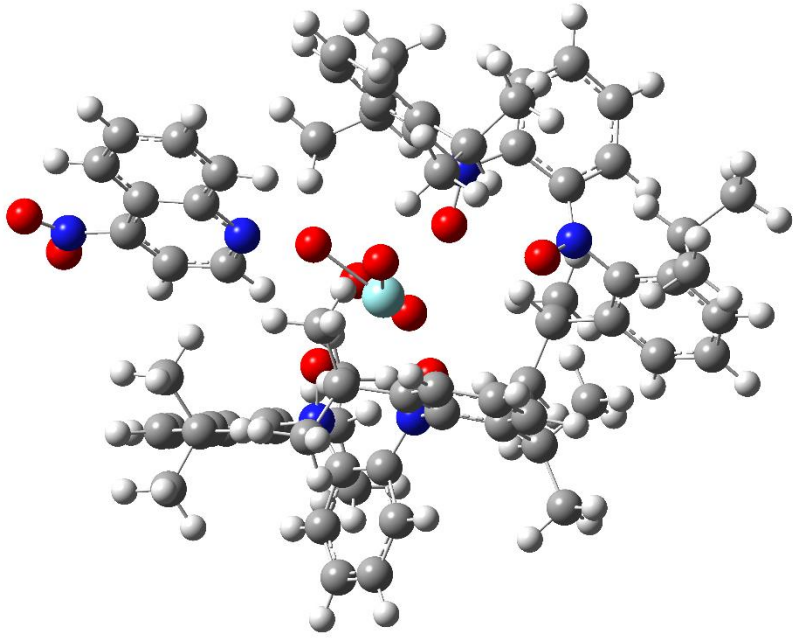

Fig. S110: spiro bisperoxo complex to oxo peroxo complex

E_{SCF}	E_{ZP}	H	G	*f*
-3805.260107	-3803.867360	-3803.777465	-3804.000693	-390

TS(38): η^3-ozone complex to peroxo complex

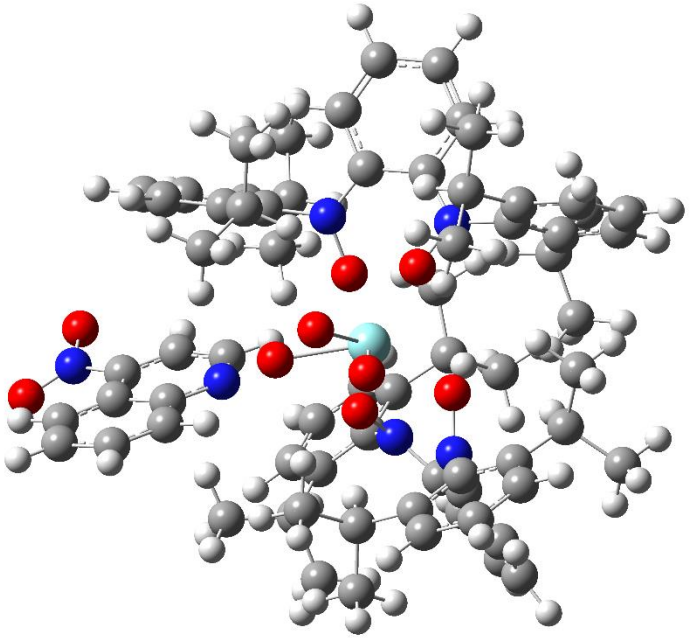

Fig. S111: η^3-ozone complex to peroxo complex

E_{SCF}	E_{ZP}	H	G	*f*
-3730.090484	-3728.699522	-3728.612067	-3728.826029	-314

TS(39): peroxo complex to oxo complex

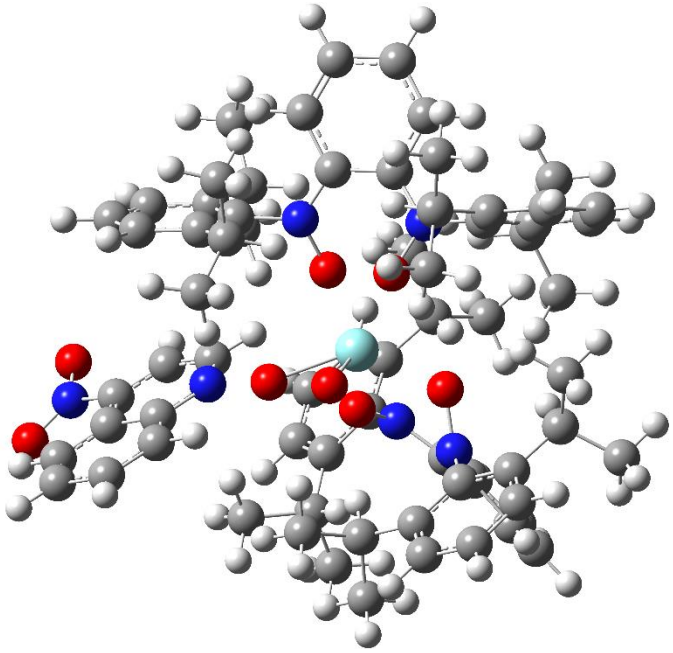

Fig. S112: peroxo complex to oxo complex

E_{SCF}	E_{ZP}	H	G	*f*
-3654.944275	-3653.556634	-3653.470027	-3653.684005	-385

2.3. RuTDCPP (Tethered) Catalytic System (B3LYP/LANL2DZ)

2.3.1 Singlet Ground States

bare complex

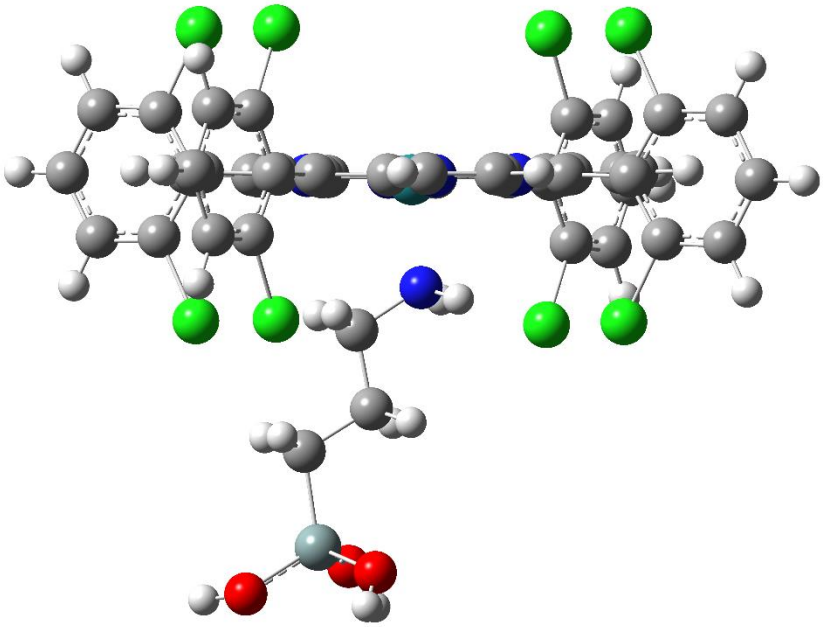

Fig. S113: bare complex

E_{SCF}	E_{ZP}	H	G
-2526.263396	-2525.583450	-2525.522619	-2525.687582

oxo complex

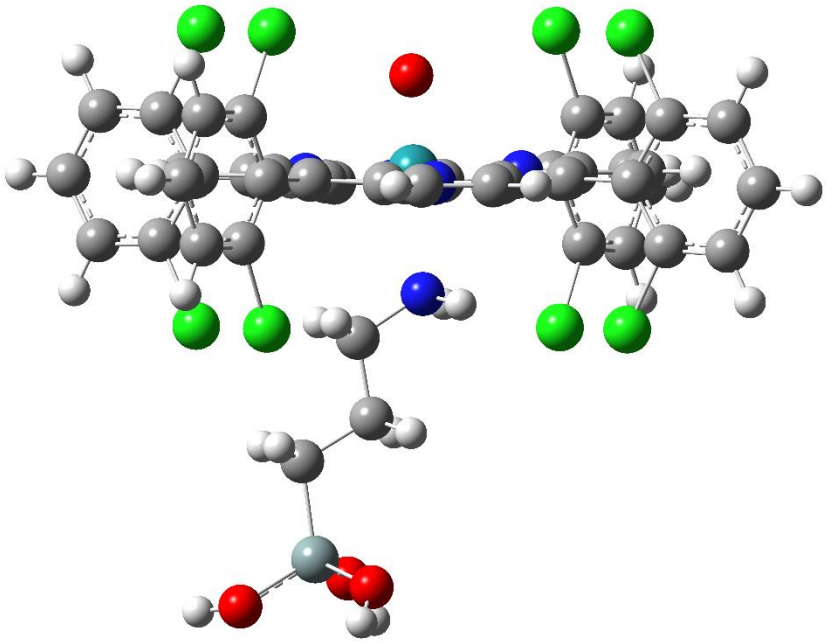

Fig. S114: oxo complex

E_{SCF}	E_{ZP}	H	G
-2601.423796	-2600.741449	-2600.679189	-2600.846757

with adsorbed propene molecule

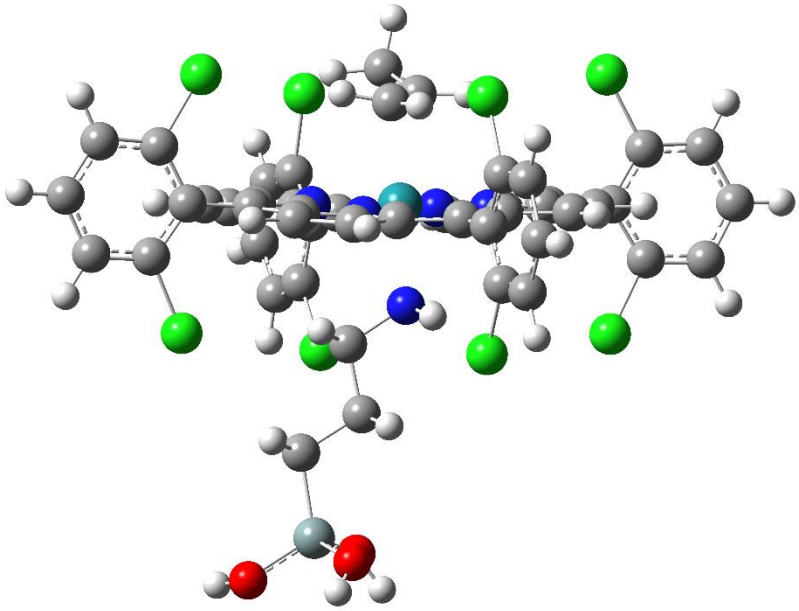

Fig. S115: with adsorbed propene molecule

E_{SCF}	E_{ZP}	H	G
-2644.173568	-2643.410832	-2643.345298	-2643.518674

with adsorbed propylene oxide molecule

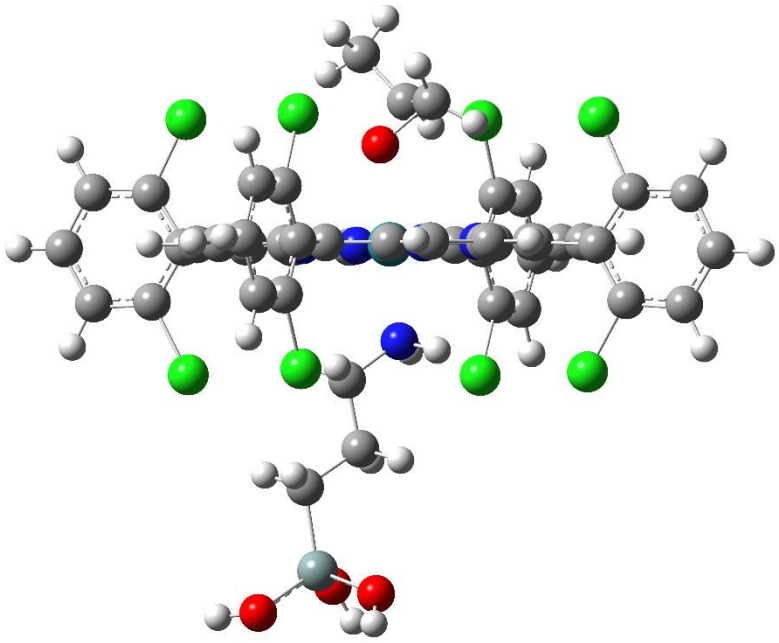

Fig. S116: with adsorbed propylene oxide molecule

E_{SCF}	E_{ZP}	H	G
-2719.370028	-2718.602755	-2718.536193	-2718.712847

with adsorbed 2,6-dimethylpyridine molecule

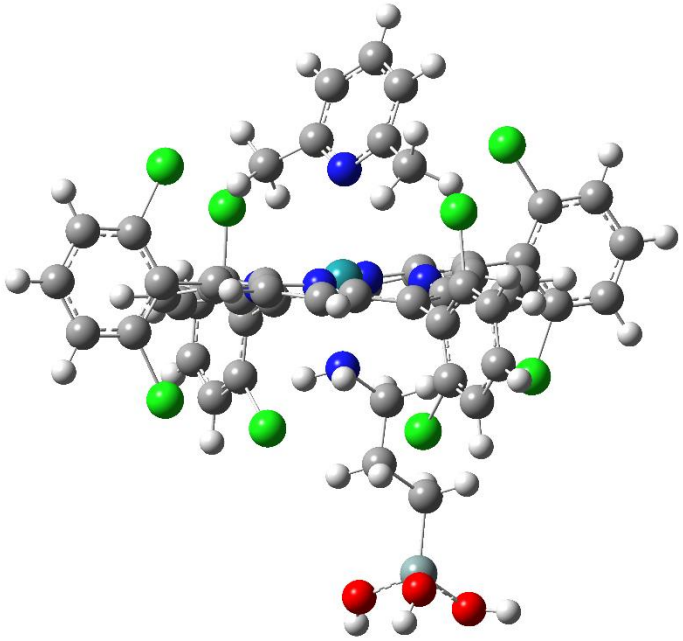

Fig. S117: with adsorbed 2,6-dimethylpyridine molecule

E_{SCF}	E_{ZP}	H	G
-2853.134976	-2852.308066	-2852.238562	-2852.420987

with adsorbed 2,6-dimethylpyridine *N*-oxide molecule

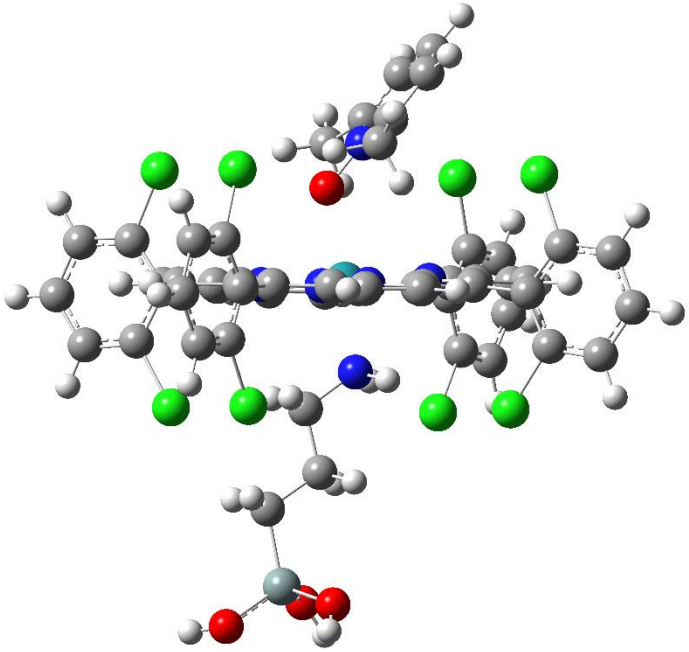

Fig. S118: with adsorbed 2,6-dimethylpyridine *N*-oxide molecule

E_{SCF}	E_{ZP}	H	G
-2928.326852	-2927.496677	-2927.425950	-2927.611029

with adsorbed pyridine molecule

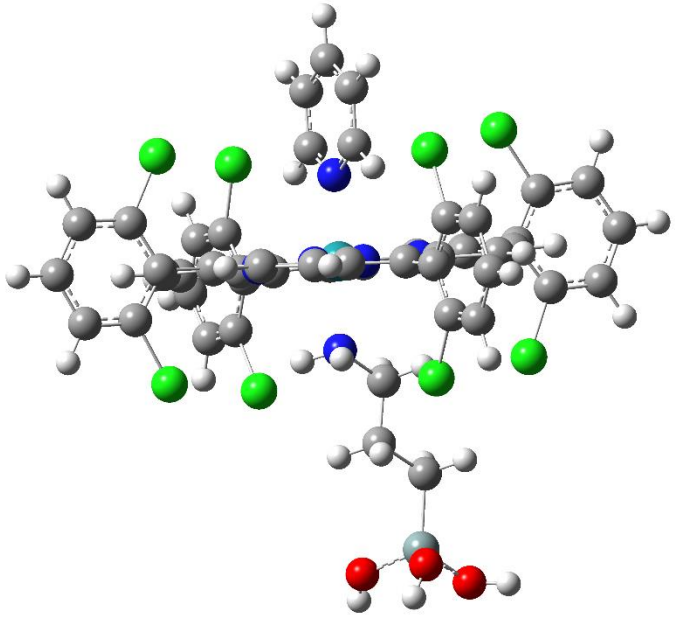

Fig. S119: with adsorbed pyridine molecule

E_{SCF}	E_{ZP}	H	G
-2774.553048	-2773.781545	-2773.715333	-2773.891439

with adsorbed pyridine *N*-oxide molecule

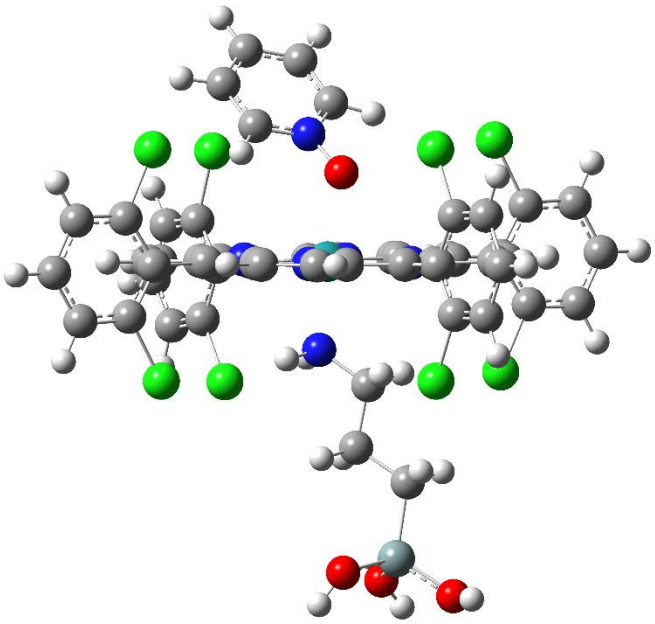

Fig. S120: with adsorbed pyridine *N*-oxide molecule

E_{SCF}	E_{ZP}	H	G
-2849.701040	-2848.926835	-2848.859219	-2849.040840

2.3.2 Triplet Ground States

bare complex

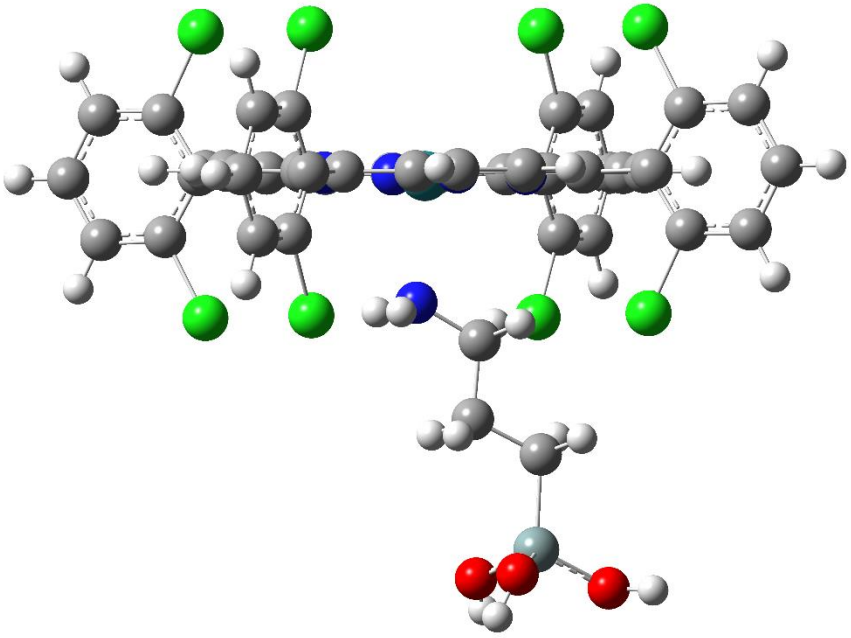

Fig. S121: bare complex

E_{SCF}	E_{ZP}	H	G
-2526.220481	-2525.543126	-2525.481466	-2525.649593

oxo complex

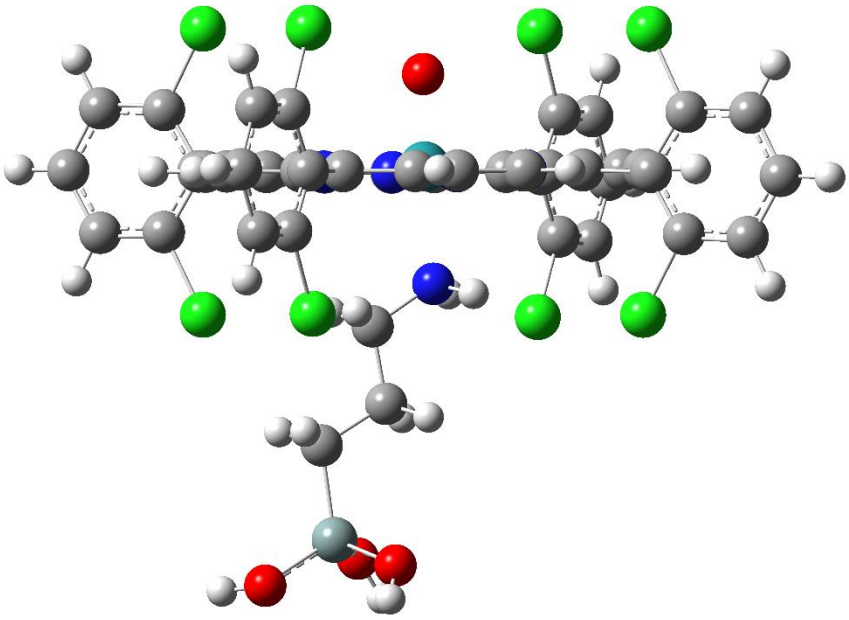

Fig. S122: oxo complex

E_{SCF}	E_{ZP}	H	G
-2601.459665	-2600.777382	-2600.715115	-2600.883810

with adsorbed propene molecule

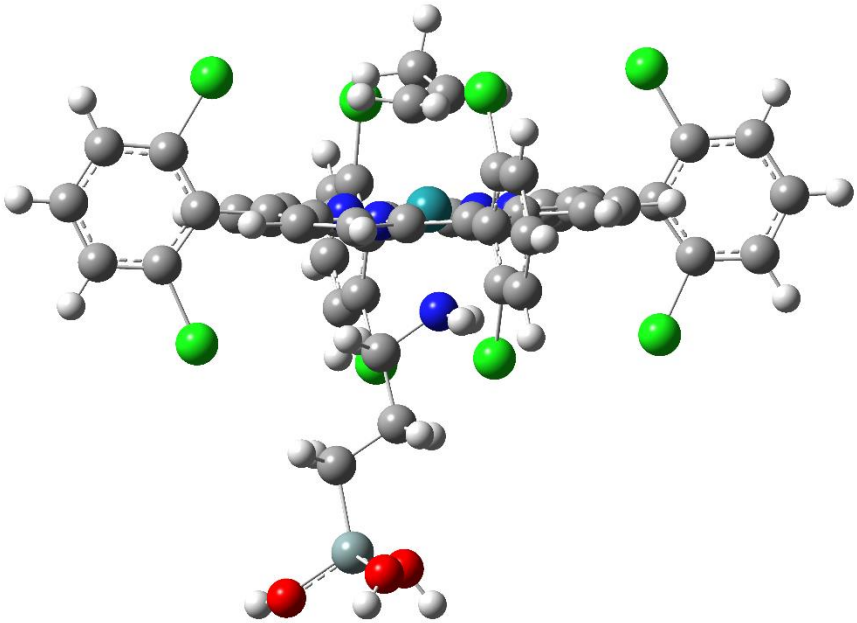

Fig. S123: with adsorbed propene molecule

E_{SCF}	E_{ZP}	H	G
-2644.126470	-2643.365759	-2643.299857	-2643.299857

with adsorbed propylene oxide molecule

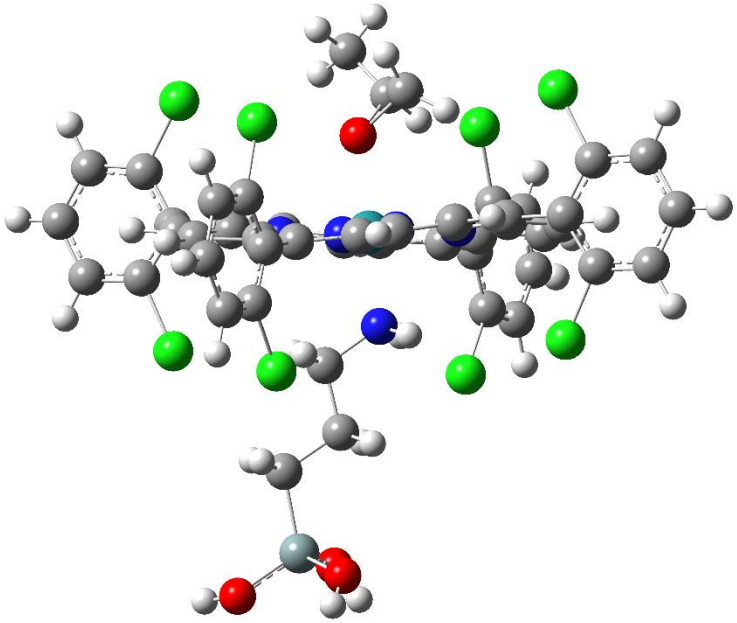

Fig. S124: with adsorbed propylene oxide molecule

E_{SCF}	E_{ZP}	H	G
-2719.310022	-2718.545566	-2718.478393	-2718.658549

with adsorbed propylene oxide molecule (*)

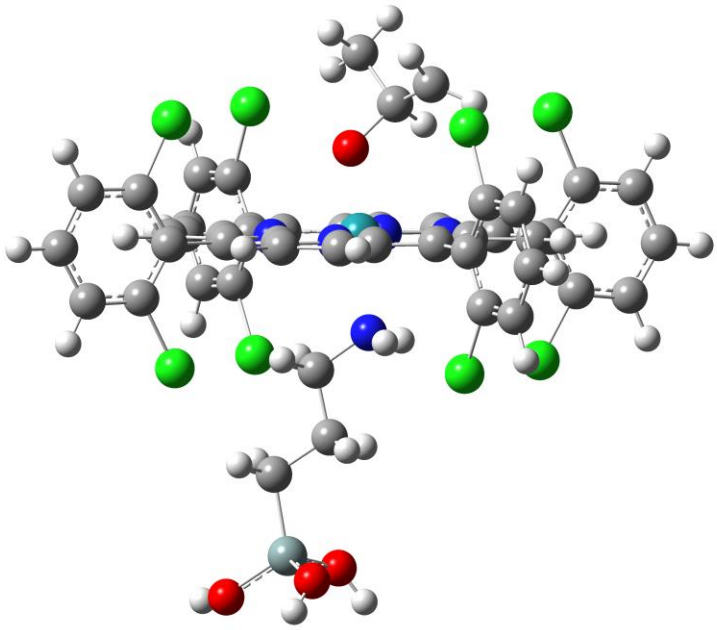

Fig. S125: with adsorbed propylene oxide molecule (*)

E_{SCF}	E_{ZP}	H	G
-2719.335928	-2718.572533	-2718.505160	-2718.684756

with adsorbed 2,6-dimethylpyridine molecule

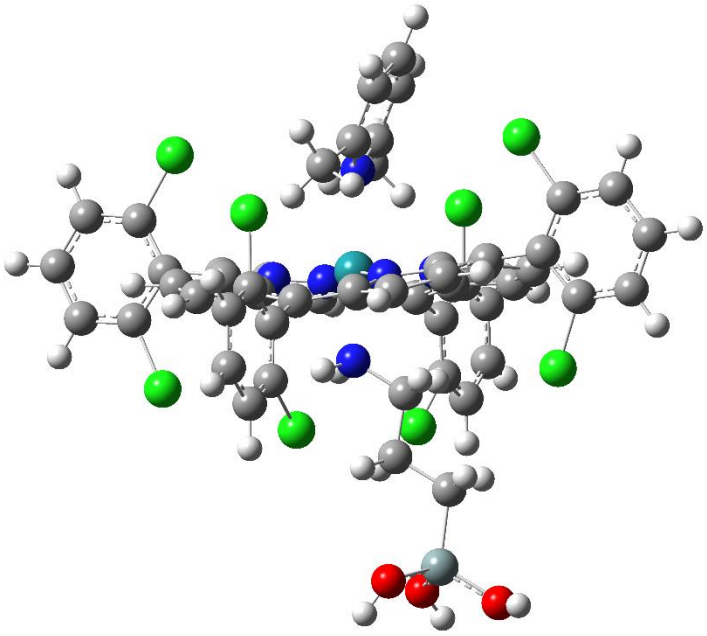

Fig. S126: with adsorbed 2,6-dimethylpyridine molecule

E_{SCF}	E_{ZP}	H	G
-2853.092973	-2852.267888	-2852.198315	-2852.380608

with adsorbed 2,6-dimethylpyridine *N*-oxide molecule

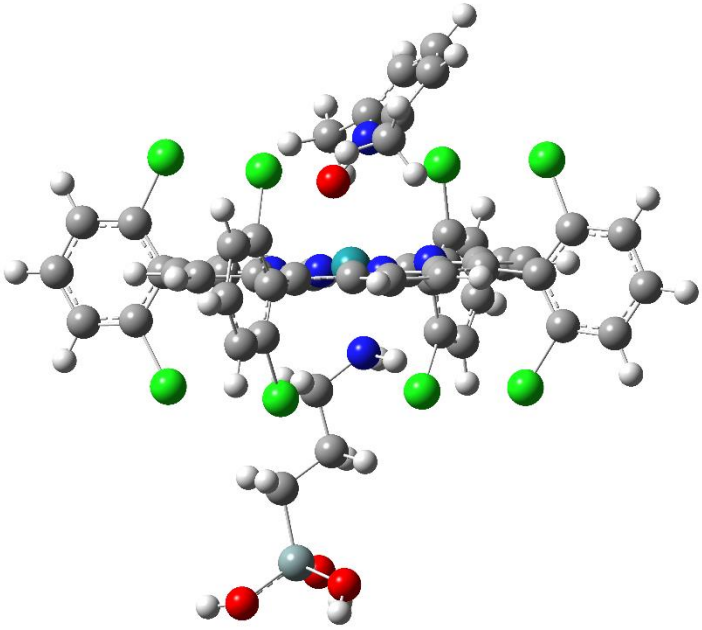

Fig. S127: with adsorbed 2,6-dimethylpyridine *N*-oxide molecule

E_{SCF}	E_{ZP}	H	G
-2928.290666	-2927.461809	-2927.391150	-2927.576285

with adsorbed pyridine molecule

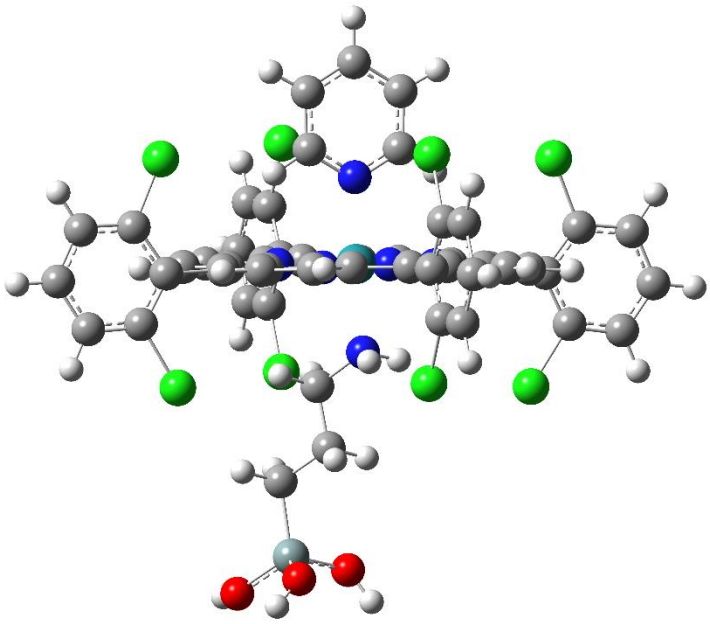

Fig. S128: with adsorbed pyridine molecule

E_{SCF}	E_{ZP}	H	G
-2774.508468	-2773.739568	-2773.672883	-2773.851102

with adsorbed pyridine *N*-oxide molecule

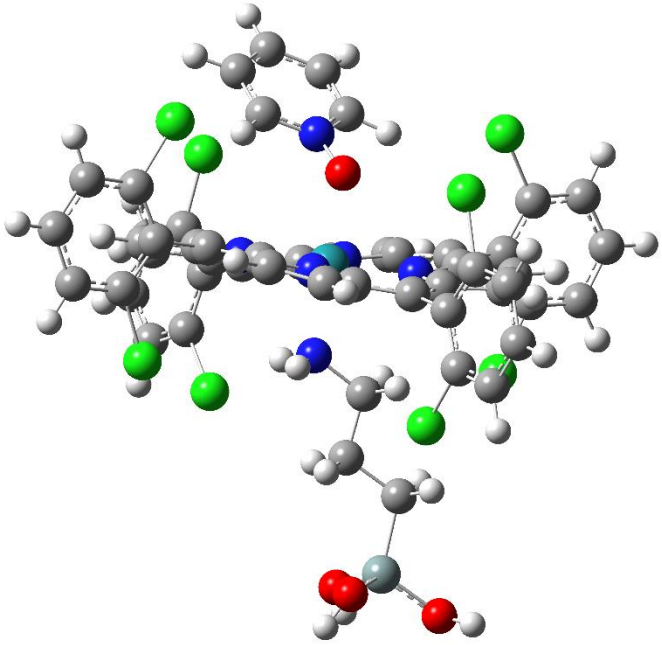

Fig. S129: with adsorbed pyridine *N*-oxide molecule

E_{SCF}	E_{ZP}	H	G
-2849.645087	-2848.873286	-2848.805364	-2848.986451

2.3.3 Quintet Ground States

bare complex

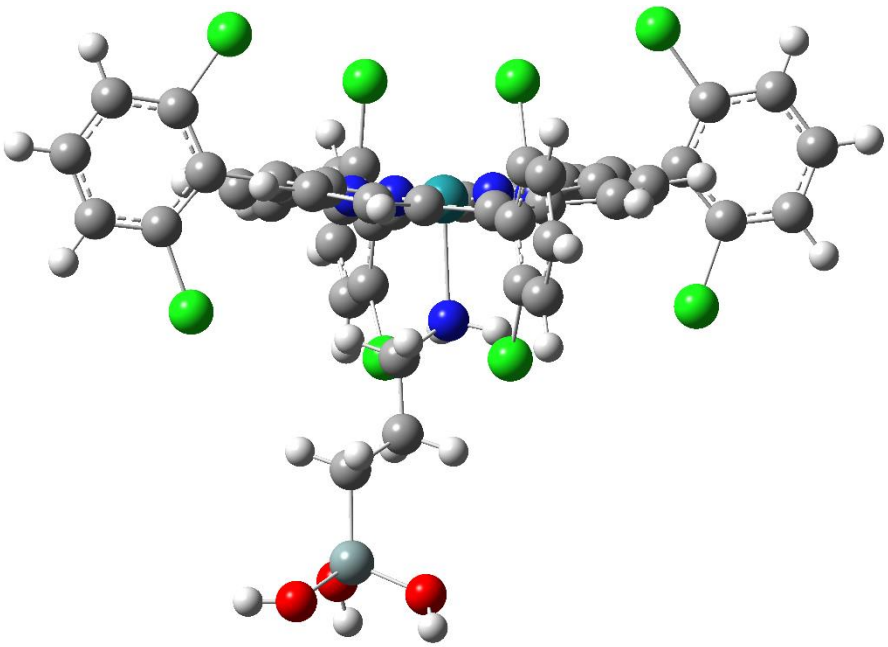

Fig. S130: bare complex

E_{SCF}	E_{ZP}	H	G
-2526.177279	-2525.502776	-2525.440655	-2525.611094

oxo complex

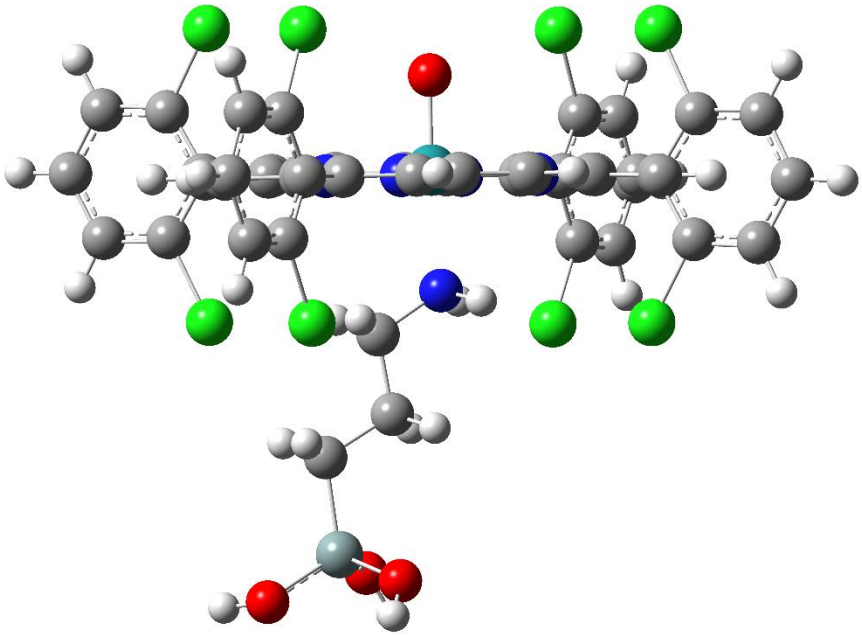

Fig. S131: oxo complex

E_{SCF}	E_{ZP}	H	G
-2601.396829	-2600.719495	-2600.656538	-2600.827603

with adsorbed propene molecule

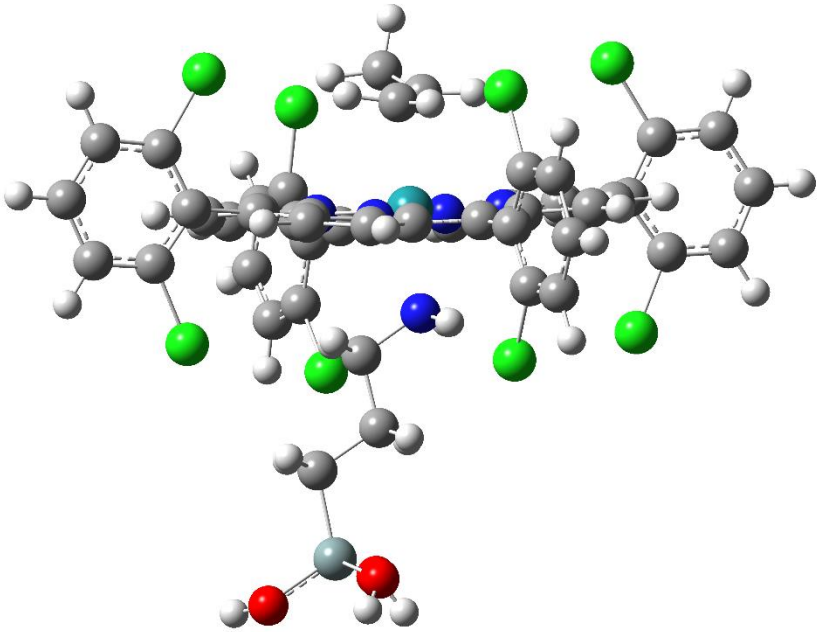

Fig. S132: with adsorbed propene molecule

E_{SCF}	E_{ZP}	H	G
-2644.068924	-2643.310632	-2643.244393	-2643.420859

with adsorbed propylene oxide molecule

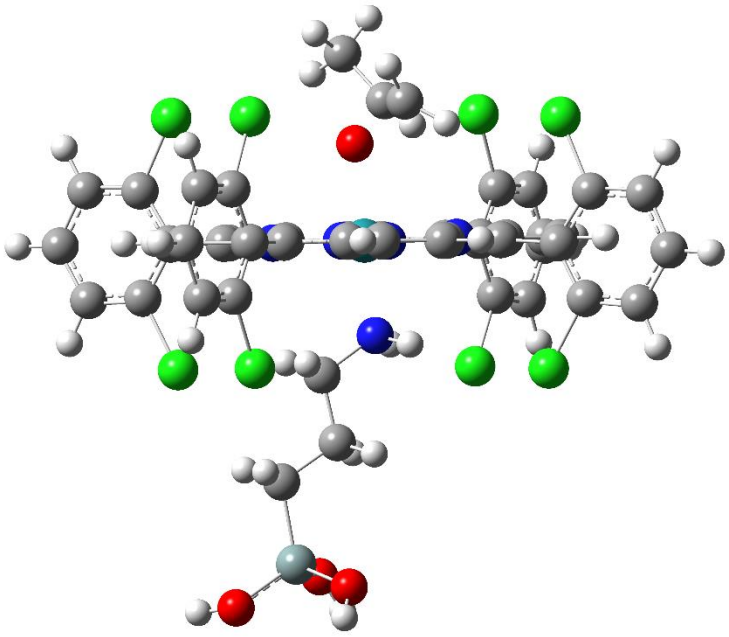

Fig. S133: with adsorbed propylene oxide molecule

E_{SCF}	E_{ZP}	H	G
-2719.266126	-2718.503830	-2718.436472	-2718.616661

with adsorbed 2,6-dimethylpyridine molecule

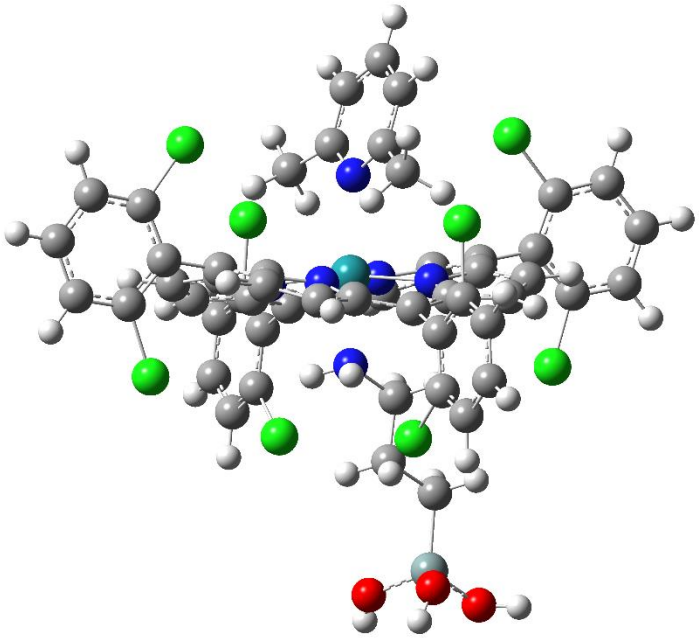

Fig. S134: with adsorbed 2,6-dimethylpyridine molecule

E_{SCF}	E_{ZP}	H	G
-2853.036978	-2852.214087	-2852.144171	-2852.327951

with adsorbed 2,6-dimethylpyridine *N*-oxide molecule

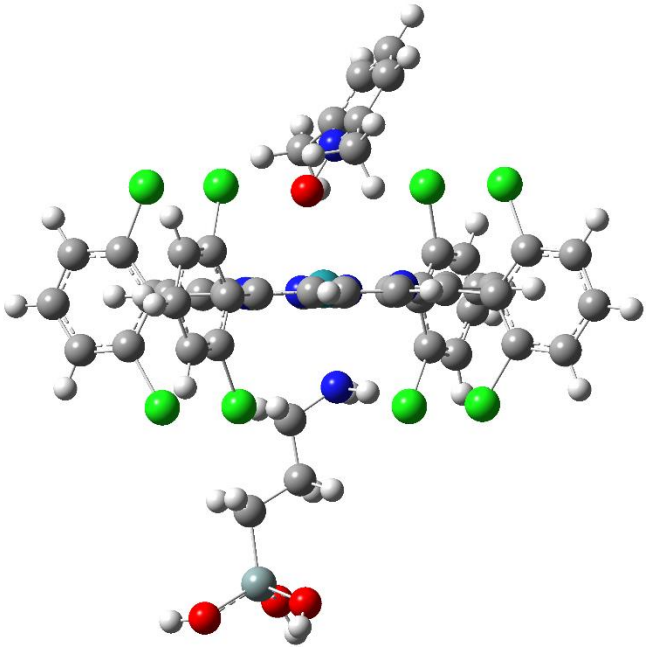

Fig. S135: with adsorbed 2,6-dimethylpyridine *N*-oxide molecule

E_{SCF}	E_{ZP}	H	G
-2928.246842	-2927.421867	-2927.349581	-2927.542356

2.3.4 Triplet Transition State

TS(10): propylene oxide like intermediate formation

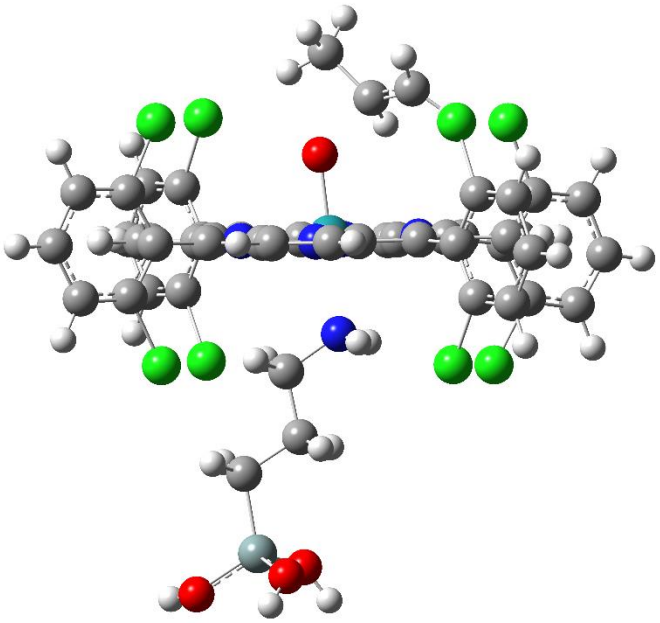

Fig. S136: propylene oxide like intermediate formation

E_{SCF}	E_{ZP}	H	G	*f*
-2719.322492	-2718.560062	-2718.492966	-2718.671878	-531

2.3.5 Approximate Crossing Point Geometries

Approximate CP(2): oxo formation (singlet geometry)

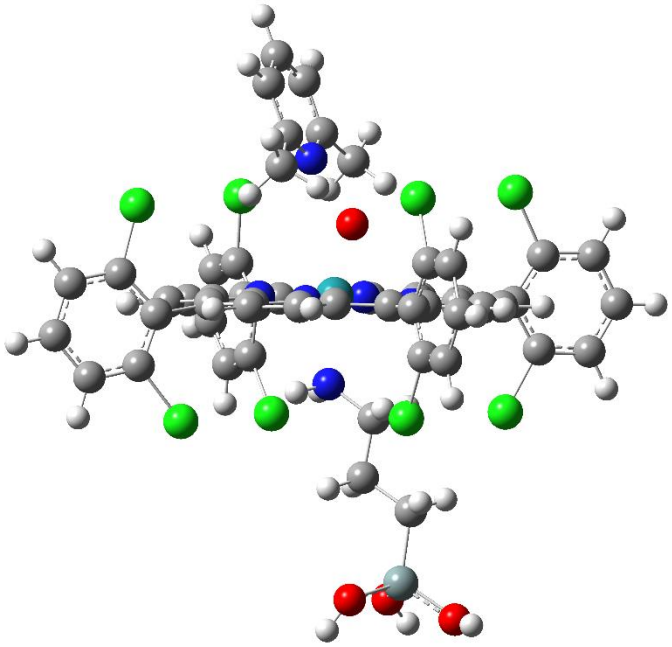

Fig. S137: oxo formation (singlet geometry)

	E_{SCF}	E_{ZP}	H	G
Singlet	-2928.281192	-2927.453587	-2927.382846	-2927.568494
Triplet	-2928.282122	n/a	n/a	n/a

N	-0.191861	-2.054995	-0.338803
N	-2.095898	-0.073184	0.633598
N	1.621623	0.081315	-1.213896
N	-0.341165	2.062739	-0.290165
C	0.844840	-2.836814	-0.850864
C	0.533619	-4.247514	-0.625705
C	-0.663041	-4.303032	0.038514
C	-1.121052	-2.928012	0.223996
H	1.158676	-5.076653	-0.925771
H	-1.191363	-5.184544	0.373262
C	-2.301689	-2.551131	0.886808
C	2.027545	-2.362194	-1.441651
C	-3.951796	-0.843211	1.789730
C	-3.998358	0.532782	1.811831
C	-2.831411	1.017640	1.099777
C	-2.754833	-1.225198	1.065225
H	-4.663350	-1.530617	2.224400
H	-4.754523	1.155910	2.267603
C	-2.471513	2.376349	0.959344
C	2.300746	1.229373	-1.587273
C	3.555405	0.852301	-2.220415
C	3.607486	-0.522965	-2.232810
C	2.384909	-1.004833	-1.607923

H	4.290117	1.542259	-2.610589
H	4.392164	-1.148305	-2.634359
C	-0.970296	4.261515	0.141460
C	0.221582	4.307279	-0.532331
C	0.632301	2.928100	-0.790386
C	-1.326002	2.853079	0.298650
H	-1.558122	5.094916	0.499462
H	0.782159	5.185918	-0.818730
C	1.843741	2.552712	-1.394637
C	-3.088923	-3.637059	1.565803
C	-4.216555	-4.266527	0.993488
C	-4.945335	-5.281674	1.630779
C	-4.548243	-5.705895	2.910128
C	-3.438489	-5.110241	3.534455
C	-2.742405	-4.099121	2.858004
H	-5.801636	-5.726989	1.135667
H	-5.100411	-6.491559	3.417839
H	-3.121082	-5.419847	4.524392
C	3.016251	-3.387580	-1.922522
C	4.029760	-3.915544	-1.091174
C	4.966595	-4.867368	-1.517879
C	4.907445	-5.331609	-2.843404
C	3.920015	-4.842790	-3.715946
C	3.003946	-3.891418	-3.243434
H	5.721083	-5.234090	-0.830195
H	3.859650	-5.190306	-4.741800
C	2.751136	3.658279	-1.857682
C	3.727279	4.242350	-1.019356
C	4.587197	5.271138	-1.428932
C	4.484984	5.758576	-2.743501
C	3.531403	5.216377	-3.622117
C	2.692083	4.188727	-3.166826
H	5.315758	5.679131	-0.736556
H	5.142647	6.555103	-3.079756
H	3.438479	5.581161	-4.639515
C	-3.321632	3.384015	1.681573
C	-2.986531	3.828483	2.983100
C	-3.740307	4.765474	3.702864
C	-4.899810	5.300611	3.115099
C	-5.287430	4.890619	1.828257
C	-4.499952	3.950454	1.147125
H	-3.428860	5.064845	4.697835
H	-6.181056	5.289746	1.360486
H	-5.497329	6.028185	3.656843
H	5.625064	-6.068416	-3.192959
Cl	-1.326144	-3.355955	3.731859
Cl	-4.791155	-3.758538	-0.656911
Cl	-5.065298	3.456909	-0.510822
Cl	-1.507175	3.159344	3.811866
Cl	1.479118	3.527096	-4.346991
Cl	3.903786	3.660391	0.699263
Cl	1.751505	-3.295252	-4.417322
Cl	4.155682	-3.359577	0.640414
H	0.241910	-0.825931	2.104349
H	0.193196	0.834262	2.114632
N	0.622289	0.018829	1.665860

C	2.111254	0.060158	1.829054
H	2.475898	0.963204	1.330292
H	2.527344	-0.800467	1.297119
C	2.560796	0.044680	3.304880
H	2.132782	0.908713	3.833481
H	2.175295	-0.860105	3.798401
C	4.107255	0.082177	3.418102
H	4.490165	0.991839	2.933381
H	4.542755	-0.767665	2.873281
Si	4.731860	0.028715	5.174698
O	4.118015	1.392630	5.948488
H	3.997921	1.537488	6.898558
O	4.224733	-1.360105	5.979113
H	4.801235	-2.025155	6.384187
O	6.420404	-0.042171	5.297408
H	7.074760	0.636146	5.074107
Ru	-0.303867	0.002977	-0.380237
C	-2.931764	-1.263096	-3.612360
C	-3.997508	-1.319896	-4.538332
C	-4.601518	-0.128153	-4.972186
C	-4.117110	1.102684	-4.499013
C	-3.049395	1.121263	-3.573761
H	-5.422478	-0.157118	-5.684353
H	-4.326587	-2.285766	-4.908642
H	-4.540659	2.042805	-4.838251
N	-2.529080	-0.055442	-3.142138
O	-0.752910	0.020864	-2.225952
C	-2.446099	2.405689	-3.072500
H	-2.778161	2.615746	-2.050988
H	-1.357823	2.313854	-3.046017
H	-2.742262	3.245617	-3.710073
C	-2.203762	-2.497273	-3.152363
H	-1.131707	-2.293736	-3.106437
H	-2.523186	-2.781656	-2.144746
H	-2.403964	-3.337027	-3.826450

Approximate CP(3): propylene oxide formation (singlet geometry)

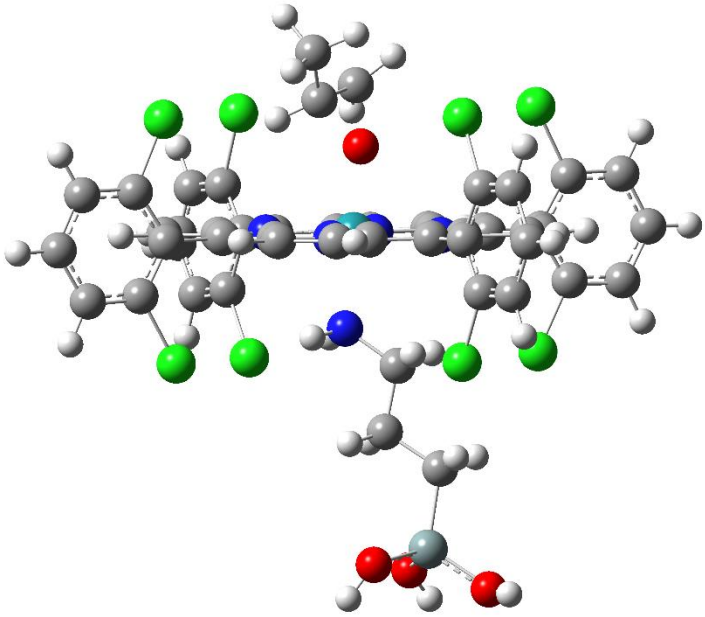

Fig. S138: propylene oxide formation (singlet geometry)

	E_{SCF}	E_{ZP}	H	G
Singlet	-2719.329388	-2718.565139	-2718.498069	-2718.675873
Triplet	-2719.324565	-2718.561366	-2718.495796	-2718.669704

N	-2.291474	0.173862	-0.029454
N	-0.118389	2.068682	-0.551958
N	-0.457060	-2.041905	-0.476911
N	1.698901	-0.168505	-1.058477
C	-3.173060	-0.869495	0.249089
C	-4.471411	-0.316667	0.616585
C	-4.361075	1.050170	0.570299
C	-2.991690	1.363998	0.176893
H	-5.345056	-0.898198	0.875079
H	-5.128589	1.779822	0.785909
C	-2.459495	2.661566	0.062040
C	-2.853517	-2.239224	0.203435
C	-0.603271	4.334308	-0.429109
C	0.717955	4.219128	-0.787298
C	1.022787	2.796871	-0.866604
C	-1.130727	2.983586	-0.286063
H	-1.168847	5.243511	-0.282719
H	1.418273	5.018447	-0.984020
C	2.274605	2.250879	-1.216837
C	0.552979	-2.963176	-0.764952
C	0.027718	-4.309180	-0.607328
C	-1.288856	-4.196423	-0.225774
C	-1.599302	-2.778616	-0.148190
H	0.589092	-5.218830	-0.766820
H	-1.984689	-4.997958	-0.021977
C	3.878487	0.334486	-1.690145

C	3.769195	-1.031409	-1.667744
C	2.398163	-1.348232	-1.274833
C	2.576980	0.880578	-1.311991
H	4.750040	0.921758	-1.942540
H	4.534598	-1.758574	-1.898957
C	1.874478	-2.646593	-1.136194
C	-3.380005	3.807014	0.373404
C	-4.202142	4.415966	-0.600810
C	-5.067005	5.484709	-0.323503
C	-5.129821	5.987648	0.987612
C	-4.334220	5.420177	1.998436
C	-3.485530	4.352953	1.672897
H	-5.674149	5.910973	-1.114931
H	-5.793756	6.815334	1.220198
H	-4.371114	5.795220	3.015588
C	-3.927006	-3.209547	0.605428
C	-4.086734	-3.633921	1.944598
C	-5.074724	-4.538532	2.357906
C	-5.962121	-5.060102	1.400186
C	-5.851282	-4.673286	0.053341
C	-4.846554	-3.765481	-0.311442
H	-5.146482	-4.826145	3.401342
H	-6.527986	-5.065711	-0.698151
C	2.808120	-3.795502	-1.393188
C	3.597771	-4.372733	-0.372993
C	4.480651	-5.440943	-0.585294
C	4.596797	-5.979074	-1.878782
C	3.834587	-5.446645	-2.932887
C	2.964852	-4.377717	-2.671705
H	5.060430	-5.839570	0.240253
H	5.275518	-6.806826	-2.063500
H	3.911960	-5.849868	-3.936948
C	3.379422	3.222081	-1.526157
C	4.244117	3.732582	-0.532435
C	5.279758	4.640313	-0.795209
C	5.481637	5.074975	-2.116719
C	4.651272	4.601407	-3.147053
C	3.627029	3.694887	-2.835649
H	5.909410	4.996591	0.012972
H	4.792176	4.927849	-4.171938
H	6.278939	5.777780	-2.341205
H	-6.734214	-5.762260	1.701460
Cl	-2.482117	3.653804	3.023910
Cl	-4.160859	3.807435	-2.314657
Cl	2.582751	3.121868	-4.206382
Cl	4.030511	3.210385	1.201812
Cl	2.006942	-3.731250	-4.075826
Cl	3.487428	-3.722637	1.326209
Cl	-4.750973	-3.300227	-2.069222
Cl	-2.966913	-2.990262	3.229281
H	-0.468871	-0.681871	1.980040
H	-0.333380	0.967612	1.898534
N	0.090376	0.085407	1.592696
C	1.504713	-0.004633	2.086434
H	2.062119	0.825411	1.641784
H	1.931586	-0.934770	1.698768

C	1.608461	0.039561	3.624306
H	1.161291	0.971115	4.000053
H	1.033281	-0.793120	4.056868
C	3.084975	-0.048468	4.089673
H	3.659479	0.779254	3.649371
H	3.541520	-0.977063	3.718420
Si	3.290592	0.000570	5.943423
O	2.581484	1.435894	6.464471
H	2.259872	1.660170	7.349983
O	2.549285	-1.311832	6.691449
H	2.983171	-1.956661	7.269957
O	4.901433	-0.113920	6.455416
H	5.618802	0.528772	6.352744
O	-0.601309	0.103147	-2.535762
C	-1.903697	-0.104021	-3.274567
C	-1.599873	-1.514725	-3.661129
H	-2.740381	-0.018059	-2.576120
C	-1.996754	0.913602	-4.403924
H	-1.807361	-2.330444	-2.974939
H	-0.955563	-1.703293	-4.517591
H	-1.127871	0.829225	-5.067662
H	-2.912249	0.755388	-4.991162
H	-2.017782	1.927821	-3.989051
Ru	-0.294228	-0.004079	-0.554689

2.4. Small Molecules (B3LYP/LANL2DZ)

(All structures shown in this section are singlets unless specified otherwise.)

O_2 (Triplet)

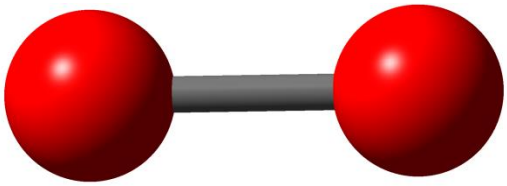

Fig. S139 O_2 (Triplet)

E_{SCF}	E_{ZP}	H	G
-150.314740	-150.311445	-150.308134	-150.331506

propene

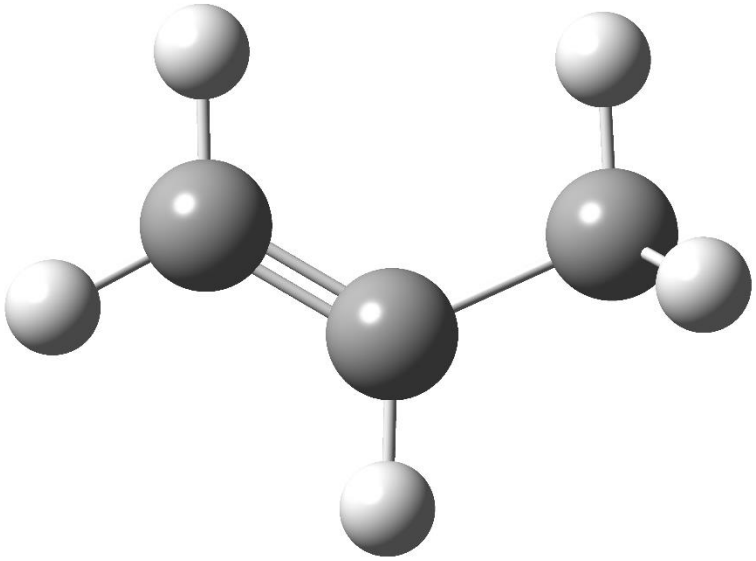

Fig. S140 propene

E_{SCF}	E_{ZP}	H	G
-117.891304	-117.811106	-117.806069	-117.836174

propylene oxide

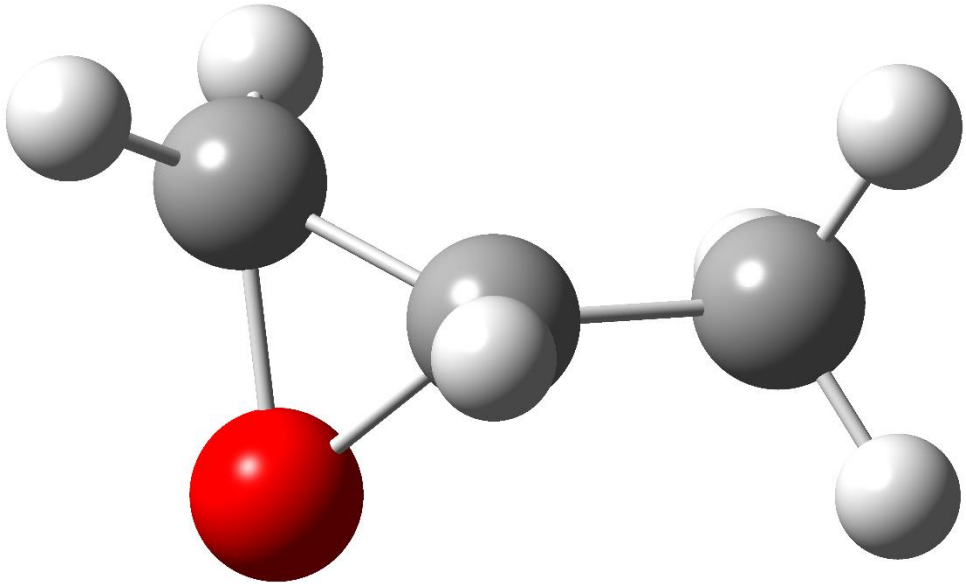

Fig. S141 propylene oxide

E_{SCF}	E_{ZP}	H	G
-193.074075	-192.988641	-192.983203	-193.015134

ethylene

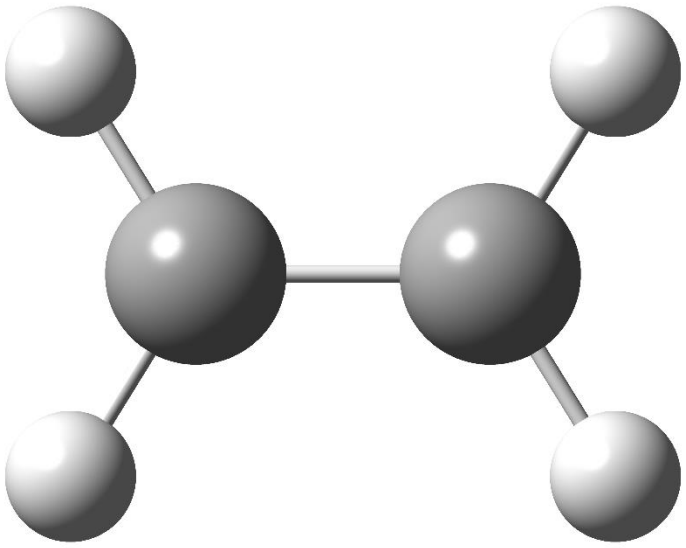

Fig. S142 ethylene

E_{SCF}	E_{ZP}	H	G
-78.578206	-78.526860	-78.522885	-78.549060

ethylene oxide

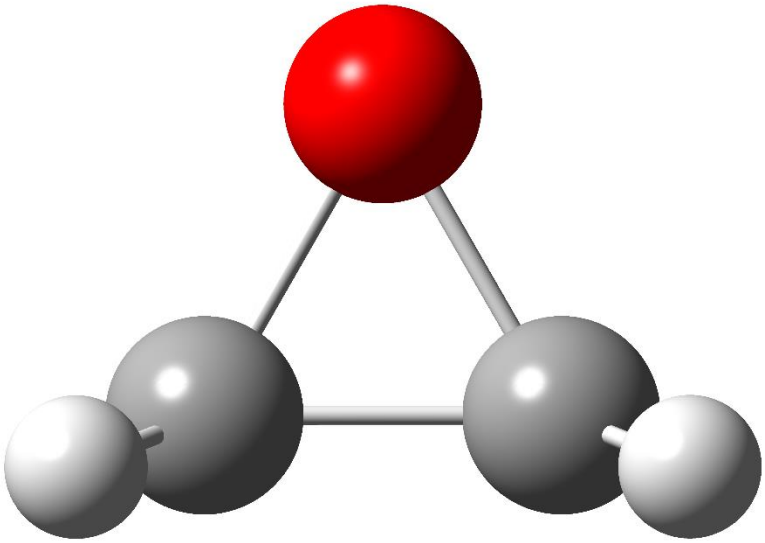

Fig. S143 ethylene oxide

E_{SCF}	E_{ZP}	H	G
-153.757542	-153.700573	-153.696408	-153.724766

2,6-dimethylpyridine

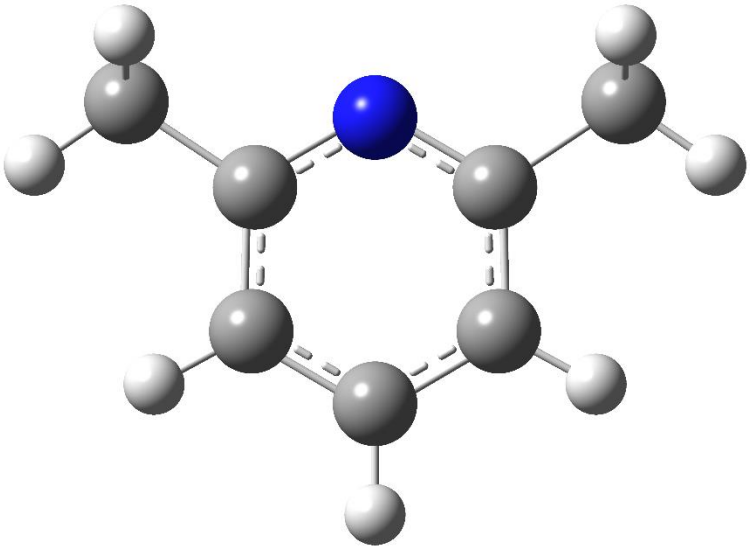

Fig. S144 2,6-dimethylpyridine

E_{SCF}	E_{ZP}	H	G
-326.869243	-326.724918	-326.716117	-326.758339

2,6-dimethylpyridine *N*-oxide

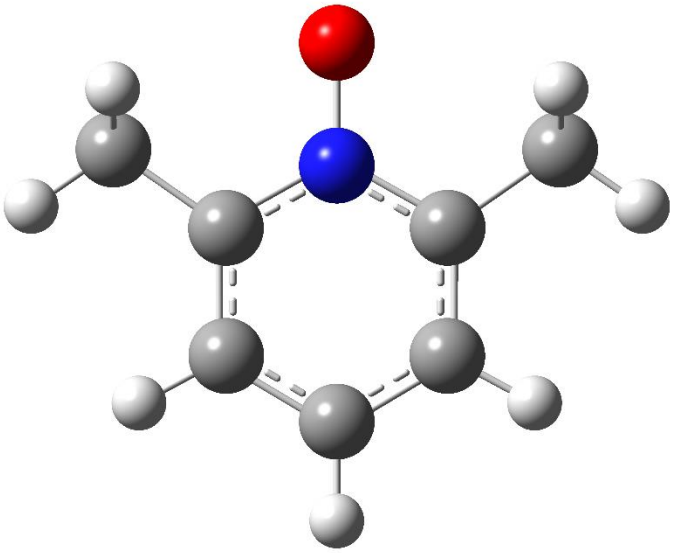

Fig. S145 2,6-dimethylpyridine *N*-oxide

E_{SCF}	E_{ZP}	H	G
-402.038435	-401.889319	-401.880186	-401.921747

2,6-dichloropyridine

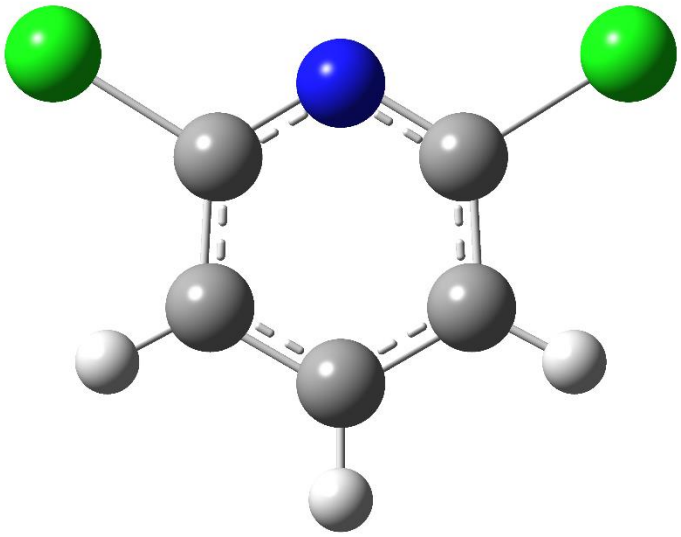

Fig. S146 2,6-dichloropyridine

E_{SCF}	E_{ZP}	H	G
-276.913551	-276.844147	-276.836610	-276.876233

2,6-dichloropyridine *N*-oxide

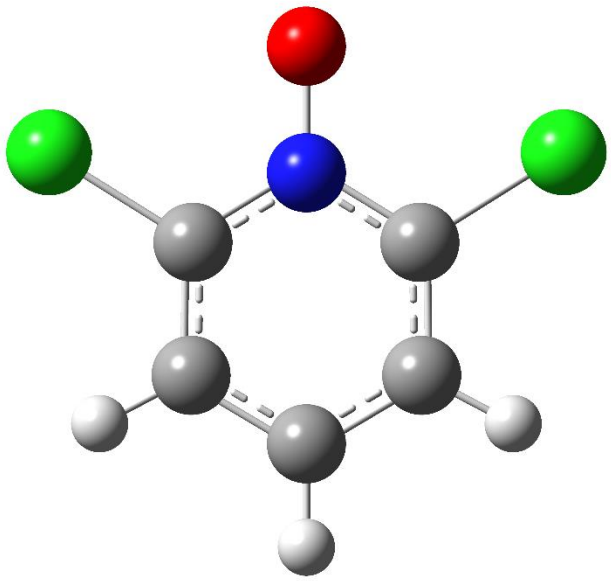

Fig. S147 2,6-dichloropyridine *N*-oxide

E_{SCF}	E_{ZP}	H	G
-352.054051	-351.980895	-351.972468	-352.014043

2-chloropyridine

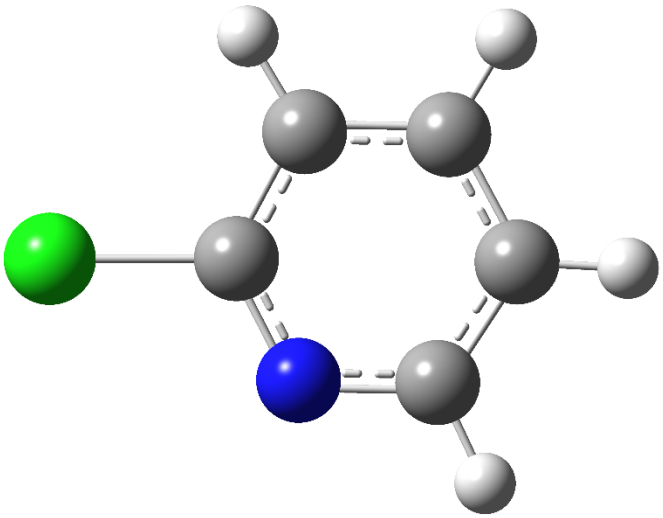

Fig. S148 2-chloropyridine

E_{SCF}	E_{ZP}	H	G
-262.577796	-262.498438	-262.492105	-262.528241

2-chloropyridine *N*-oxide

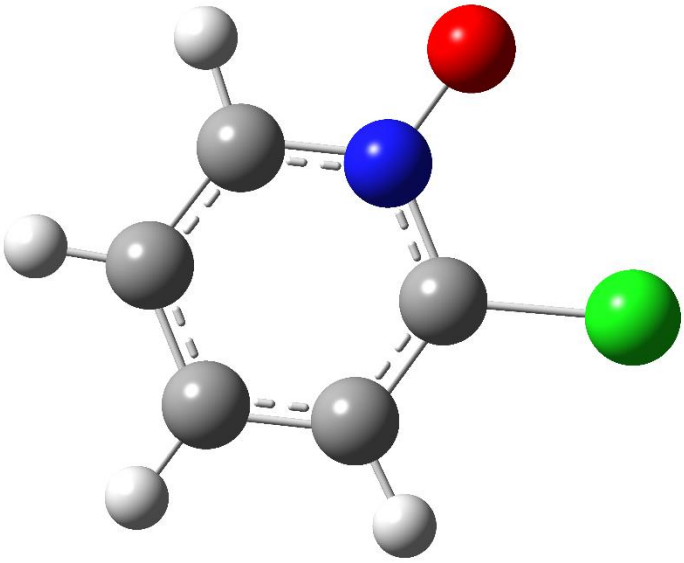

Fig. S149 2-chloropyridine *N*-oxide

E_{SCF}	E_{ZP}	H	G
-337.729224	-337.646024	-337.638824	-337.677018

pyridine

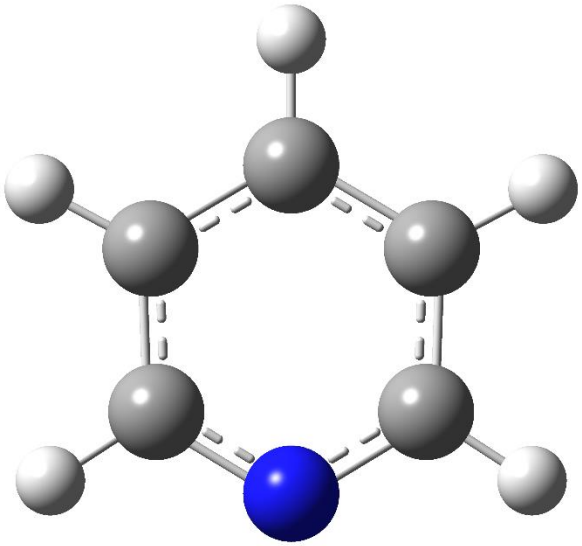

Fig. S150 pyridine

E_{SCF}	E_{ZP}	H	G
-248.239415	-248.150160	-248.144974	-248.177576

pyridine *N*-oxide

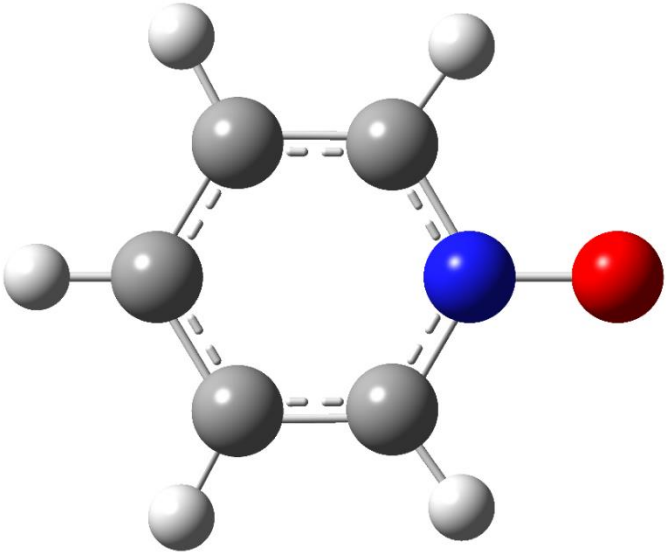

Fig. S151 pyridine *N*-oxide

E_{SCF}	E_{ZP}	H	G
-323.403187	-323.309974	-323.303963	-323.338723

4-nitroquinoline

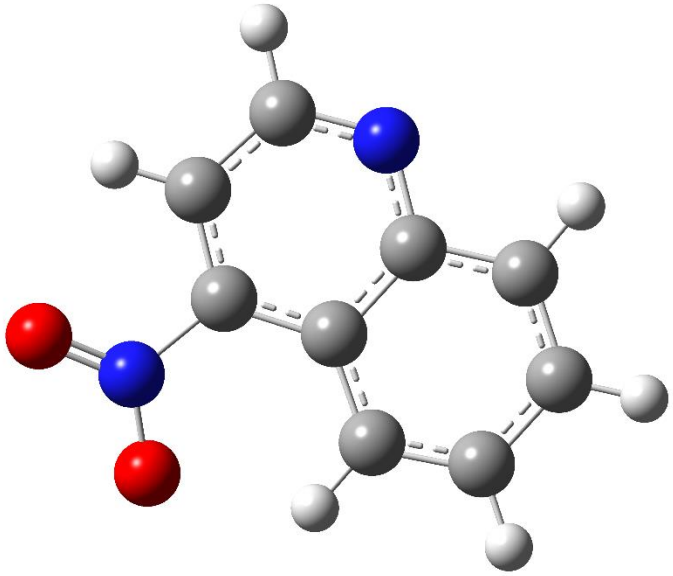

Fig. S152 4-nitroquinoline

E_{SCF}	E_{ZP}	H	G
-606.322250	-606.184258	-606.174073	-606.220041

4-nitroquinoline *N*-oxide

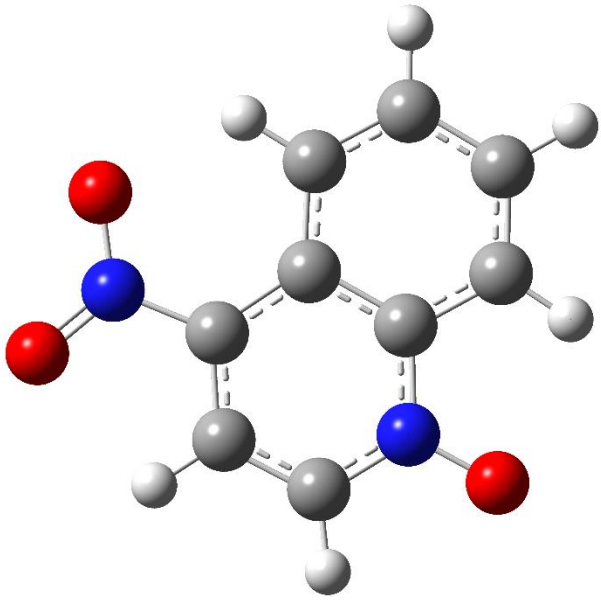

Fig. S153 4-nitroquinoline *N*-oxide

E_{SCF}	E_{ZP}	H	G
-681.491158	-681.348929	-681.337880	-681.385715

2.5. Higher Levels of Theory and Basis Sets Tests

2.5.1 B3LYP/LANL2DZ with Tight Convergence Criteria

O_2 (Triplet)

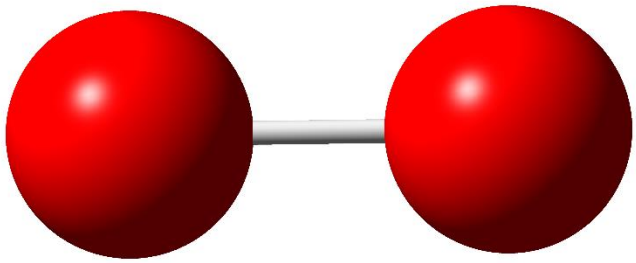

Fig. S154 O_2 (Triplet)

E_{SCF}	E_{ZP}	H	G
-150.314740	-150.311443	-150.308132	-150.331504

2,6-dimethylpyridine (Singlet)

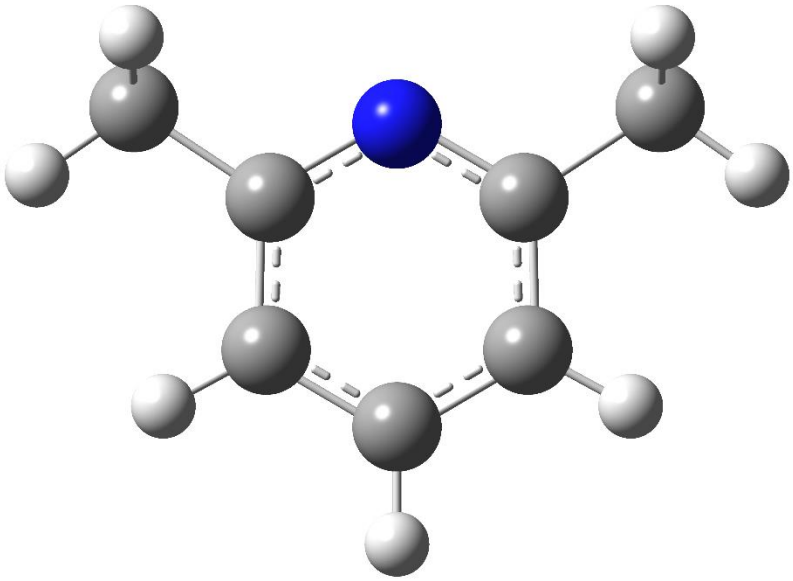

Fig. S155 2,6-dimethylpyridine (Singlet)

E_{SCF}	E_{ZP}	H	G
-326.869253	-326.724866	-326.716101	-326.757958

2,6-dimethylpyridine *N*-oxide (Singlet)

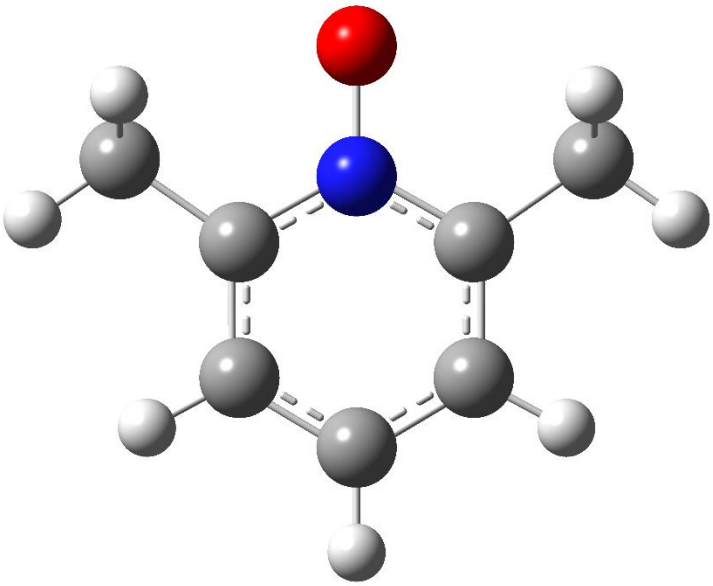

Fig. S156 2,6-dimethylpyridine *N*-oxide (Singlet)

E_{SCF}	E_{ZP}	H	G
-402.038437	-401.889326	-401.880184	-401.921774

oxo complex with adsorbed Me_2PyO molecule (Triplet)

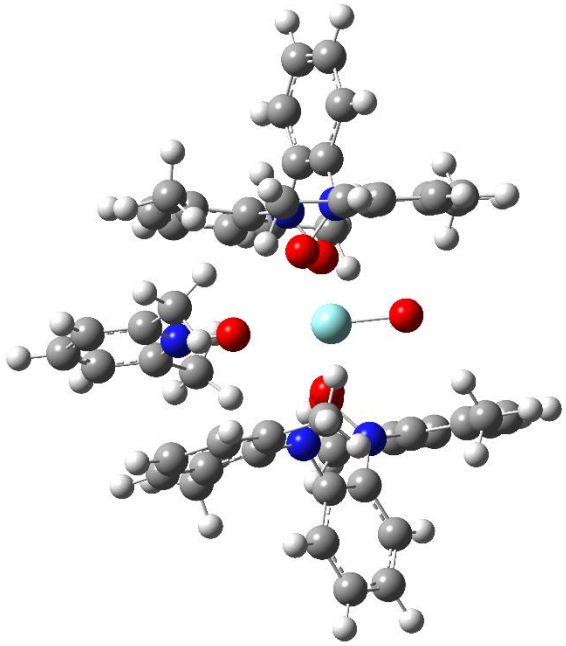

Fig. S157 oxo complex with adsorbed Me_2PyO molecule (Triplet)

E_{SCF}	E_{ZP}	H	G
-2746.658262	-2745.718113	-2745.655289	-2745.818217

η^3-ozone complex to peroxo complex (Triplet)

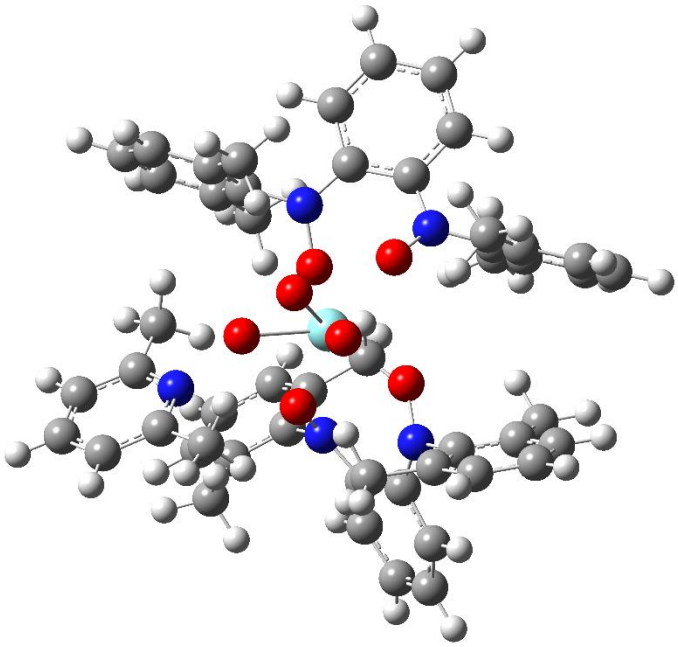

Fig. S158 η^3-ozone complex to peroxo complex (Triplet)

E_{SCF}	E_{ZP}	H	G	*f*
-2821.749736	-2820.808876	-2820.744891	-2820.909609	-255

peroxo η^3-ozone complex to spiro bisperoxo complex (Triplet)

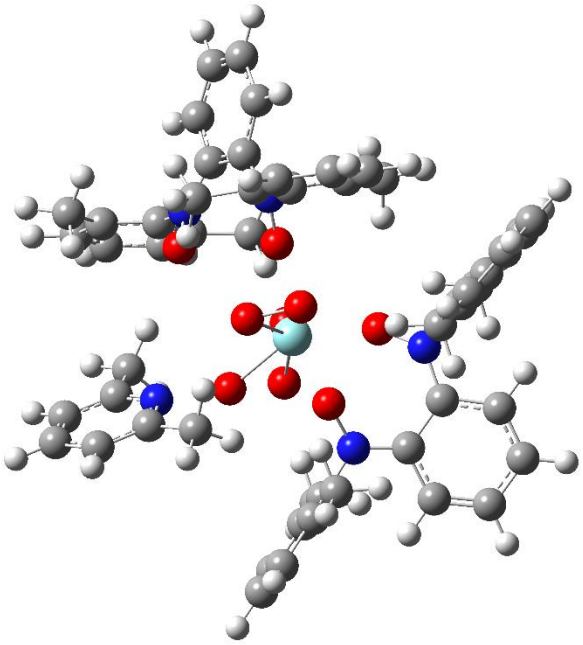

Fig. S159 peroxo η^3-ozone complex to spiro bisperoxo complex (Triplet)

E_{SCF}	E_{ZP}	H	G	*f*
-2972.067602	-2971.121520	-2971.054402	-2971.228083	-210

2.5.2 B3LYP/LANL2DZ with PCM

O_2 (Triplet)

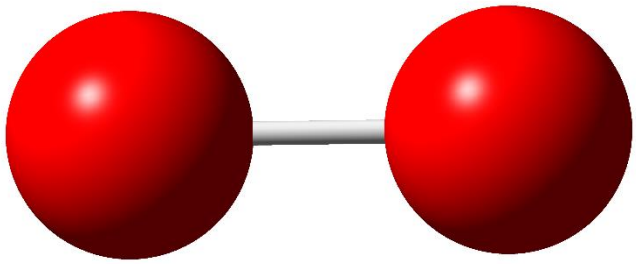

Fig. S160 O_2 (Triplet)

E_{SCF}	E_{ZP}	H	G
-150.314977	-150.311687	-150.308376	-150.331748

2,6-dimethylpyridine (Singlet)

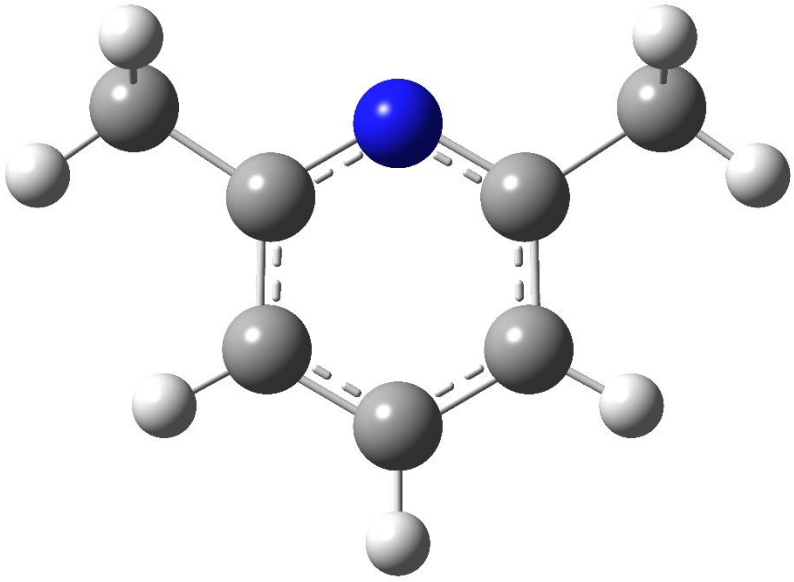

Fig. S161 2,6-dimethylpyridine (Singlet)

E_{SCF}	E_{ZP}	H	G
-326.874122	-326.729807	-326.721084	-326.762625

2,6-dimethylpyridine *N*-oxide (Singlet)

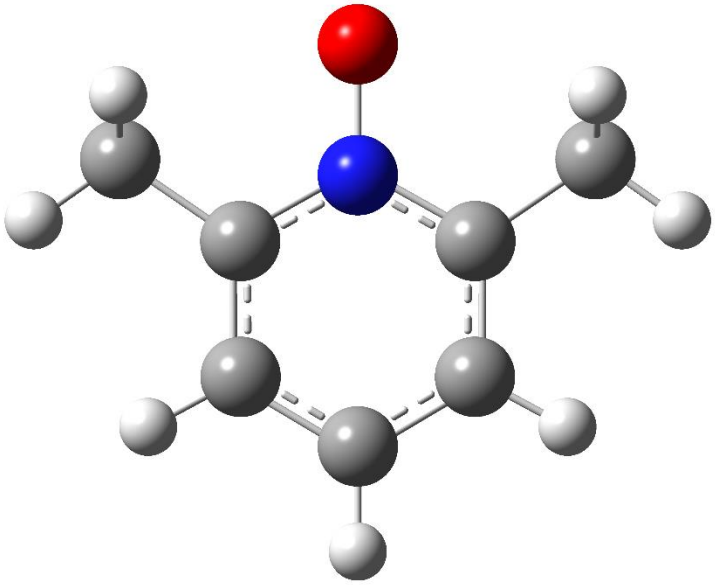

Fig. S162 2,6-dimethylpyridine *N*-oxide (Singlet)

E_{SCF}	E_{ZP}	H	G
-402.046771	-401.897803	-401.888637	-401.930286

oxo complex with adsorbed Me_2PyO molecule (Triplet)

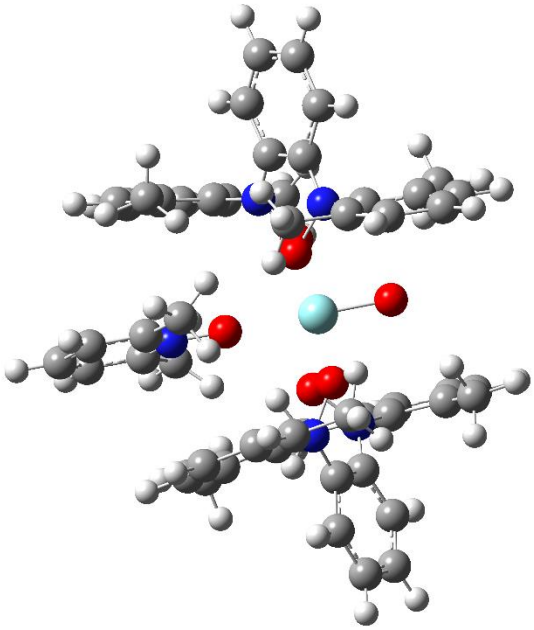

Fig. S163 oxo complex with adsorbed Me_2PyO molecule (Triplet)

E_{SCF}	E_{ZP}	H	G
-2746.685457	-2745.745359	-2745.682819	-2745.844385

η^3-ozone complex to peroxo complex (Triplet)

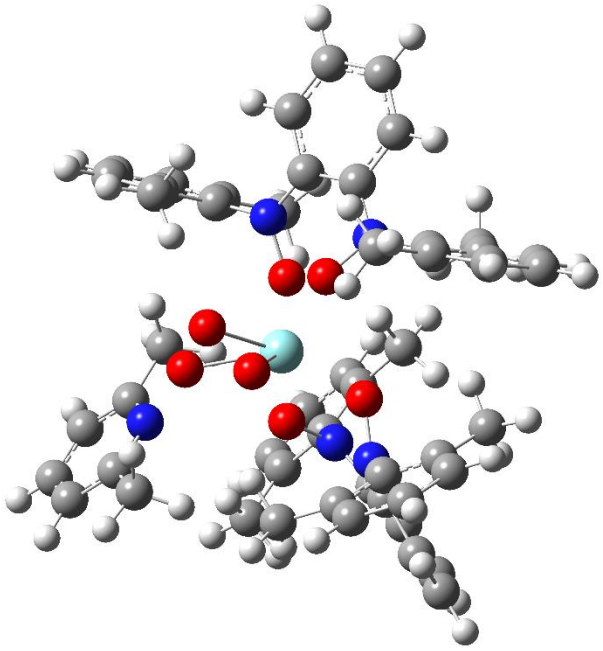

Fig. S164 η^3-ozone complex to peroxo complex (Triplet)

E_{SCF}	E_{ZP}	H	G	*f*
-2821.777516	-2820.837287	-2820.773240	-2820.937699	-266

peroxo η^3-ozone complex to spiro bisperoxo complex (Triplet)

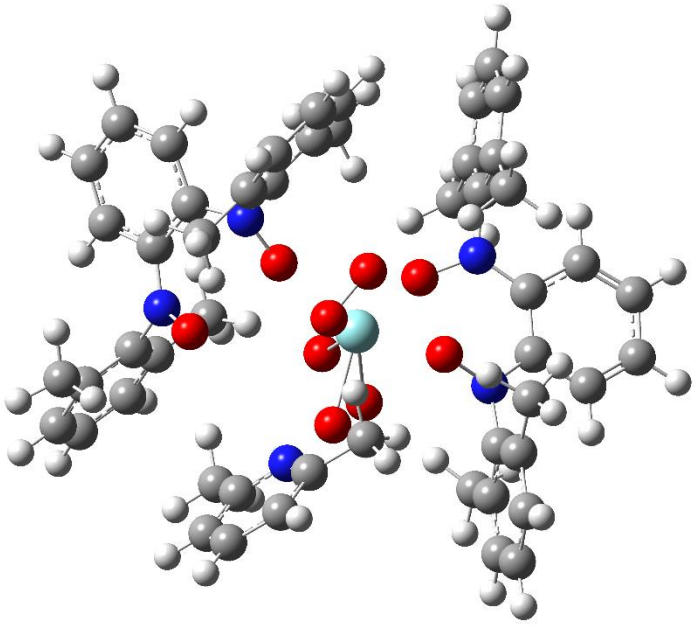

Fig. S165 peroxo η^3-ozone complex to spiro bisperoxo complex (Triplet)

E_{SCF}	E_{ZP}	H	G	*f*
-2972.096590	-2971.150547	-2971.083683	-2971.255242	-225

2.5.3 B3LYP/Custom Basis Set

O_2 (Triplet)

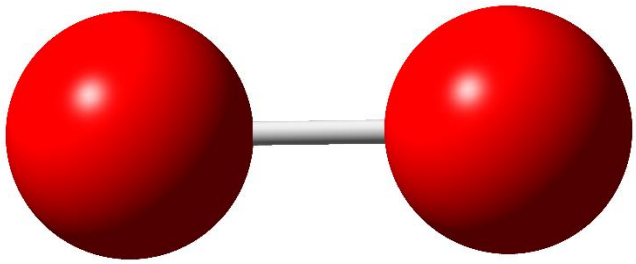

Fig. S166 O_2 (Triplet)

E_{SCF}	E_{ZP}	H	G
-150.360532	-150.356817	-150.353510	-150.376803

2,6-dimethylpyridine (Singlet)

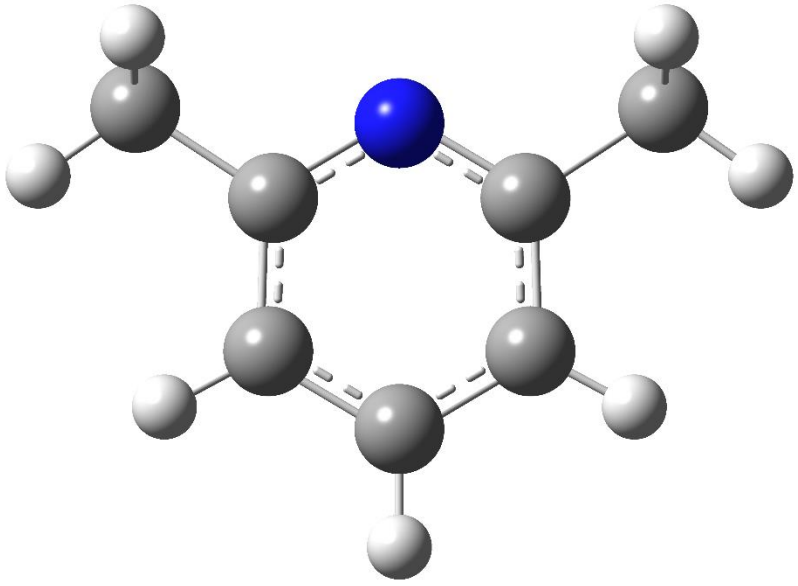

Fig. S167 2,6-dimethylpyridine (Singlet)

E_{SCF}	E_{ZP}	H	G
-326.889109	-326.744760	-326.735974	-326.778016

2,6-dimethylpyridine *N*-oxide (Singlet)

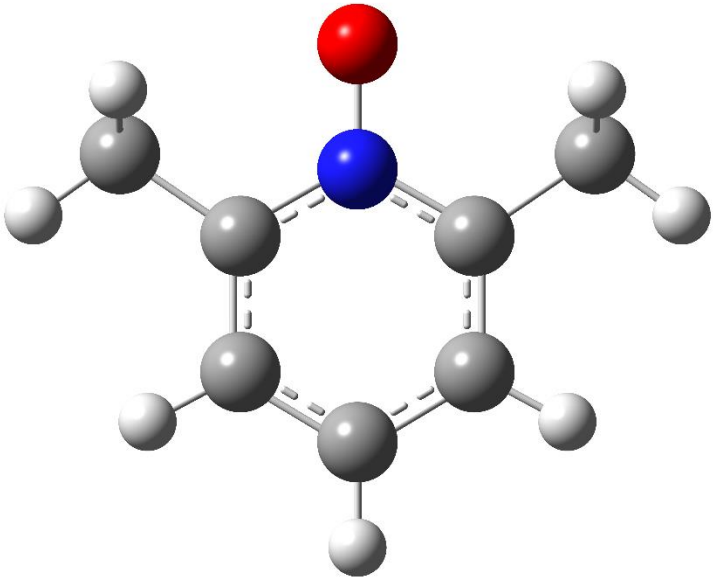

Fig. S168 2,6-dimethylpyridine *N*-oxide (Singlet)

E_{SCF}	E_{ZP}	H	G
-402.082333	-401.932739	-401.923678	-401.965089

oxo complex with adsorbed Me_2PyO molecule (Triplet)

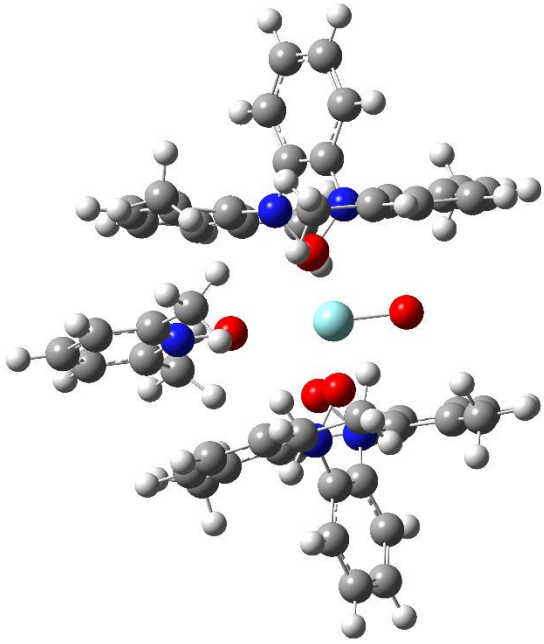

Fig. S169 oxo complex with adsorbed Me_2PyO molecule (Triplet)

E_{SCF}	E_{ZP}	H	G
-2746.856025	-2745.915836	-2745.852830	-2746.016972

η^3-ozone complex to peroxo complex (Triplet)

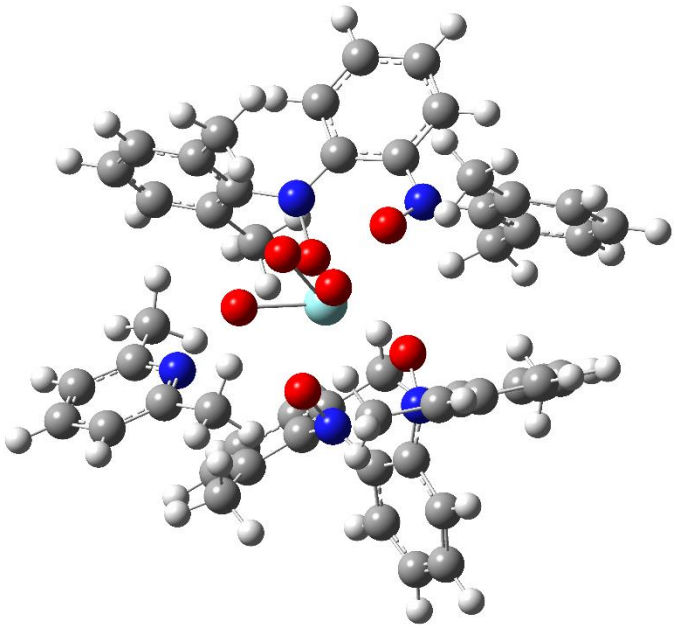

Fig. S170 η^3-ozone complex to peroxo complex (Triplet)

E_{SCF}	E_{ZP}	H	G	*f*
-2821.961601	-2821.020573	-2820.956514	-2821.121604	-233

peroxo η^3-ozone complex to spiro bisperoxo complex (Triplet)

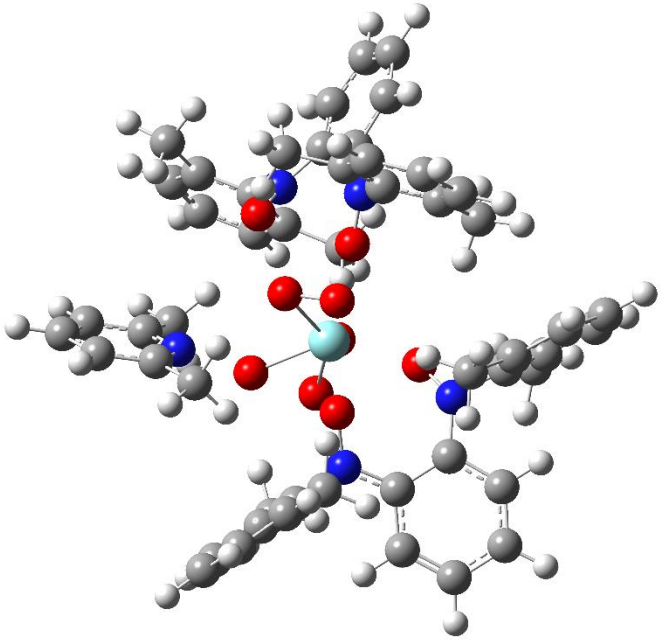

Fig. S171 peroxo η^3-ozone complex to spiro bisperoxo complex (Triplet)

E_{SCF}	E_{ZP}	H	G	*f*
-2972.324674	-2971.377757	-2971.310667	-2971.485082	-343

2.5.4 B3LYP/Custom Basis Set with PCM

O_2 (Triplet)

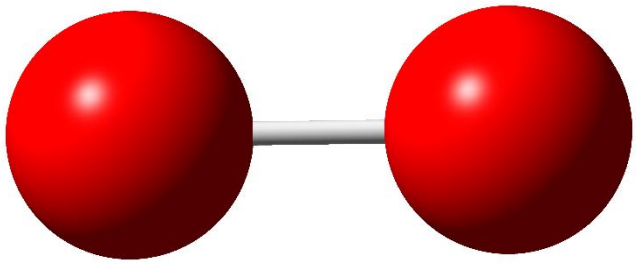

Fig. S172 O_2 (Triplet)

E_{SCF}	E_{ZP}	H	G
-150.360636	-150.356920	-150.353613	-150.376906

2,6-dimethylpyridine (Singlet)

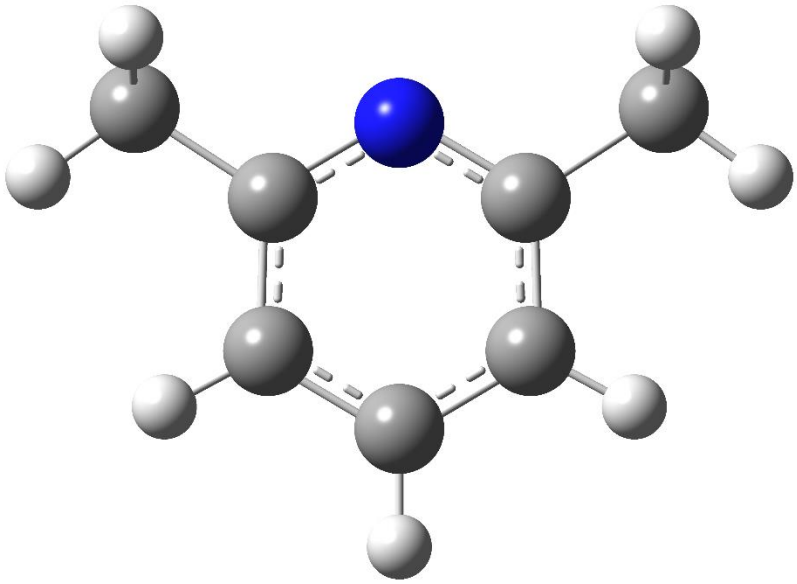

Fig. S173 2,6-dimethylpyridine (Singlet)

E_{SCF}	E_{ZP}	H	G
-326.893479	-326.749252	-326.740480	-326.782382

2,6-dimethylpyridine *N*-oxide (Singlet)

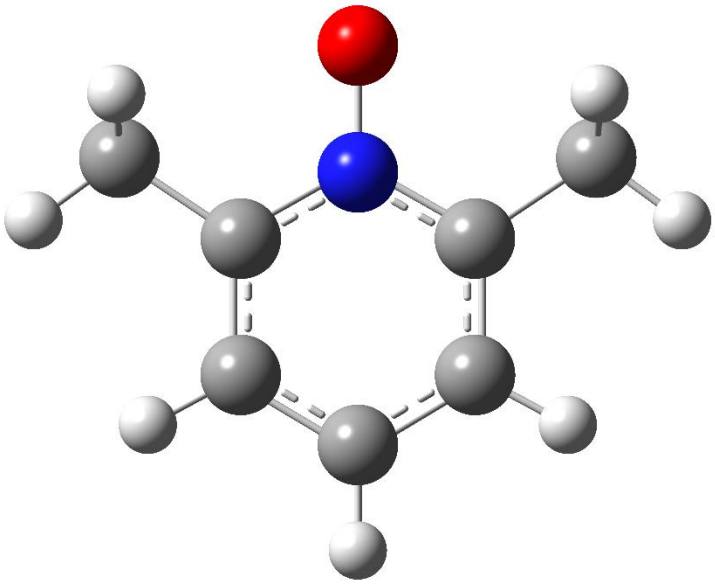

Fig. S174 2,6-dimethylpyridine *N*-oxide (Singlet)

E_{SCF}	E_{ZP}	H	G
-402.090161	-401.940802	-401.931710	-401.973201

oxo complex with adsorbed Me_2PyO molecule (Triplet)

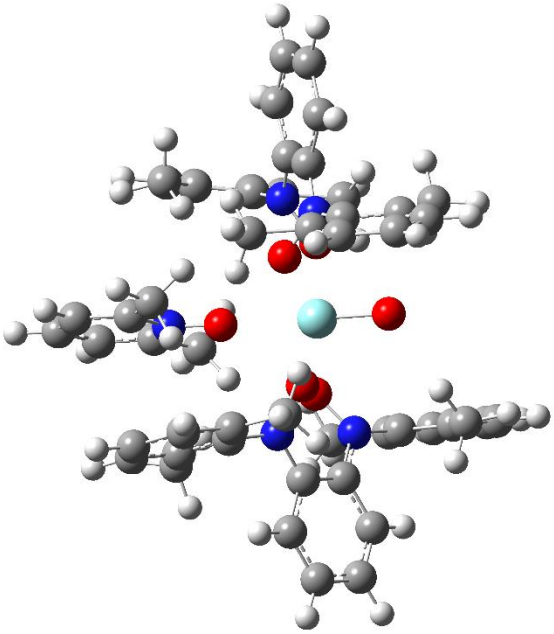

Fig. S175 oxo complex with adsorbed Me_2PyO molecule (Triplet)

E_{SCF}	E_{ZP}	H	G
-2746.880325	-2745.940640	-2745.877803	-2746.040004

η^3-ozone complex to peroxo complex (Triplet)

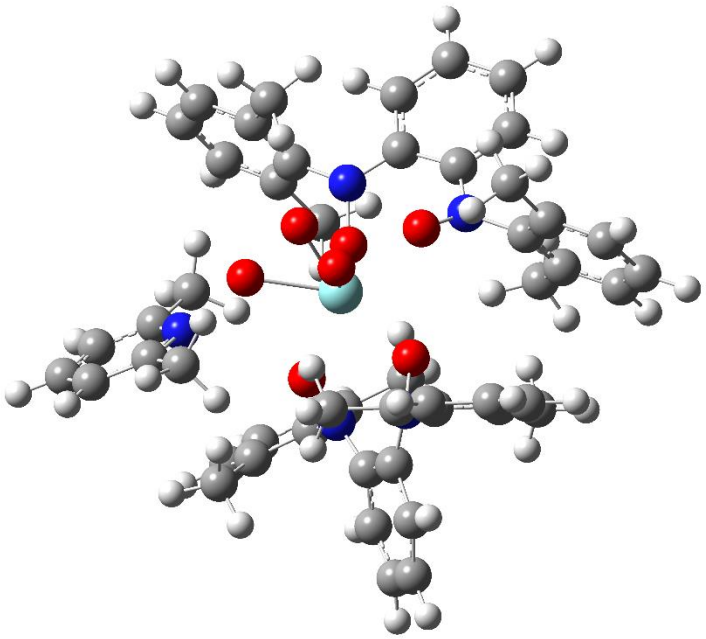

Fig. S176 η^3-ozone complex to peroxo complex (Triplet)

E_{SCF}	E_{ZP}	H	G	*f*
-2821.984055	-2821.043300	-2820.979346	-2821.143349	-390

peroxo η^3-ozone complex to spiro bisperoxo complex (Triplet)

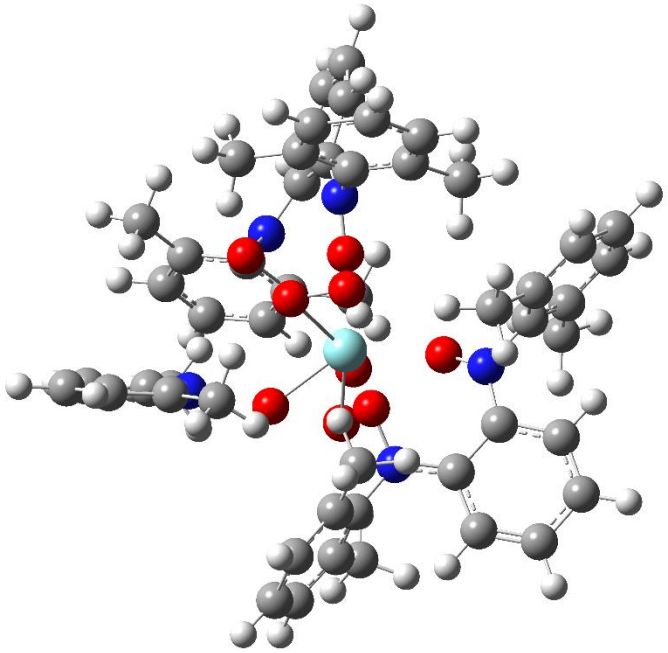

Fig. S177 peroxo η^3-ozone complex to spiro bisperoxo complex (Triplet)

E_{SCF}	E_{ZP}	H	G	*f*
-2972.350593	-2971.403716	-2971.336943	-2971.508462	-358